UNIVERSITY OF CALIFORNIA

Santa Barbara

Ecological implications of copper-based nanoparticles in aquatic complex matrices: Fate, behavior, and toxicity assessment

A dissertation submitted in partial satisfaction of the

requirements for the degree Doctor of Philosophy

in Environmental Science and Management

by

Caroline Patricio Vignardi

Committee in charge:

Professor Hunter S. Lenihan, Chair

Professor Patricia A. Holden

Professor Arturo A. Keller

March 2019

The dissertation of Caroline Patricio Vignardi is approved.

_____

Patricia A. Holden

_____

Arturo A. Keller

_____

Hunter S. Lenihan, Committee Chair

March 2019

Ecological implications of copper-based nanoparticles in aquatic complex matrices:

Fate, behavior, and toxicity assessment

Caroline Patricio Vignardi

ACKNOWLEDGEMENTS

First, I would like to thank Elohim God the Father and God the Mother for all blessings, especially the love and support I have received from all those who made this work a reality. My committee, for their invaluable comments and opportunities, and their generosity in sharing lab space, equipment, and expertise. I would like to especially thank my advisor for giving me the chance to carry out this research and for all his support and encouragement throughout, for which I am eternally grateful. No amount of thanks can express my gratitude to my Brazilian friends, especially my Brazilian advisor Phan. To my extended family, Ren (partner!!!) and his lovely wife Julie, Mohsen (Mo!!!), Yemi (Doc!!!), Kelly (best assistant), Henrik, Angela, Keila, Aga, Joe, Nicolas, Jess, Luis, and my boyfriend Niklas (the love of my life), thank you for your love and support over the many years of study and for the advice you have given and the examples that you have set. To my heavenly family, especially Oxnard Zion, for setting an example of dedication and perseverance that will help make me faithful to any path I choose. To all the UCSB and Bren staff, especially Sage, for his incalculable help in managing the experimental designs, which made much of this research possible. I am also very grateful to all at the Lenihan lab, especially Sean, Laura, Jose, and Phoebe, all my assistants, all at Holden lab, especially Monika, Marina, Ying, Timnit, Laurie, and Tania, and all at Keller lab, especially Anastasiya, Yuxiong, Lijuan, Jon, Nicol, and mi amigo Cruz, for their advice, perspectives, help, and friendship throughout this process. Finally, to my family, my deepest thanks for your never-ending support and faith in me. This manuscript is dedicated to you.

VITA OF CAROLINE PATRICIO VIGNARDI
March 2019

EDUCATION

Bachelor of Marine Biology, University of Santa Cecilia, Santos, Brazil, January 2010 (summa cum laude)
Master of Science in Biological Oceanography, University of São Paulo, São Paulo, Brazil, August 2012
Doctor of Philosophy in Environmental Science and Management, University of California, Santa Barbara, March 2019 (expected)

PROFESSIONAL EMPLOYMENT

2010: Teaching Assistant, Effects of Environmental Factors on the Physiology of Fish, Department of Biological Oceanography, University of São Paulo, São Paulo, Brazil
2011: Teaching Assistant, Aquaculture, Department of Biological Oceanography, University of São Paulo, São Paulo, Brazil
2012: Teaching Assistant, Special Topics in Marine Ecology II: Biological Processes, Department of Biological Oceanography, University of São Paulo, São Paulo, Brazil
2012: Researcher Assistant, Comandante Ferraz Antarctic Station, King George Island, Admiralty Bay, Antarctica
2016: Teaching Assistant, Bren School of Environmental Science and Management, University of California, Santa Barbara

PUBLICATIONS

Hasue, F. M., Passos, M. J. A. C. R., Santos, T. C. A., Rocha, A. J. S., Vignardi, C. P., Sartorio, P. V., Gomes, V., Phan, V. N. 2012. Assessment of genotoxicity and depuration of anthracene in juvenile coastal fish *Trachinotus carolinus* using the comet assay. Brazilian Journal of Oceanography, v. 61, p. 215-222, 2013. DOI: 10.1590/S1679-87592013000400002.

Gomes, V., Phan, V. N., Passos, M. J. A. C. R., Rocha, A. J. S., Hasue, F. M., Machado, A. S. D., Sartorio, P. V., Ferreira, J. P. L., Vignardi, C. P., Campos, D. Y. F., Ito, M. 2013. Study on the effects of ultraviolet radiation (UV) and organic contaminants on Antarctic marine animals from shallow waters. Annual Activity Report Book APA, 126-130. DOI: http://dx.doi.org/10.4322/apa.2014.109.

Gomes, V., Rocha, A. J. S., Passos, M. J. A. C. R., Botelho, M. T., Hasue, F. M., Vignardi, C. P., Phan, V. N. 2014. Biomonitoring of genotoxicity of shallow waters around the brazilian antarctic station comandante ferraz (eacf), admiralty bay, king george island, antarctica, using amphipod crustaceans. Annual Activity Report Book APA, 104-108. DOI: http://dx.doi.org/10.4322/apa.2015.020.

Vignardi, C. P., Hasue, F. M., Sartorio, P. V., Cardoso, C. M., Machado, A. S. D., Santos, T. C. A., Nucci, J. M., Passos, M. J. A. C., Gomes, V., Phan, V. N. 2015. Titanium dioxide nanoparticles exhibit genotoxicity, potential cytotoxicity and possible tissue accumulation in

marine fish, *T. carolinus* (Linnaeus, 1766). Aquatic Toxicology 158, 218-229. DOI: 10.1016/j.aquatox.2014.11.008.

Cardoso, C.M.; Sartorio, P.V.; Machado, A.S.D.; Vignardi, C.P.; Rojas, D.C.C; Passos, M.J.A.; Rocha, A. J. S., Phan, V.N.; Gomes, V. 2015. Hsp70 and p53 expressions and behavior of juvenile pompano, *Trachinotus carolinus* (Perciformes, Carangidae), at controlled temperature increase. Journal of Experimental Marine Biology and Ecology 470, 34-42. DOI: 10.1016/j.jembe.2015.04.024.

Rocha, A. J. S., Botelho, M. T., Hasue, F. M., Passos, M. J. A. C. R., Vignardi, C. V., Phan, V. N., Gomes, V. 2015. Genotoxicity of shallow waters near the Brazilian Antarctic Station "Comandante Ferraz" (EACF), Admiralty Bay, King George Island, Antarctica. Brazilian Journal of Oceanography 63(1), 63-70. DOI: 10.1590/S1679-87592015080906301.

Rocha, A. J. S., Botelho, M. T., Hasue, F. M., Passos, M. J. A. C. R., Cardoso, C. M., Vignardi, C. P., Phan, V. N., Gomes, V. 2017. Hsp70 and p53 expression in *Gondogeneia antarctica* amphipods collected in shallow waters around the Brazilian Antarctic Station “Comandante Ferraz” (EACF), Admiralty Bay, King George Island, Antarctica. Pan-American Journal of Aquatic Sciences 12(2), 97-107.

Machado, A. S. D., Cardoso, C. M., Sartorio, P. V., Costa, E. F. S., Vignardi, C. P., Hasue, F. M., Viadanna, P. H. O., Santos, D. M., Yasumaru, F. A., Marion, C., Gomes, V., Phan, V. N. 2017. Lethal thermal maximum temperature induces behavioral responses and protein expressions (Hsp70 and p53) in juvenile common carp (*Cyprinus carpio* Linnaeus). Pan-American Journal of Aquatic Sciences 12(4), 295-309.

Vignardi, C. P., Tran, K., Muller, E. B., Means, J. C., Murray, J., Ortiz, C., Keller, A. A., Smith, N., Couture, J., Lenihan, H. S. Effects of Cu nanopesticides on the energy budget of the estuarine amphipod *Leptocheirus plumulosus*. *In preparation*.

Vignardi, C. P., Adeleye, A. S., Oranu, E., Miller, R. J., Keller, A. A., Holden, P. A., Lenihan, H.S. Aging of copper nanoparticles in the marine environment regulates toxicity to phytoplankton. *In preparation*.

Vignardi, C. P., Adeleye, A. S., Oranu, E., Miller, R. J., Keller, A. A., Holden, P. A., Lenihan, H. S. Aging in freshwater increases copper nanoparticle toxicity to marine phytoplankton. *In preparation*.

AWARDS

Department of Biological Oceanography CAPES scholarship, University of Sao Paulo, Sao Paulo, 2010-2012.

Science without borders CAPES scholarship, Sao Paulo, 2014-2018.

UC Santa Barbara Earth Research Institute (ERI) Travel Award, 2017.

FIELDS OF STUDY

Major Field: Aquatic Ecology and Toxicology

Studies in Ecotoxicology of Engineered Nanomaterials (ENMs) Research with Professors Hunter S. Lenihan, Adeyemi S. Adeleye, and researcher Robert J. Miller.

Studies in Impacts of Emerging Pesticides with Professors Hunter S. Lenihan, Jay C. Means, Erik B. Muller, and researcher Jill Mulray.

ABSTRACT

Ecological implications of copper-based nanoparticles in aquatic complex matrices: Fate, behavior, and toxicity assessment

by

Caroline Patricio Vignardi

Engineered nanomaterials (ENMs) are likely to undergo some degree of modification when released into the environment, which can influence the fate, behavior, and toxicity of nanoparticles (NPs). The environmental factors in natural aquatic ecosystems, such as water chemistry, hydrology, disturbance, and biotic interactions, can transform or "age" toxic chemicals through physical, chemical, and biological processes, including aggregation and disaggregation, adsorption, redox reaction, dissolution, complexation and biotransformation. The extent of aging can vary considerably over time and within a single or a number of water bodies, such as a river that flows into the ocean through an estuary. However, the ecological effects of NPs under realistic environmental exposure scenarios are not yet fully understood. Adding to these challenges are problems arising from traditional ecotoxicological risk assessments, which are inevitably hampered by narrow subsets of relevant species, toxicants, exposure conditions, and levels of impact. The present work examined the toxicity of copper-based nanoparticles (CBNPs), which frequently enter natural aquatic ecosystems due to their increasing application in consumer products, by assessing their impact on marine phytoplankton and estuarine amphipods, organisms that are central to aquatic ecosystems. Standard toxicological methods were used, along with physiological measurements, studies

of fate and transport, and mechanistic biological models based on Dynamic Energy Budget (DEB) theory. The aim of the work was to understand 1) the influence of aging processes on CBNPs under environmentally relevant test conditions, 2) the impact of aged CBNPs on a marine phytoplankton population, 3) the potential impact of CBNPs on non-target estuarine organisms, and 4) the potential for detecting and predicting the toxic effects of CBNPs on an individual, to generate model estimates of effects on populations and communities. CBNPs were found to be toxic to benthic estuarine organisms at concentrations of CBNPs already found in the natural environment. However, sublethal toxicity may not be detected by traditional ecotoxicological tests. Additionally, aging was found to influence the fate and transport of CBNPs through oxidation, aggregation, and dissolution processes, increasing Cu toxic ion bioavailability to pelagic organisms over time. While current studies increasingly consider more realistic environmental exposure scenarios, this work, as well as that of other researchers, suggests that CBNPs behave differently under prolonged environmental exposure, and nanoecotoxicological research should focus on sublethal impacts, integrated with mechanistic biological models and based on Dynamic Energy Budget (DEB) theory.

TABLE OF CONTENTS

I. Introduction 12

I.I References 17

Chapter 1. Effects of Cu nanopesticides on the energy budget of the estuarine amphipod *Leptocheirus plumulosus* 20

1.1 Abstract 21

1.2. Introduction 23

1.3. Methods 26

1.4. Results 35

1.5. Discussion 40

1.6. References 46

1.7. Appendix. Supporting Information 61

Chapter 2. Aging of copper nanoparticles in the marine environment regulates toxicity to phytoplankton 75

2.1. Abstract 76

2.2. Introduction 78

2.3. Methods 80

2.4. Results 85

2.5. Discussion 92

2.6. References 94

2.7. Appendix. Supporting Information 108

Chapter 3. Aging in freshwater increases copper nanoparticle toxicity to marine phytoplankton. 137

3.1. Abstract 138

3.2. Introduction 139

3.3. Methods 141

3.4. Results 147

3.5. Discussion 152

3.6. References 156

3.7. Appendix. Supporting Information 169

II. Conclusions 182

I. Introduction

Nanotechnology has the potential to greatly improve several fields of scientific research due to the unique phenomena of controlling matter at dimensions of between approximately 1 and 100 nanometers (nm). This enables new applications which are not possible when working with bulk materials[1]. Over the last decade, a large range of products containing engineered nanomaterials (ENMs) has entered industrial use. The release of these materials into the environment, whether from coatings or other products, is a rapidly increasing form of environmental contamination[2–4].

Their unique properties make ENMs extremely reactive due to their high surface area relative to volume. Additionally, ENMs can behave in completely different ways depending on the characteristics of the surrounding media, and their composition, size, and surface charge[5]. The fate and transformation processes of nanoparticles (NPs) in the environment are therefore directly linked to natural environmental properties, including ionic strength, salinity, alkalinity, natural organic matter concentrations and hydrodynamics, all of which can trigger a series of events that modify the bioavailability, uptake, and toxicity of NPs[6,7].

Predicting ecosystem level consequences using traditional ecotoxicity methodology has proven difficult[8]. Assessing the fate and transport processes of ENMs, and their impact on organisms and ecosystem processes, therefore requires an understanding of the transformations of the nanomaterials in the environment. This is particularly true for metallic ENMs that in natural aqueous solutions undergo varying rates of aggregation, complexation, sedimentation and dissolution, all of which are influenced by particle morphology and concentration, as well as the ionic strength of the medium and the presence and type of the natural organic matter (NOM)[9].

Aquatic ecosystems are at risk of contamination by NPs via unintentional release, including industrial spills and waste disposal, and/or direct applications, such as the use of copper-based nanoparticles in antifouling paint and nanopesticides[10,11]. A critical role for science then is to assess the environmental implications and predict the impacts of NPs before they are released in high enough volumes to create environmental problems. One major role we can play is to create realistic environmental scenarios, in mesocosms or other controlled virtual environments, in which we design and execute experiments that help us predict, recognize, assess, and in some cases manage to reduce the severity of NP impacts in nature. In that spirit, I have undertaken a set of experiments to better understand interactions between nanoparticles, aquatic ecosystems, and aquatic organisms.

While copper is an essential element for all living organisms, it is also a heavy metal and therefore toxic to many organisms in concentrations above certain thresholds. The dual nature of copper complicates environmental risk assessment as aquatic organisms possess different mechanisms of absorption, defense, and elimination of Cu particles[12]. Once released into the environment, copper-based nanoparticles (CBNPs) can remain suspended in water indefinitely, dissolve or agglomerate and be deposited in sediment[5,13]. In marine or marine influenced ecosystems, for example, the rapid aggregation and precipitation of ENMs suggests that pelagic organisms may be exposed to these nanomaterials for shorter periods than organisms in the benthic environment, where particles deposit and accumulate. Benthic microbes, plants, and animals may therefore be exposed to relatively high concentrations of particles with aggregate sizes above the nanometer range, and over relatively longer periods of time[7,14]. Estuarine ecosystems, which receive a large proportion of contaminants released from the terrestrial environment into the aquatic environment, are especially interesting and challenging to study because of the dynamic nature of physiochemical conditions and the

diverse biological communities that inhabit both the water column and benthos. Generating a better understanding of the environmental implications and impacts of copper ENMs in estuarine ecosystems therefore benefits ecosystem management but also provides a fascinating system to explore the environmental chemistry of nanomaterials.

Many estuarine species, many of which produce important ecosystem services, are at risk from the release of nanomaterials into upstream riverine aquatic systems. These include marine phytoplankton, which are responsible for a large part of carbon recycling and primary production, and benthic invertebrates, such as amphipods, that are important prey species in marine and estuarine benthic food webs. Both phytoplankton and amphipods are vulnerable to metal pollution, including from nanomaterials, in sediments and the water column, and so have been extensively used in toxicity assessments[5,15,16].

While a large number of studies have examined the impacts of ENMs over the last decade, there are still crucial gaps in our knowledge of the ecological risk of CBNPs, especially in terms of their behavior, transformation processes, and toxicity under environmentally realistic conditions[11,17,18]. The influence of aqueous ionic strength in aquatic ecosystems is a particularly challenging area of inquiry[19,20]. Salinity influences Cu fate and transport and therefore toxicity by metal speciation[6]. Moreover, salinity can change rapidly over time, space and the environment, thereby modifying potential exposure, uptake, and toxicity to a wide variety of organisms, including phytoplankton and amphipods[19,20]. While studies have confirmed the toxicity of CBNPs, no study has examined the impact of these ENMs in scenarios of ecological exposure to sentinel organisms, which are needed to predict ecosystem level impacts[21].

The objective of my dissertation was to address and better understand the potential ecological impacts of CBNPs as they transform in complex environmental matrices.

Specifically, I assessed how CBNPs behave under environmentally realistic conditions in freshwater, estuarine, and seawater systems, the impacts of CBNPs on key water properties, the uptake and body burdens of Cu particles in phytoplankton and amphipods, and how the lethal and sublethal responses of aquatic organisms were influenced by CBNPs. These topics were addressed using exposure scenarios designed to mimic the real world, taking into account the potential for aging, biological uptake and NPs speciation at low levels of CBNPs, and particularly applications involving the direct release of CBNPs, such as commercial antifouling paints and pesticides in agriculture. The scenarios I created and resulting questions I addressed have been highly recommended in recent major literature reviews[11,21]. Closely-controlled toxicity tests involving ecologically important species, phytoplankton or amphipods were used, and Dynamic Energy Budget (DEB) models were employed to translate and integrate information obtained from laboratory assays, to provide insights on the broader ecological risks of CBNPs[22,23].

Chapter 1 compared how non-target estuarine amphipods responded to Cu-based nanopesticides and conventional Cu-based pesticides at environmentally relevant concentrations. The lethal and sublethal effects on Cu speciation and Cu body burdens in amphipods were examined, and lethal and sublethal effects were quantified in the laboratory experiments. The data generated from the experiments were then used in mechanistic biological models based on Dynamic Energy Budget (DEB) theory as a means of advancing our general understanding of CBNPs on aquatic organisms.

Chapter 2 explored the aging process of copper nanoparticles (Cu NPs) in a mesocosm designed to simulate the surface water of an estuarine ecosystem, with the specific goal of examining the aging process that Cu NPs experience when they enter an estuary from a river, and the eventual impacts the NPs may have on estuarine phytoplankton. In contrast to prior

works on nanoparticle-aging in aqueous media, which have used artificially high concentrations of NPs, I examined the aging process, behavior, transformation, bioavailability and toxicity of Cu NPs at environmentally realistic, very low levels of Cu, and focused on the aging process as it likely occurs during the relatively slow transport of materials through a large estuary, over a period of days to weeks. This approach was used to mimic conditions that occur in the real world, as some of the major predicted exposure scenarios involve Cu NPs from boats coated with antifouling paints[10], with generally constant ambient conditions, except for the aging period.

In chapter 3, I examined the aging process of copper nanoparticles (Cu NPs) in a freshwater mesocosm, with the specific goal of examining the aging process that Cu NPs undergo as they flow downriver to an estuary, where they can impact estuarine phytoplankton. Freshwater ecosystems have characteristics that make them less likely to influence Cu NPs properties, including the presence of fewer Cu binders, such as chloride ions and natural organic matter (NOM), which are important for controlling Cu speciation, bioavailability, and toxicity in aquatic ecosystems[14]. Uncovering some of the underlying mechanisms that control the physicochemical processes of Cu NPs which age in freshwater systems before reaching the ocean is environmentally relevant, and critically important for marine organisms.

The data generated from these experiments were used by the Center for the Environmental Implications of Nanotechnology (UC CEIN) and the city of Santa Barbara, to predict the impacts of emergent pollutants on individuals as well as populations of marine phytoplankton and estuarine amphipods. This research will also fundamentally contribute to our understanding of the ecosystem-level impacts of Cu NPs to allow safer use of Cu-based nanoproducts.

I.I References

1. Satalkar, P., Elger, B. S. & Shaw, D. M. Defining Nano, Nanotechnology and Nanomedicine: Why Should It Matter? *Sci Eng Ethics* **22**, 1255–1276 (2016).
2. Nel, A. *et al.* Nanomaterial toxicity testing in the 21st century: use of a predictive toxicological approach and high-throughput screening. *Acc. Chem. Res.* **46**, 607–621 (2013).
3. Scheufele, D. A. *et al.* Scientists worry about some risks more than the public. *Nat Nanotechnol* **2**, 732–734 (2007).
4. Service, R. F. Nanotechnology Grows Up. *Science* **304**, 1732–1734 (2004).
5. Keller, A. A. *et al.* Stability and Aggregation of Metal Oxide Nanoparticles in Natural Aqueous Matrices. *Environ. Sci. Technol.* **44**, 1962–1967 (2010).
6. Klaine, S. J. *et al.* Nanomaterials in the environment: Behavior, fate, bioavailability, and effects. *Environmental Toxicology and Chemistry* **27**, 1825–1851 (2008).
7. Garner, K. L. & Keller, A. A. Emerging patterns for engineered nanomaterials in the environment: a review of fate and toxicity studies. *Journal of Nanoparticle Research* **16**, (2014).
8. Bernhardt, E. S. *et al.* An Ecological Perspective on Nanomaterial Impacts in the Environment. *Journal of Environment Quality* **39**, 1954 (2010).
9. Garner, K. L., Suh, S. & Keller, A. A. Assessing the Risk of Engineered Nanomaterials in the Environment: Development and Application of the nanoFate Model. *Environ. Sci. Technol.* **51**, 5541–5551 (2017).
10. Adeleye, A. S., Oranu, E. A., Tao, M. & Keller, A. A. Release and detection of nanosized copper from a commercial antifouling paint. *Water Research* **102**, 374–382 (2016).

11. Keller, A. A. *et al.* Comparative environmental fate and toxicity of copper nanomaterials. *NanoImpact* **7**, 28–40 (2017).
12. Gomes, T. *et al.* Accumulation and toxicity of copper oxide nanoparticles in the digestive gland of Mytilus galloprovincialis. *Aquatic Toxicology* **118**–**119**, 72–79 (2012).
13. Conway, J. R., Adeleye, A. S., Gardea-Torresdey, J. & Keller, A. A. Aggregation, Dissolution, and Transformation of Copper Nanoparticles in Natural Waters. *Environ. Sci. Technol.* **49**, 2749–2756 (2015).
14. Adeleye, A. S., Conway, J. R., Perez, T., Rutten, P. & Keller, A. A. Influence of Extracellular Polymeric Substances on the Long-Term Fate, Dissolution, and Speciation of Copper-Based Nanoparticles. *Environ. Sci. Technol.* **48**, 12561–12568 (2014).
15. Hanna, S. K., Miller, R. J., Muller, E. B., Nisbet, R. M. & Lenihan, H. S. Impact of engineered zinc oxide nanoparticles on the individual performance of Mytilus galloprovincialis. *PLoS ONE* **8**, e61800 (2013).
16. Miller, R. J. *et al.* Photosynthetic efficiency predicts toxic effects of metal nanomaterials in phytoplankton. *Aquatic Toxicology* **183**, 85–93 (2017).
17. Lowry, G. V. *et al.* Environmental occurrences, behavior, fate, and ecological effects of nanomaterials: an introduction to the special series. *J. Environ. Qual.* **39**, 1867–1874 (2010).
18. Rossbach, L. M. *et al.* Sub-lethal effects of waterborne exposure to copper nanoparticles compared to copper sulphate on the shore crab (Carcinus maenas). *Aquatic Toxicology* **191**, 245–255 (2017).
19. Peijnenburg, W. J. G. M. *et al.* A Review of the Properties and Processes Determining the Fate of Engineered Nanomaterials in the Aquatic Environment.

http://dx.doi.org/10.1080/10643389.2015.1010430 (2015). Available at: https://openaccess.leidenuniv.nl/handle/1887/51414. (Accessed: 25th February 2019)

20. Mouneyrac, C., Syberg, K. & Selck, H. Ecotoxicological Risk of Nanomaterials. in *Aquatic Ecotoxicology* 417–440 (Elsevier, 2015). doi:10.1016/B978-0-12-800949-9.00017-6
21. Holden, P. A. *et al.* Considerations of Environmentally Relevant Test Conditions for Improved Evaluation of Ecological Hazards of Engineered Nanomaterials. *Environ. Sci. Technol.* **50**, 6124–6145 (2016).
22. Muller, E. B., Lin, S. & Nisbet, R. M. Quantitative Adverse Outcome Pathway Analysis of Hatching in Zebrafish with CuO Nanoparticles. *Environ. Sci. Technol.* **49**, 11817–11824 (2015).
23. Muller, E. B., Nisbet, R. M. & Berkley, H. A. Sublethal toxicant effects with dynamic energy budget theory: model formulation. *Ecotoxicology* **19**, 48 (2009).

Chapter 1. Effects of Cu nanopesticides on the energy budget of the estuarine amphipod *Leptocheirus plumulosus*

This work will be submitted for publication. Target journal: Aquatic Toxicology.

Key words: DEBtox; sublethal effects; amphipods; ecotoxicity; copper; nanopesticides; estuarine.

1.1 Abstract

New era nanopesticides have great promise for global agriculture due to their extended, low dose release profiles that are intended to increase effectiveness but reduce incidental environmental harm. Whether nano-engineered pesticides cause reduced levels of toxicity to non-target aquatic organisms is unclear but important to assess. Predicting how aquatic species respond to incidental exposure to nanopesticides, including copper (Cu)-based nano-formulations, is challenging not only because of the expected low concentrations (ppb levels) in the environment, but also because two forms of toxicity may occur, that are related to Cu ion exposure and the other exposure to Cu nanoparticles. We conducted laboratory experiments to test how a model estuarine organism, the amphipod *Leptocheirus plumulosus,* responded to Cu-based nanopesticides at concentrations similar to those found in estuarine water located downstream of agricultural fields in Santa Barbara county, CA, USA. Results showed that Cu body burden in amphipods increased approximately linearly with the nominal exposure concentration, and survivorship declined regardless of the Cu formulation, but only at relatively very high concentrations. Amphipods displayed minimal sublethal effects in terms of traditional ecotoxicological responses, specifically growth rates, movement, and respiration, when exposed to concentrations reflective of field conditions. However, results of Dynamic Energy Budget (DEB) modeling based on patterns of increased levels of respiration, and a related reduction in biomass, indicated potential for population-level effects of exposure to very low-levels of the two pesticides CuPRO and Kocide, as well as the control contaminant $CuCl_2$. Our results indicate that toxicity assessment of environmental trace concentrations of emerging pollutants, including Cu nanopesticides, may go undetected with traditional ecotoxicological tests. We present a process integrating

sublethal toxicity test and DEB modeling that can improve our capacity to detect and predict environmental impacts of very low levels of nanomaterials released into the environment.

1.2. Introduction

Pollution of estuarine ecosystems is a serious problem that is growing in scope as we introduce new chemicals into the environment. Estuaries are important as they provide many ecosystem services, including nutrient cycling, habitat for economically valuable species, and the maintenance of biodiversity [1–3]. Estuaries also sequester and harbor microorganisms that degrade anthropogenic contaminants [4,5]. Thus, the fate, transport, and ecological impacts of emerging pollutants, including nanomaterials, are key concerns in estuarine ecosystem science and management [6–8]. To date, many concepts about the ecological implications and impacts of nanomaterials and other emerging contaminants come from traditional ecotoxicological risk assessments that are hampered unavoidably by narrow subsets of relevant species, toxicants, exposure conditions, and levels of impact [9]. Problems arising from our reliance on traditional methods include the high uncertainty generated by relatively wide margins of error that typically accompany data from those studies [10].

Estuaries are major recipients of pesticide-laden run-off from agricultural fields and urban landscapes, and therefore represent model systems to assess the effects of incidental exposure to pesticides in downstream ecosystems [11,12]. Nano-based products are increasingly used for commercial applications, including an emerging suite of pesticides used in large-scale agriculture [13], which are generally referred to as nanopesticides [14,15]. One of the most common forms of nanopesticides are Cu-based chemicals, and include two popular brands, CuPRO 2005 (CuPRO) and Kocide 3000 (Kocide) [15]. All Cu-based pesticides function primarily by releasing toxic Cu ions. Conventional Cu-based pesticides, including $CuCl_2$ or $CuSO_4$, are very effective at controlling agricultural pests [16] but can also release relatively large amounts of dissolved Cu into natural water bodies that eventually harm non-target organisms [17]. To reduce environmental impacts, Cu-based nanopesticides are engineered (and

thus advertised) to be as effective as conventional products but less ecologically harmful because they release affective doses of Cu ions very slowly, thereby repelling pests but exposing non-target organisms to relatively very low levels of Cu. The degree to which the nanopesticides perform to reduce exposure and harm to downstream organisms is poorly understood.

The behavior and toxicity of Cu nanomaterials have been addressed in simple aqueous solutions [18–20], including in seawater [21–23]. Most environmental impact studies of Cu nanopesticides have focused on crop plants and soil organisms[24]. The few published studies of toxicity to aquatic organisms concern primarily zebrafish, a model freshwater organism [15]. That work indicates that Cu nanopesticides, specifically CuPRO and Kocide, are less toxic to the zebrafish embryo hatching process compared with a conventional $CuCl_2$-based pesticide. Not surprisingly, lower toxicity of the two nanopesticides was attributed to relatively low rates of Cu ion dissolution after particle introduction. Toxicity in the experiments was also detected at concentrations much higher than those measured thus far in natural waters [25,26]. Whether Cu nanopesticides are toxic to non-target estuarine organisms at environmentally relevant concentrations has not been adequately tested.

As the volume of nanopesticides production and potential for discharge into the aquatic environment increases, so does potential for wide-ranging ecological impacts[24]. Amphipods (small arthropod crustaceans) have been used as bioassay organisms to test the ecological impacts of pesticides in aquatic habitats because they live in water and sediment that accumulate contaminants; are highly sensitive and therefore vulnerable to many pesticides, including those that release Cu and other metal ions[10]; and are ecologically valuable in estuarine food webs, mainly as detritivores and/or prey for fish and other predators [17,22,27,28].

Acute and chronic toxicity tests are also widely used for amphipods (and other estuarine and marine species), and therefore are included in a wide range of ecological risk assessments [29].

Detecting nanopesticide constituents and other nanomaterials in agricultural, urban, and natural ecosystems, and assessing their toxicity at environmentally relevant, usually extremely low concentrations has proven very difficult [6]. However, recent advancements have been made through the use of mechanistic biological models based on Dynamic Energy Budget (DEB) theory [30] to link tissue and organ injuries, or the alteration of physiological processes and behavior, to changes in growth, maintenance, and reproduction in individual organisms[31,32]. In turn, estimates of the toxic effects to an individual provide the basis for generating model estimates of effects in populations and communities [6,10]. In dynamic process-based models, underlying mechanisms of the toxic response are assumed, allowing extrapolation beyond test conditions [9]. DEB theory describes the principle of an organism's energy balance, with differential equations describing how the energy that is taken up from substrates is assimilated and used for critical processes for the population maintenance costs[31,33]. The process-oriented structure of this approach makes toxicity assessment statistics independent of exposure time and of choice of sublethal endpoints or experimental conditions. As such, the multitude of impacts of a chemical can be delineated simultaneously, delivering common ecotoxicological parameters to all affected endpoints [10,34].

Here, we report the results of a study designed to test whether environmentally relevant concentrations (µg - mg L^{-1} in seawater) of Cu-based nanopesticides are toxic to a non-target estuarine amphipod *Leptocheirus plumulosus*, a species used frequently in ecotoxicity research and management[35]. We compare the relatively toxicity of the two most commonly used Cu-nanopesticides, CuPRO and Kocide, with $CuCl_2$, the major constituent of conventional Cu-based pesticides. Our strategy involved laboratory experiments to measure

the dose-dependent responses in mortality, growth, behavior (i.e., movement), and respiration, followed by the use of the experimental data in DEB models that provide predictions about the population level effects of exposure to sublethal concentrations of the Cu pesticides. Our results indicate that mechanistic DEB models provide a powerful tool for detecting and assessing the ecological implications of nanomaterials at environmentally relevant concentrations.

1.3. Methods

The copper compounds used in this study were characterized by the central materials library maintained by University of California's Center for Environmental Implications of nanotechnology (UC CEIN) [36]. A detailed summary of the chemicals can be found in the Supporting Information for this paper (Table S1). Reagent grade $CuCl_2$ salt was purchased from Sigma Aldrich (St. Louis, Mo), and the nanopesticides ($Cu(OH)_2$) Kocide 3000 from Dupont (Wilmington, DE), and CuPRO 2005 from SePRO (Carmel, IN). The nanopesticides physicochemical characterizations were analyzed for primary particle size distribution and morphology using a scanning electron microscopy (FEI XL40 Sirion) equipped with an Oxford INCA energy-dispersive X-ray spectroscopy (EDS) probe. The size and surface charge of particles at pH 7 (0.5 mM phosphate buffer) were determined by measuring hydrodynamic diameter (HDD) and zeta (ζ) potential using a Zetasizer Nano-ZS90 (Malvern, UK). Purity and copper content (wt %) of particles was assessed via inductively coupled plasma optical emission spectroscopy (ICP-OES, Thermo Scientific)[15,37,38].

Briefly, the main copper phase (XRD) of Kocide and CuPRO was orthorhombic $Cu(OH)_2$ with a primary particle size distribution of ~ 50-1000 nm for Kocide, and ~ 10 nm for CuPRO and a surface charge (mV) of particles at pH 7 (0.5 mM phosphate buffer) of -40.9 ±

2.7 for Kocide and -47.8 ± 1.1 for CuPRO. The agglomerate hydrodynamic diameter (nm) was 1532 ± 580 for Kocide and 4779 ± 4767 for CuPRO. Copper content of particles was 26.5 (wt %) for Kocide (impurities included C, O, Na, Al, Si, S, and Cl) and 34.0 (wt %) for CuPRO (impurities included C, O, Na, Al, Si, P, and Ca). We report the physicochemical kinetics of aggregation, sedimentation, dissolution, speciation, and complex formation of the $Cu(OH)_2$ particles elsewhere [39]. The exposure concentrations of dissolved, nanoparticle, and bulk forms of Cu (mg L^{-1}) in the microcosms are provided in Table S2.

Amphipod culturing and testing

Brood stocks of estuarine amphipods *Leptocheirus plumulosus* (Family: Aoridae) were obtained from Aquatic Biosystems (Fort Collins, CO, USA). The cultures were maintained in polystyrene bins containing fine quartz and containing 3 L of aerated, filtered seawater (0.5 μm) adjusted to 20 ppt salinity with deionized water at 20.0 °C ± 0.5. Cool fluorescent lights (500 μmol m^{-2} s^{-1}) provided illumination with a 14:10 h Light : Dark photoperiod. Approximately 50 % of culture water was removed from culture bins two times per week and replaced with fresh 20 ppt seawater. The amphipods were fed with a suspension of finely ground fish flakes (TetraMin® Blacksburg, VA, USA) after each water change. To avoid metal contamination, all materials were washed in a 10 % HNO_3 acid bath and rinsed thoroughly with deionized water followed by ultrapure water rinse prior to use.

Cu compound preparation and dispersion

Cu-based nanopesticide dispersions were prepared 45 min prior to the start of the experiment. A stock suspension of 10 mg Cu L^{-1} was prepared by diluting each Cu compound in ultrapure water (Barnstead NANOpure Diamond™, 18.2 MV/cm) adjusted to

salinity 20 ppt with filtered natural seawater (0.45 µm). To disperse Cu particles, the suspensions were sonicated for 30 min (Branson model 2510 sonic bath; Danbury, CT). The stock solutions were then diluted with additional seawater to the desired final nominal Cu concentrations of 0.1, 0.25, 1.0, and 2.5 mg L^{-1}. The final exposure concentrations tested were selected based upon a series of pilot experiments that tested amphipod mortality over a range of 1-1000 µg L^{-1} in seawater, concentrations of Cu nanopesticides expected to occur in the environment[24].

Water quality and Cu compound speciation

Water quality parameters were monitored daily to ensure amphipod viability. Digital meters were used to measure temperature, dissolved oxygen concentration, and pH, the salinity was measured using a refractometer, and the hardness, alkalinity, and ammonia concentrations were determined with water quality test strips (QUANTOFIX®). The three different Cu-based pesticides were introduced into microcosms simulating natural conditions to gain insight into how these particles might behave and/or are transformed in estuarine seawater over time. Therefore, we sampled aliquots from mesocosms with nominal Cu concentrations of 0.25 and 2.5 mg L^{-1}, and seawater controls, after 1, 4, and 7 days of exposure. Immediately after collection, the water samples were analyzed for Cu concentrations (mg L^{-1}) in the test media during the experiments to determine physicochemical Cu speciation kinetics. The dissolved fraction (soluble Cu) was quantified after ultrafiltration in Amicon Ultra-4 3 kDa centrifugal filter tubes with maximum pore size ~2 nm (Millipore, Billerica, MA), and centrifuged for 30 min at 4000 × g. The nanoparticulate fraction (nano Cu) between 2 and 200 nm, was determined as the fraction of total Cu derived by filtering out particles larger than 200 nm (Target 0.2 µm PVDF syringe

filter, Fisher Scientific), after accounting for the dissolved fraction left in the filtrate. The final filtrates and the total copper bulk solution were placed in metal-free tubes (VWR International, 15 mL), acidified with 2.5 % trace metal grade nitric acid (HNO_3, Fisher Scientific, Pittsburgh, PA), and stored at 4°C until examined. Instrumental analyses measured dissolved, nanoparticulate, and the total Cu content via inductively coupled mass atomic emission spectroscopy (ICP-MS, Thermo ICAP 6300, Thermo Fisher Scientific) with a detection limit of 50 μg L^{-1}. All analyses were run in triplicate, with standards and blank solutions measured every 15 samples, for quality assurance. In addition, the bulk fraction of Cu (>200 nm) was accounted for via mass balance as follows: Total Cu – (dissolved Cu + nano Cu).

Cu exposure and body burden in amphipods

Toxicity of the materials was determined by performing 7-day experiments without sediment, modified from Hanna et al. [22] The toxicity endpoints were assessed through assays conducted in 1 L glass jars (height 20 cm, inner diameter 8 cm), and nylon screen bottoms (600 microns) within the test jars were added as an artificial substrate to allow amphipods to be retained. To reduce stress caused from handling, 20 organisms were carefully placed into the microcosms containing only pure seawater for a 48 h-acclimation period. After 48 h, toxicity tests were initiated by introducing fresh media containing the Cu compounds test solutions (0.1, 0.25, 1.0, and 2.5 mg Cu L^{-1}) or the seawater control, with a total final volume of 700 mL. Only mature amphipods (3-4 weeks old) were used.

All tests using control and treatment combinations (i.e., the Cu compounds x concentrations) were conducted in four replicate microcosms per treatment, each of which were randomly placed together in the same climate-controlled room used for culture

preparation. Amphipods were not fed during the experiments to isolate toxicant effects, as Cu is known to react rapidly with organic material and changes in estuarine ionic strength. All microcosms were covered with a petri dish to avoid evaporation and entry of the dust into the test solutions. Gentle aeration was provided to maintain adequate oxygen saturation (>80 %). Environmental parameters were recorded daily.

To examine potential tissue bioaccumulation of Cu in amphipods, body burden of Cu in whole organism tissues was determined at the end of the experiment by collecting surviving organisms. The organisms were washed in an ethylenediaminetetraacetic acid (EDTA) solution (0.01 M EDTA, 0.1 M KH_2PO_4/ K_2HPO_4 buffer pH 6.0, salinity adjusted to 20 ppt) to remove Cu bound to external surfaces and dried in oven at 60°C for 3 days. The dried organisms pooled from each replicate was then acidified with trace metal grade nitric acid (2.5 % HNO_3). Total Cu content of the surviving amphipods was analyzed by ICP-MS. Samples were analyzed in triplicate, and metal standard solutions and blanks were analyzed after every ten samples. Detection limits for metals ≥1 μg L^{-1}.

Toxicity endpoints

Microcosm exposures were carried out according to US EPA guidelines [26]. The number of dead organisms in each microcosm was counted and recorded daily. Decomposed and missing organisms (presumed cannibalized) were counted as dead. Corpses were removed, dried, and weighed daily. In addition to mortality, the number of individuals exhibiting any abnormal behavior or appearance was counted and recorded daily. At day 7, live and dead biomass (mg) and individual organism length (mm) were recorded.

To assess effects of the pesticides on behavior, motility was measured at the beginning and at the end of the experiment by placing organisms on 24 well/plates (maximum 5

organisms per well) and recording a series of image sequences (10 images/sec, 10 seconds in total) with a camera coupled on a stereomicroscope (Olympus SZX12). The images were analyzed by Fiji software, an image processing package [40], using MTrackJ plugin [41]. The motility length parameter was determined and is defined as the total length of the movement track from the start (first) point of the track to the final current point (inclusive).

Models

For the analysis of survival and biomass data, we used two dose metrics, the nominal concentration and the body burden of Cu. We used the general metric *M* in model derivations and specified the metric for each application. We assumed that there is potentially a level of the dose metric, M_{0*}, below which detrimental effects did not occur (with '*r*' and '†' substituting '∗' to represent respiration and survival, respectively), and defined the effective dose metric as

$$M_{E*} = \max\left(0, M - M_{0*}\right) \quad (1)$$

Biomass Dynamics

The amount of living biomass, W_L, declined due to respiration (at rate *R*) and mortality (at rate *D*) and increased due to cannibalism and/or feeding on corpses (at rate *C*). To retain simplicity, we assumed that the conversion efficiency of biomass recycling was 100 %. Dead biomass was removed daily (at rate *E*). We approximated this removal process by assuming it to be a continuous process that matched the difference between the rates of mortality and cannibalism, i.e. $C = D - E$. Accordingly, the dynamics of living biomass is given by the following balance equation

$$\frac{dW_L}{dt} = -R + E \tag{2}$$

We assumed that the respiration rate was proportional to the amount of living biomass,

$$R = \mu W_L \tag{3}$$

in which μ is the specific population respiration rate. We assumed that the respiration rate coefficient increased linearly with the dose metric defined in Equation 1,

$$\mu = \mu_0 \left(1 + \frac{M_{Er}}{M_{Kr}} \right) \tag{4}$$

in which μ_0 and M_{Kr} is the background respiration rate coefficient (i.e., specific population respiration rate in absence of toxic effects) and toxicant scaling parameter, respectively. EC_x values for respiration can be calculated from Equation 1 and 4 once M_K and M_0 have been estimated. For the EC_{50}, defined as the value of the dose metric at the respiration rate is twice that of the control, the result is

$$\mathrm{EC}_{50} = M_{Kr} + M_{0r} \tag{5}$$

In the Supporting Information, we show that the rate of manual dead biomass removal was satisfactorily described with the (phenomenological) exponential decay function

$$E = \gamma W_{rm} e^{-\gamma t} \tag{6}$$

in which W_{rm} and γ are parameters. Substitution of Equation 3 and 6 into 2 gives

$$\frac{dW_L}{dt} = -\mu W_L - \gamma W_{rm} e^{-\gamma t} \tag{7}$$

with μ specified in Equation 4. Equation 7 can be solved with standard methods to yield

$$W_L = W_{L0} e^{-\mu t} + \frac{\gamma W_{rm}}{\gamma - \mu}\left(e^{-\gamma t} - e^{-\mu t}\right) \quad (8)$$

in which W_{L0} is the initial amount of living biomass.

Survival Model

The fraction of individuals surviving until time *t*, *S(t)*, is often modeled with the survivor function

$$\frac{dS}{dt} = -S(t)h(t) \quad (9)$$

in which *h(t)* is the hazard rate ('instantaneous probability to die'). Following Jager et al. (2011) [9], we assumed that the hazard rate was proportional to an abstract damage variable representing the cumulative impacts of ageing and toxic effects on survival potential. We assumed that this damage quantity accumulated at a constant rate in absence of toxicants and, in addition to this background accumulation, that this damage quantity accumulated at a rate proportional to the dose metric given in Equation 1. We also assumed that initial damage was negligible. Then, provided the dose metric is invariant, the hazard rate increases linearly in time and

$$h = k_{\dagger}^{'}\left(1 + \frac{M_{E\dagger}}{M_{K\dagger}}\right)t \quad (10)$$

in which $k_{\dagger}^{'}$ is the killing rate. Substitution of Equation 10 into 9 and subsequent solving with all individuals alive at *t*=0 yields

$$S(t) = e^{-0.5k_{\dagger}^{'}\left(1+\frac{M_E}{M_K}\right)t^2} \quad (11)$$

which describes a Weibull distribution. We defined LC_x as the value of the dose metric at which survival is reduced *x* % relative to that in the control. From Equation 1 and 11,

$$LC_x = \frac{-2M_K}{k_\dagger' t^2} \ln\left(1 - 0.01x\right) + M_0 \quad (12)$$

Statistical analyses

Experiments

Separate two-way ANOVAs were used to test for differences in the mean total dissolved and nanoparticle Cu concentration (mg L^{-1}) in microcosms, Cu body burden in amphipods, and amphipod survival, length, biomass, and motility, all as a function of Cu pesticide type, nominal Cu concentration in the pesticides (mg L^{-1}), and their interaction. Prior to ANOVA, all data were square root transformed and tested for heteroscedasticity of variances using Levene's test. Transformed data passed subsequent Levene's tests for homogeneity of variances ($P > 0.05$). Differences between specific treatments were determined with Tukey's honestly significant difference (HSD) post hoc tests ($P < 0.05$). All statistical analyses and graphics were conducted in R (R Development Core Team) and Excel.

Models

Parameters of the biomass model were estimated with likelihood methods assuming additive normally distributed measurement error. Parameters of the survival model were estimated by maximizing the log likelihood function of the multinomial distribution [9]. Fit results were evaluated with 95 % confidence intervals, which were calculated from negative log likelihood profiles.

1.4. Results

Cu Speciation

Dissolved Cu was detected in all experimental microcosms, including in trace amounts in the seawater controls (Figure 1). Mean total dissolved Cu concentration was < 1 mg L^{-1} across for all treatments, and varied with pesticide type ($CuCl_2$, CuPRO, and Kocide) and nominal Cu concentrations (i.e., 0 mg L^{-1}, 0.25 mg L^{-1}, and 2.5 mg L^{-1}), as indicated by a significant two-way interaction in the ANOVA (2-way ANOVA; Pesticide x Concentration; $F_{2,14} = 48.5$; $P < 0.0001$; Table S3). The total amount of dissolved Cu increased rapidly with increasing nominal Cu concentration across all three Cu pesticides (Figure 1) but was much higher for the conventional Cu pesticide ($CuCl_2$) than the two nanopesticides at 0.25 mg L^{-1} and 2.5 mg L^{-1} nominal concentrations (Tukey's HSD test, $P < 0.05$). However, there was no difference in dissolved Cu between the Kocide and CuPRO treatments at 0.25 mg L^{-1} and 2.5 mg L^{-1} nominal concentrations (Tukey's HSD tests, $P > 0.05$).

Mean total nanoparticle Cu concentration also varied with pesticide type and nominal concentrations (2-way ANOVA; Pesticide x Concentration; $F_{2,14} = 18.97$; $P < 0.001$; Table S4) in the microcosms. Low parts-per-billion (0.02-0.20 μg L^{-1}) of nanoparticulate Cu were detected in all microcosms, except seawater controls (Figure 1). Again, the total amount of nanoparticle Cu increased significantly with increasing nominal Cu concentration across all three types of pesticides (Tukey's HSD, $P < 0.001$). Total nanoparticle Cu did not vary among nanopesticides at the 0.25 mg L^{-1} nominal concentration (Tukey's HSD, $P > 0.001$) but was significantly lower in the CuPRO than the $CuCl_2$ or Kocide treatments at the 2.5 mg L^{-1} nominal concentration (Tukey's HSD, $P < 0.001$).

Bulk forms of Cu, specifically particles >200 nm in size, were undetectable or in very low concentrations (< 25 μg L^{-1}) at the 0.25 mg L^{-1} nominal concentrations for the two

nanopesticides. By contrast, bulk Cu particles were the most predominant Cu species in the 2.5 mg L^{-1} treatments. No large Cu particles were detected in the controls and $CuCl_2$ treatments.

Cu body burden in amphipods

Copper was present at detectable levels in amphipods from all treatments, including seawater controls, after seven days of exposure (Figure 2). Body burden of Cu generally increased with nominal concentrations of Cu for all Cu formulations and were generally higher for the nanopesticides than the $CuCl_2$. Concentrations of Cu in amphipod tissues were 140 µg Cu g DW^{-1} in the 0 mg L^{-1} (i.e., control), and 220–266, 203–254, 256–345, and 331–447 µg Cu g DW^{-1} in the 0.1, 0.25, 1, and 2.5 mg L^{-1} treatments, respectively (Figure 2). There was a significant effect of both main factors 'Pesticide' (2-way ANOVA; Pesticide; $F_{3,39} = 15.00$; $P < 0.0001$; Table S5) and 'Concentration' (2-way ANOVA; Concentration; $F_{3,39} = 26.68$; $P < 0.0001$; Table S5), which indicates that the type of pesticides and their Cu concentrations are associated with significantly different Cu body burdens. Kocide and CuPRO were taken up by amphipods at a higher rate than for $CuCl_2$ (Tukey HSD; $P < 0.05$), a pattern driven mostly by differences observed at 1.0 and 2.5 mg L^{-1}.

Toxicity

Survivorship was relatively high in the controls but generally decreased with increasing nominal concentrations of all three Cu formulations (Figure 3). The result of ANOVA indicated that mortality was greater for all pesticides at the two highest nominal concentrations (2-way ANOVA; Concentration; $F_{3,39} = 20.79$; $P < 0.0001$; Table S6). There

was no significant difference in survivorship as a function of the type of pesticide or the interaction of pesticides and concentration ($P > 0.05$; Table S6).

The total mean length and biomass of amphipods did not vary as a function of the Cu formulation (2-way ANOVA; $P > 0.05$; Tables S7 and S8) but tended to be lower in all formulations at 1 and 2.5 mg L^{-1} concentrations than in the seawater control. However, the differences were not statistically significant (Tukey's HSD tests; $P > 0.05$). For the total mean motility, measured as the total length (mm) that the amphipods swam in 10 seconds, we observed high variance among replicates for all treatments. Such variance greatly influenced the over overall motility assessment, and no significant difference across the three pesticides and concentrations was detected (Tukey's HSD tests; $P > 0.05$; Table S9).

Dynamic Energy Model

There was a clear dose-response in sublethal and lethal impacts of each of the Cu-based pesticide formulations on *L. plumulosus*: the amount of biomass left after seven days decreased while mortality increased with exposure concentrations (Figure 4 and Figure 5). The biomass decline and survival data were analyzed with simple bioenergetic and survivorship models in order to obtain toxic effect statistics that are independent of exposure time and other specifics of experimental protocols. In addition, the analyses serve to determine differences in toxicity profiles between ionic and nano copper speciation. For the analysis of survival and biomass data, one can use several dose metrics, including nominal concentrations, scaled or unscaled body burdens, and measures of accumulated damage. To keep the presentation simple, the dose metric in the analyses is either the nominal Cu concentration (C) or the body burden of copper (c).

The model describing the decline of living biomass contains six parameters (Equations 4 and 8), of which the value of one, the initial amount of living biomass, is fixed at the mean amount of biomass of 20 individuals at the start of the experiment (Table 1). The two parameters quantifying the daily removal of corpses have been estimated by fitting the phenomenological function describing the removal process (Equation S1) to the means of the amounts of biomass removed at each treatment (Figure S1). Accordingly, there are 13 sets of estimated values of the parameters describing biomass removal, one for each of the four exposure levels of the three copper formulations, in addition to that of the control (Table 2). These values have been fixed in the estimation procedure of the background respiration rate and the toxic effect parameters.

The background respiration rate has been estimated by fitting the model describing the decline of living biomass during the experiment (Equations 4 and 8) to the control data (Table 1), which value has been used for the analysis of toxic effects of Cu exposure. With nominal concentration as the dose metric, the toxic effect parameters are the no-effect and tolerance concentration for respiration; with body burden as dose metric, the two effect parameters are the no-effect and tolerance body burden for respiration.

To estimate toxic effect parameters, the biomass decline model was fitted to data from each copper formulation exposure separately, as well as to all data combined. Strikingly, with both the nominal concentration and body burden as the dose metric, the model with parameter values estimated from all data combined predicted the observed decline in biomass with increasing exposure level about equally well, regardless of copper formulation (Figure 4). In fact, the sums of log likelihoods decreased only 0.03 - 0.68 when the values of the no-effect and tolerance metrics were fixed on their respective values estimated from all data combined, instead of estimating them from the data from each copper formulation separately

(Table S11). This indicates that there was no significant difference in sublethal toxic effects on *L. plumulosus* among copper formulations. The estimate for the no-effect concentration was slightly negative but did not differ significantly from 0 at the 95 % level (results not shown); therefore, we set this value at 0 in subsequent analyses. Although the no-effect body burden also did not differ significantly from 0 (Table 1), its estimated value was substantial and was used in predictions and calculations here, as copper is an essential nutrient.

Accordingly, the EC_{50} as calculated from Equation 5 and the parameter values listed in Table 1 is 1.27 mg Cu L^{-1} and 145.4 µg Cu g DW^{-1} for nominal concentrations and body burdens, respectively.

The approach and results of the analysis of the survival data with the model in Equation 10 largely paralleled those of the biomass decline data. The parameter quantifying background mortality, the killing acceleration, was estimated by fitting Equation 10 to the survival data in the control (Table 1). This value was used to estimate the two toxic effect parameters for each of the dose metrics, the no-effect and tolerance concentration or body burden for survival, by fitting the survival model to data from each copper formulation separately and to all data combined. The sum of log likelihoods of the fits to the separate data sets with the no-effect and tolerance levels as free parameters decreased relatively little (0.01 - 0.48; Table S12) when the toxic effect parameters were fixed at their respective values estimated from all data combined. This shows that lethal toxicity of copper in *L. plumulosus* did not differ among copper formulations. The no-effect levels for survival for both nominal concentration and body burden did not significantly differ from 0 at the 95 % level. The estimate for the former is marginally negative, while the latter is substantial. Following the same reasoning as for the no-effect levels for respiration, we set the no-effect nominal concentration at 0 and used the estimated no-effect body burden in subsequent analyses and

presentations. The model predictions of survival at each of the copper formulations with nominal concentrations as the dose metric are shown in Figure 5; predictions with body burdens as the dose metric are comparable (results not shown).

The parameter estimates reveal differences between the sensitivities in lethal and sublethal impacts. The estimated value for the no-effect body burden for survival is substantially higher than that for respiration, which is plausible given that sublethal effects should precede an increase in mortality. The tolerance levels for both metrics indicate that lethal impacts increased more rapidly with increasing exposure levels than sublethal effects once the corresponding no-effect levels had been exceeded. In other words, the range of exposure levels at which the full spectrum of lethal impacts was observed was narrower than that of sublethal effects. EC_{50} and LC_{50} values cannot be easily compared, as the latter, but not the former, depends on exposure time (Equations 5 and 12). The exposure time at which the predicted LC_{50} equals the predicted EC_{50} can be solved from Equation 12. With the parameter estimates in Table 1, this exposure time was 6.2 days with the nominal concentration and 6.9 days with the body burden as the dose metric; $LC_{50} > EC_{50}$ for shorter exposure times, while $LC_{50} < EC_{50}$ for longer exposure times, implying that lethal impacts appeared somewhat more pronounced than sublethal impacts in the experiments analyzed in this study.

1.5. Discussion

Our objective in this study was to assess whether aquatic ecosystems exposed to agriculture runoff containing nano-Cu pesticides (e.g., CuPRO and Kocide) are at greater or

lower ecological risk than runoff containing conventional Cu pesticides (e.g., $CuCl_2$). Ecological risk posed in this study was compared as a function of the response of estuarine amphipods exposed to concentrations of the pesticides across a range from very low concentrations, those mimicking what might be expected in estuaries downstream of agriculture[24], to very high concentrations, especially those that are known to cause toxic responses. To better understand the response of amphipods we examined and compared the availability of Cu in different forms produced by each pesticide, Cu body burden in amphipods, and both conventional toxicity responses and more cryptic responses revealed by Dynamic Energy Budget modeling. Overall, we found little indication of elevated ecological risk for downstream aquatic organisms posed by the use of nano-Cu pesticides. Less Cu was released by Cu nanopesticides compared with ionic $CuCl_2$, and despite slightly higher Cu body burdens in amphipods exposed to the nanomaterials, there was little differences in related toxicity.

Dissolution of Cu in aqueous media increases with ionic strength (IS) and the presence and type of natural organic matter (NOM) [42,43]. In their study of nano-Cu's physiochemical behavior in natural waters, Adeleye et al. (2014) [42] reported that the dissolution of Cu nanopesticides increased with IS due to formation of soluble Cl^- complexes, more so in the presence of NOM. Relatively slow dissolution of Cu from the two nanopesticides in our experiment probably resulted from the estuarine salinity (20 ppt) and the release of NOM from the amphipods only, as there was no other source of NOM in the experiment.

Dissolved Cu had an overall higher concentration than nanoparticle Cu concentration, and generally increased with increasing nominal Cu concentration. Amphipod microcosms exposed to Kocide nanopesticide at highest nominal concentration, however, had similar concentrations of dissolved and nanoparticle Cu (Figure 1). This outcome probably emerged

because Kocide particles broke up in aqueous media or $CuCl_2$ precipitates were formed [42]. The large surface area and pore size distribution of Cu nanopesticides (15.71 ± 0.16 m^2 g^{-1}) may have enhanced nanoparticle Cu concentration due to surface roughness and porosity, especially in Kocide treatments [42]. Differences that we observed in Cu speciation between Kocide and CuPRO nanopesticides are probably related to their different surface charges and content of stabilizer in each compound [39].

Enhanced mean total Cu body burden in amphipods was slightly higher in Kocide and CuPRO relative to conventional Cu pesticide. Amphipods are a non-selective filter and deposit feeders so are likely to ingest (agglomerates of) metal and metal oxide nanoparticles and ions bound to dissolved and particulate organic matter with relative ease [42], and/or dissolved forms are taken up by amphipods via passage across permeable membranes [44]. Amphipods can also eliminate Cu during molting. These observations, coupled with Cu speciation results in our experiment, indicate that there is no strong evidence to suggest differences among ionic and nano-Cu pesticides in amphipod's Cu body burdens.

$CuCl_2$, Kocide, and CuPRO in microcosms with 1.0 mg L^{-1} impacted the non-target aquatic organisms in a manner very similar to that with 2.5 mg L^{-1} (Figure 3). Thus, separate and combined effects of nominal concentrations and Cu body burdens on the toxicity to downstream aquatic organisms appear robust to moderate levels of Cu concentrations that are highly expected in aquatic systems due to probable increases in Cu nanopesticides application in upstream agricultural areas[24]. By contrast, we never observed sublethal responses in the form of growth (i.e., change in length or biomass) or movement in any bioassay (Tables S7, S8, and S9).

The overall patterns from our experimental results indicated that at very low concentrations of Cu-based pesticides, we observed little indication of toxicity in amphipods

using conventional toxicity tests. Therefore, at very low environmental concentrations, we do not expect differences in toxicity to downstream estuarine organism between the pesticide types. It should be noted, however, that the relatively rapid release of Cu ions from $CuCl_2$ based pesticides may enhance the negative impacts of conventional pesticides soon after their application. By contrast, longer dissolution times for nano-Cu pesticides may extend their negative impacts to non-target organisms.

Results of our toxico-dynamical modeling provided important insights for developing new approaches to the ecological risk assessment for trace concentrations of Cu and other toxic materials. Sublethal effects were also quantified in our study as the impact of ionic copper ($CuCl_2$) and nano-copper (Kocide and CuPRO) on population level respiration, which was indirectly assessed through changes in amphipod biomass. The results give rise to the following conclusions. First, in all cases, we observed a normal dose-response, meaning that mortality and respiration increased with exposure level. Second, the toxicodynamic models describe the lethal and sublethal effects of copper exposure about equally well with either the nominal concentration or body burden (of copper) as dose metric (Figure 4 and Figure 5). This fitness to use either nominal or body burden as the dose metrics for the analysis of survival and biomass data was in agreement with the observation that body burdens increase approximately linearly with nominal concentrations (Figure 4) and indicates that body burdens equilibrated relatively rapidly. Third, the no-effect body burden for survival and respiration of copper was substantial, which is not surprising, since copper is an essential micronutrient. Fourth, and strikingly, the estimated model parameters quantifying lethal and sublethal effects do not differ significantly among treatments (

Table 1, S11, and S12). This shows that ionic and nano-copper have similar toxic effects on amphipods. We speculate that this was due to the fact that amphipods are detritus feeders

and thereby ionic as well as aggregates of copper compounds are bioavailable to them. This was corroborated by Figure 2, which suggest there was little difference among copper formulation with respect to bioaccumulation potential. Fifth, the estimated no-effect body burden for survival was lower than that for respiration, although the 95 % confidence intervals are relatively wide. This is to be expected, since sublethal effects usually are observed before survival is impacted. However, it should be noted that the impact of copper exposure on survival was mitigated by cannibalism, which occurred especially at the higher exposure levels. Survivors likely benefitted from their cannibalistic activity through an increase in life expectancy. This assumed benefit was concealed in the analysis of sublethal impact data, as calculated respiration rates were normalized to population biomass content. Cannibalism is a process that emerges at the population level, which signifies that the extrapolation from individual to population level impacts should be done with care [45].

Lethal impacts were quantified with the Stochastic Death (SD) variant of the General Unified Threshold Model of Survival (GUTS), which assumes that the instantaneous probability an individual dies at a certain moment is proportional to the amount of damage due to stress it has accumulated in its body [9,46]. The amount of damage is an abstract additive quantity that gauges the impairment of components of biochemical machinery due to ageing, starvation and toxicant exposure, among other potential stress factors. Thus, a benefit of the damage concept is that it integrates impacts of multiple stress factors (in this study: starvation and toxic effects due to copper exposure). It also provides a process-based description that translates the exposure level of a chemical, which may interact with the biochemical machinery via multiple unknown molecular initiating events, into an adverse outcome, in this case death [47]. Due to the paucity of available data, we neither considered the Individual Threshold variant of GUTS [48], nor included the possibility of damage repair [49] in our

analysis. This requires information from recovery experiments, but it is unlikely that such information would change our calculation of LC_x values [46].

A major strength of toxicodynamic models is that the toxic effect parameters that can be estimated from data, namely a no-effect level and a stress coefficient scaling the magnitude of toxic impact, do not depend on exposure time [48]. Summary statistics, such as the EC_x and LC_x, can then be calculated for any chosen exposure time (Equation 5 and 12) [48,50]. This means that the toxicity parameters estimated in this study can be used to predict the impacts of ionic and nano copper on the respiration and survival in amphipods at other exposure scenarios, including those with alternate exposure times and concentrations, as well feeding regimes.

As we have shown here with regards to the differences in toxicological effects observed in the laboratory and modeling, additional efforts should be made to the development of toxicity studies and toxicokinetic−toxicodynamic models to forecast the short- and long-term toxicity, contributing to environmental regulation for the use of the nanomaterials in benefits of the society [51]. For instance, nano-Cu pesticides may be enhanced in their capacity to reducing the particle size (greater number of particles per gram), thus helping to decrease adverse ecological effects by releasing less of the active ingredient (AI) in the environment [52]. However, future research on the ecological implications of Cu-based nanopesticides for long-term exposure periods should consider that Cu-based nanopesticides have a potential for runoff for several months or more after being applied to cultivated land[53], and their behavior will depend on ENM composition and environmental parameters[24].

1.6. References

1. Kennish, M. J. *Practical Handbook of Estuarine and Marine Pollution*. (CRC Press, 2017). doi:10.1201/9780203742488
2. Lenihan, H. S. *et al.* Cascading of habitat degradation: Oyster reefs invaded by refugee fishes escaping stress. *Ecological Aplications* **11**, 764–782 (2001).
3. Needles, L. A. *et al.* Managing Bay and Estuarine Ecosystems for Multiple Services. *Estuaries and Coasts* **38**, 35–48 (2015).
4. Boorman, L. A. Salt marshes – present functioning and future change. *Mangroves and Salt Marshes* **3**, 227–241 (1999).
5. Kehrig, H. A., Pinto, F. N., Moreira, I. & Malm, O. Heavy metals and methylmercury in a tropical coastal estuary and a mangrove in Brazil. *Organic Geochemistry* **34**, 661–669 (2003).
6. Holden, P. A. *et al.* Considerations of Environmentally Relevant Test Conditions for Improved Evaluation of Ecological Hazards of Engineered Nanomaterials. *Environmental Science and Technology* **50**, 6124–6145 (2016).
7. Holden, P. A. *et al.* Ecological nanotoxicology: integrating nanomaterial hazard considerations across the subcellular, population, community, and ecosystems levels. *Acc. Chem. Res.* **46**, 813–822 (2013).
8. Klaine, S. J. *et al.* Nanomaterials in the environment: Behavior, fate, bioavailability, and effects. *Environmental Toxicology and Chemistry* **27**, 1825–1851 (2008).
9. Jager, T., Albert, C., Preuss, T. G. & Ashauer, R. General unified threshold model of survival - A toxicokinetic-toxicodynamic framework for ecotoxicology. *Environmental Science and Technology* **45**, 2529–2540 (2011).

10. Muller, E. B., Lin, S. & Nisbet, R. M. Quantitative Adverse Outcome Pathway Analysis of Hatching in Zebrafish with CuO Nanoparticles. *Environmental Science and Technology* **49**, 11817–11824 (2015).
11. Bernardino, A. F. *et al.* Predicting ecological changes on benthic estuarine assemblages through decadal climate trends along Brazilian Marine Ecoregions. *Estuarine, Coastal and Shelf Science* **166**, 74–82 (2015).
12. Chapman, P. M. & Wang, F. Assessing sediment contamination in estuaries. *Environmental Toxicology and Chemistry* **20**, 3–22 (2001).
13. Kookana, R. S. *et al.* Nanopesticides: guiding principles for regulatory evaluation of environmental risks. *J. Agric. Food Chem.* **62**, 4227–4240 (2014).
14. Kah, M., Kookana, R. S., Gogos, A. & Bucheli, T. D. A critical evaluation of nanopesticides and nanofertilizers against their conventional analogues. *Nature Nanotechnology* **13**, 677 (2018).
15. Lin, S. *et al.* Understanding the transformation, speciation, and hazard potential of copper particles in a model septic tank system using zebrafish to monitor the effluent. *ACS Nano* **9**, 2038–2048 (2015).
16. de Oliveira-Filho, E. C., Lopes, R. M. & Paumgartten, F. J. R. Comparative study on the susceptibility of freshwater species to copper-based pesticides. *Chemosphere* **56**, 369–374 (2004).
17. Kiaune, L. & Singhasemanon, N. Pesticidal copper (I) oxide: environmental fate and aquatic toxicity. *Rev Environ Contam Toxicol* **213**, 1–26 (2011).
18. Keller, A. A. *et al.* Stability and aggregation of metal oxide nanoparticles in natural aqueous matrices. *Environmental Science and Technology* **44**, 1962–1967 (2010).

19. Schirmer, K., Behra, R., Sigg, L. & Sutter, M. J.-F. Ecotoxicological Aspects of Nanomaterials in the Aquatic Environment. *Safety aspects of Engineered Nanomaterials* **0**, 141–162 (2013).

20. Adeleye, A. S., Oranu, E. A., Tao, M. & Keller, A. A. Release and detection of nanosized copper from a commercial antifouling paint. *Water Research* (2016). doi:10.1016/j.watres.2016.06.056

21. Bielmyer-Fraser, G. K., Jarvis, T. A., Lenihan, H. S. & Miller, R. J. Cellular Partitioning of Nanoparticulate versus Dissolved Metals in Marine Phytoplankton. *Environ. Sci. Technol.* **48**, 13443–13450 (2014).

22. Hanna, S. K., Miller, R. J., Zhou, D., Keller, A. A. & Lenihan, H. S. Accumulation and toxicity of metal oxide nanoparticles in a soft-sediment estuarine amphipod. *Aquatic Toxicology* **142**–**143**, 441–446 (2013).

23. Torres-Duarte, C. *et al.* Developmental effects of two different copper oxide nanomaterials in sea urchin (Lytechinus pictus) embryos. **10**, 671–679 (2016).

24. Keller, A. A. *et al.* Comparative environmental fate and toxicity of copper nanomaterials. *NanoImpact* **7**, 28–40 (2017).

25. Nason Jeffrey A., Bloomquist Don J. & Sprick Matthew S. Factors Influencing Dissolved Copper Concentrations in Oregon Highway Storm Water Runoff. *Journal of Environmental Engineering* **138**, 734–742 (2012).

26. US EPA. *Ecological Effects Test Guidelines. Gammarid amphipod acute toxicity test.* (2016).

27. Edding, M. & Tala, F. Copper Transfer and Influence on a Marine Food Chain. *Bulletin of Environmental Contamination and Toxicology* **57**, 617–624 (1996).

28. Schuler, L. J., Hoang, T. C. & Rand, G. M. Aquatic risk assessment of copper in freshwater and saltwater ecosystems of South Florida. *Ecotoxicology* **17**, 642–659 (2008).
29. Mcgee, B. L. *et al.* A FIELD TEST AND COMPARISON OF ACUTE AND CHRONIC SEDIMENT TOXICITY TESTS WITH THE ESTUARINE AMPHIPOD LEPTOCHEIRUS PLUMULOSUS IN CHESAPEAKE BAY, USA. *Environmental Toxicology and Chemistry* **23**, 1751–1761 (2004).
30. Baas, J., Jager, T. & Kooijman, B. A review of DEB theory in assessing toxic effects of mixtures. *Science of the Total Environment* **408**, 3740–3745 (2010).
31. Nisbet, R. M., Mccauley, E. & Johnson, L. R. Dynamic energy budget theory and population ecology: lessons from Daphnia. doi:10.1098/rstb.2010.0167
32. Muller, E. B., Nisbet, R. M. & Berkley, H. A. Sublethal toxicant effects with dynamic energy budget theory: model formulation. *Ecotoxicology* **19**, 48 (2009).
33. Kooijman, S. A. L. M. Metabolic acceleration in animal ontogeny: An evolutionary perspective. *Journal of Sea Research* **94**, 128–137 (2014).
34. Lecomte-Pradines, C. *et al.* A dynamic energy-based model to analyze sublethal effects of chronic gamma irradiation in the nematode *Caenorhabditis elegans*. *Journal of Toxicology and Environmental Health, Part A* **80**, 830–844 (2017).
35. Series on Testing and Assessment: Ecotoxicity Testing - OECD. Available at: http://www.oecd.org/chemicalsafety/testing/seriesontestingandassessmentecotoxicitytesting.htm. (Accessed: 3rd February 2019)
36. Godwin, H. A. *et al.* The University of California Center for the Environmental Implications of Nanotechnology. *Environ. Sci. Technol.* **43**, 6453–6457 (2009).

37. Adeleye, A. S., Conway, J. R., Perez, T., Rutten, P. & Keller, A. A. Influence of Extracellular Polymeric Substances on the Long-Term Fate, Dissolution, and Speciation of Copper-Based Nanoparticles. *Environ. Sci. Technol.* **48**, 12561–12568 (2014).

38. Hong, J. *et al.* Toxic effects of copper-based nanoparticles or compounds to lettuce (Lactuca sativa) and alfalfa (Medicago sativa). *Environ Sci Process Impacts* **17**, 177–185 (2015).

39. Conway, J. R., Adeleye, A. S., Gardea-Torresdey, J. & Keller, A. A. Aggregation, dissolution, and transformation of copper nanoparticles in natural waters. *Environmental Science and Technology* (2015). doi:10.1021/es504918q

40. Schindelin, J. *et al.* Fiji: An open-source platform for biological-image analysis. *Nature Methods* **9**, 676–682 (2012).

41. Meijering, E., Dzyubachyk, O. & Smal, I. Methods for cell and particle tracking. *Methods Enzymol* **504**, 183–200 (2012).

42. Adeleye, A. S., Conway, J. R., Perez, T., Rutten, P. & Keller, A. A. Influence of extracellular polymeric substances on the long-term fate, dissolution, and speciation of copper-based nanoparticles. *Environmental Science and Technology* (2014). doi:10.1021/es5033426

43. Garner, K. L. & Keller, A. A. Emerging patterns for engineered nanomaterials in the environment: a review of fate and toxicity studies. *Journal of Nanoparticle Research* **16**, (2014).

44. Rainbow, P. S. Trace metal bioaccumulation: Models, metabolic availability and toxicity. *Environment International* **33**, 576–582 (2007).

45. Gergs, A., Preuss, T. G. & Palmqvist, A. Double Trouble at High Density: Cross-Level Test of Resource-Related Adaptive Plasticity and Crowding-Related Fitness. *PLOS ONE* **9**, e91503 (2014).

46. Ashauer, R., O'Connor, I., Hintermeister, A. & Escher, B. I. Death Dilemma and Organism Recovery in Ecotoxicology. *Environ. Sci. Technol.* **49**, 10136–10146 (2015).

47. Murphy, C. A. *et al.* Linking adverse outcome pathways to dynamic energy budgets: A conceptual model. *A Systems Biology Approach to Advancing Adverse Outcome Pathways for Risk Assessment* 281–302 (2018). doi:10.1007/978-3-319-66084-4_14

48. Jager, T., Heugens, E. H. W. & Kooijman, S. A. L. M. Making sense of ecotoxicological test results: towards application of process-based models. *Ecotoxicology* **15**, 305–314 (2006).

49. Klanjscek, T., Muller, E. B. & Nisbet, R. M. Feedbacks and tipping points in organismal response to oxidative stress. *J. Theor. Biol.* **404**, 361–374 (2016).

50. Miller, R. J. *et al.* Photosynthetic efficiency predicts toxic effects of metal nanomaterials in phytoplankton. *Aquatic Toxicology* **183**, 85–93 (2017).

51. Grillo, R., de Jesus, M. B. & Fraceto, L. F. Editorial: Environmental Impact of Nanotechnology: Analyzing the Present for Building the Future. *Front. Environ. Sci.* **6**, (2018).

52. Kah, M., Beulke, S., Tiede, K. & Hofmann, T. Nanopesticides: State of Knowledge, Environmental Fate, and Exposure Modeling. *Critical Reviews in Environmental Science and Technology* **43**, 1823–1867 (2013).

53. Kocide 3000-O - Biochemicals - Certis USA. Available at: http://certisusa.com/pest_management_products/biochemicals/kocide3000-O.htm. (Accessed: 3rd February 2019)

Table 1. Symbols and parameter estimates from biomass and survival data sets.

	Interpretation	Value [95 % CI] or (SE)[1]	Units
	Body burden of Cu	Variable	µg Cu g DW^{-1}
	Tolerance body burden for effect on respiration	145.4 [75.7 475.3]	µg Cu g DW^{-1}
	Tolerance body burden for effect on survival	45.4 [18.0 184.8]	µg Cu g DW^{-1}
	No-effect body burden on respiration	148.6 [-117.1 218.6]	µg Cu g DW^{-1}
	No-effect body burden for survival	188.0 [-37.0 251.8]	µg Cu g DW^{-1}
	Nominal concentration of Cu	Variable	mg L^{-1}
	Tolerance concentration for effect on respiration	1.27 (0.30)	mg L^{-1}
	Tolerance concentration for effect on survival	0.44 (0.13)	mg L^{-1}
	No-effect concentration on respiration	0	mg L^{-1}
	No-effect concentration for survival	0	mg L^{-1}
	Biomass removal rate (corpses)	Variable	mg day^{-1}
	Hazard rate	Variable	day^{-1}
	Killing acceleration	12.5 (12.1) x 10^{-3}	day^{-2}
	Dose metric, either or	Variable	-
	Dose metric parameter, either or	Variable	-
	Respiration rate	Variable	mg day^{-1}
	Survival probability	Variable	-
	Time	Variable	day
	Amount of living biomass	Variable	mg
	Initial amount of living biomass	11.73	mg
	Dead biomass removal parameter	See Table S10[2]	mg
	Dead biomass removal parameter	See Table S10 [2]	day^{-1}
	Specific population respiration rate	Variable	day^{-1}
	Background population respiration rate	28.4 (14.9) x 10^{-3}	day^{-1}

[1] 95 % confidence interval if two values in square brackets are given; standard errors for single values are in parentheses.
[2] Parameter values varied among treatments.

Table 2. Parameters estimated from biomass removal data with Equation S1.

	$CuCl_2$		CuPRO		Kocide	
Nominal [Cu]	γ	W_{rm}	γ	W_{rm}	γ	W_{rm}
mg L^{-1}	day^{-1}	mg	day^{-1}	mg	day^{-1}	mg
0	0.24	0.23	0.24	0.23	0.24	0.23
0.1	0.08	1.13	0.14	2.64	0.07	3.68
0.25	0.38	1.57	0.02	12.77	0.03	8.65
1	0.49	3.43	0.09	6.10	0.03	11.21
2.5	0.69	3.77	0.31	3.26	0.08	7.60

List of captions

Table 1. Symbols and parameter estimates from biomass and survival data sets. 52

Table 2. Parameters estimated from biomass removal data with Equation S1.....53

Figure 1. Mean (95 % C.I.) dissolved and nanoparticle Cu concentrations (mg L^{-1}) in amphipods' microcosms exposed to conventional Cu pesticide ($CuCl_2$), commercial Cu nanopesticides (Kocide and CuPRO), and seawater controls, as a function of nominal Cu concentrations 0, 0.25 and 2.5 mg L^{-1}. N = 3 replicate microcosms per treatment. Results of a Tukey's honestly significant difference (HSD) post hoc test are provided above each bar (between treatments: a < b < c, at $P < 0.05$; from controls: *, **, at $P<0.01$, and $P<0.001$, respectively). Italicized letters represent nanoparticle Cu concentrations. 56

Figure 2. Mean (95 % C.I.) total body burden of copper (µg Cu g DW $^{-1}$) in estuarine amphipods exposed to conventional Cu pesticide ($CuCl_2$), commercial Cu nanopesticides (Kocide and CuPRO), and seawater controls, as a function of nominal Cu concentrations 0, 0.25 and 2.5 mg L^{-1}. N = 4 replicate microcosms per treatment, each with 20 amphipods. Results of a Tukey's honestly significant difference (HSD) post hoc test are provided above each bar (between treatments: a < b < c, at $P < 0.05$; from controls: *, at $P < 0.01$). .57

Figure 3. Mean (95 % C.I.) cumulative survivorship (%) of amphipods exposed to conventional Cu pesticide ($CuCl_2$), commercial Cu nanopesticides (Kocide and CuPRO), and seawater controls, as a function of nominal Cu concentrations 0, 0.25 and 2.5 mg L^{-1}. N = 4 replicate microcosms per treatment, each with 20 amphipods. Results of a Tukey's honestly significant difference (HSD) post hoc test are provided above each bar (between treatments: a > b, at $P < 0.05$). 58

Figure 4. Predicted mean biomass versus mean measured biomass levels after seven days of exposure to $CuCl_2$ (open circles), CuPRO (squares) or Kocide (triangles) using (A) nominal

concentrations and (B) body burdens as dose metrics. Closed circle represents controls. Colors represent exposure (nominal) concentrations of 0.1 (mg L^{-1}), (black open symbols), 0.25 (mg L^{-1}), (blue), 1.0 (mg L^{-1}), (green) and 2.5 (mg L^{-1}), (red), respectively. Predictions are based on parameter values estimated from all data combined (Table 1) with Equations 4 and 8. 59

Figure 5. Model fits to survival data with C_{nec} = 0 and C_k estimated from all Cu species data with nominal Cu concentrations as dose metric; 0 (black), 0.1 (red), 0.25 (blue), 1 (purple) and 2.5 (green) mg L^{-1} nominal Cu concentrations. A: $CuCl_2$; B: CuPRO; C: Kocide. Symbols represent means (n=4); error bars are standard deviations. Points represent measured data, and curves are model predictions. 60

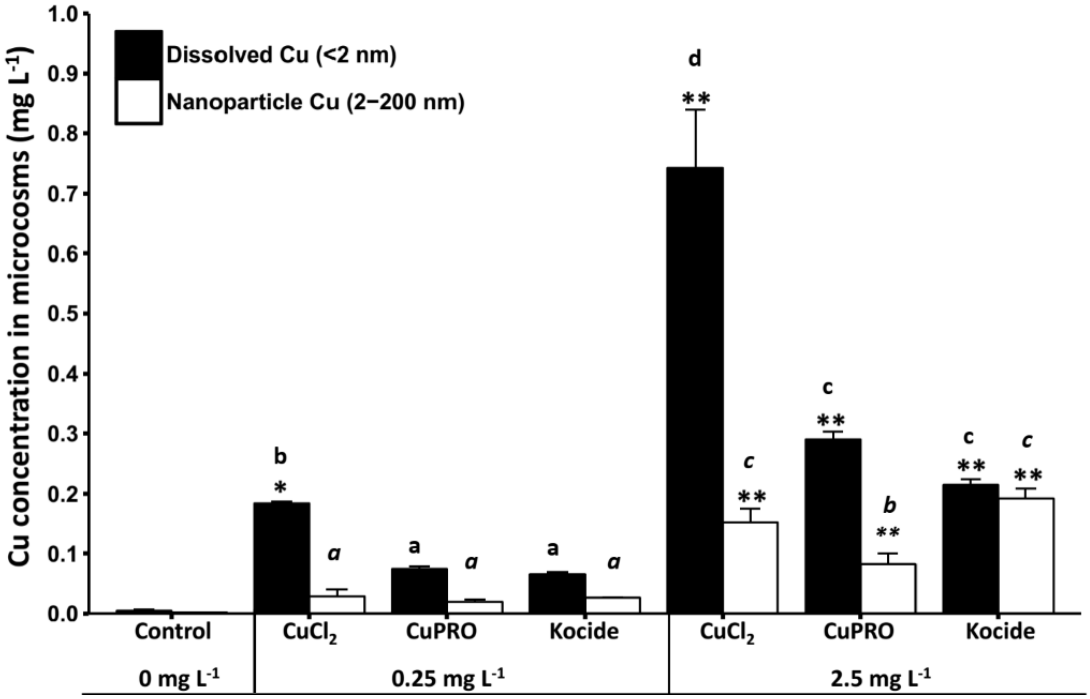
Cu concentration in microcosms (mg L-1)
1.0
0.9
0.8
0.7
0.6
0.5
0.4
0.3
0.2
0.1
0.0
Dissolved Cu (<2 nm)
Nanoparticle Cu (2−200 nm)
b
*
a
a
a
d
**
c
**
c
**
b
**
c
**
c
**
Control
CuCl2
CuPRO
Kocide
CuCl2
CuPRO
Kocide
0 mg L-1
0.25 mg L-1
2.5 mg L-1

Figure 1.

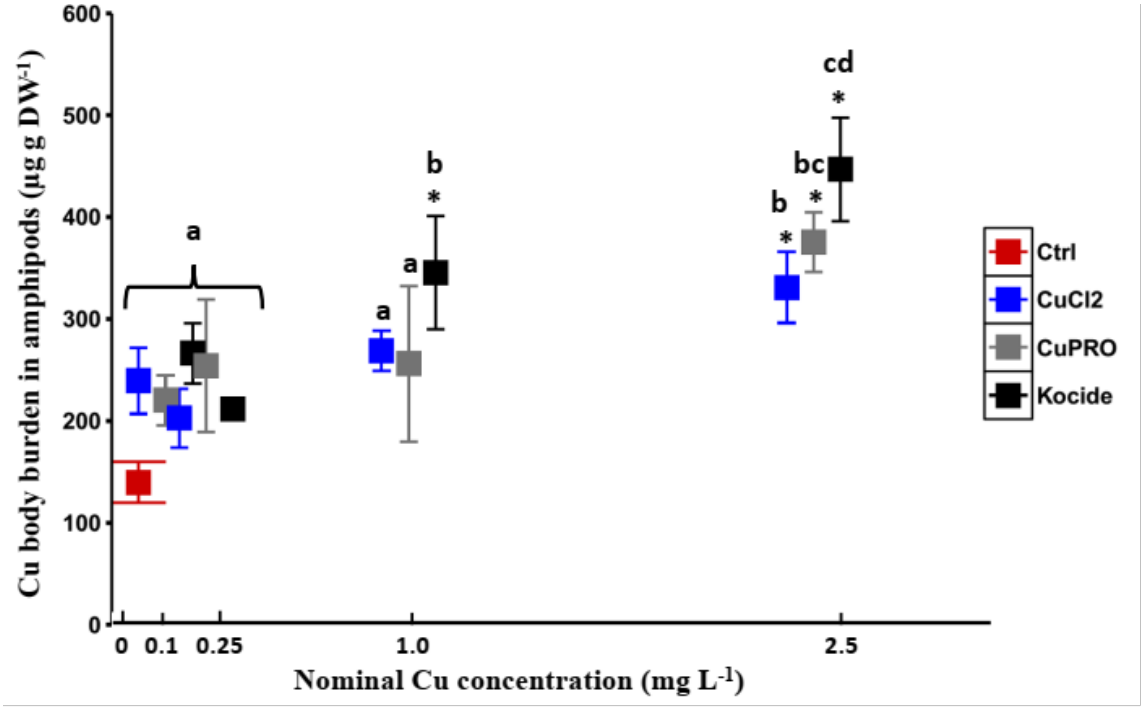
Cu body burden in amphipods (µg g DW-1)
600
500
400
300
200
100
0
0 0.1 0.25
1.0
2.5
Nominal Cu concentration (mg L-1)
a
a
b
*
b
*
b
*
bc
*
cd
*
Ctrl
CuCl2
CuPRO
Kocide

Figure 2.

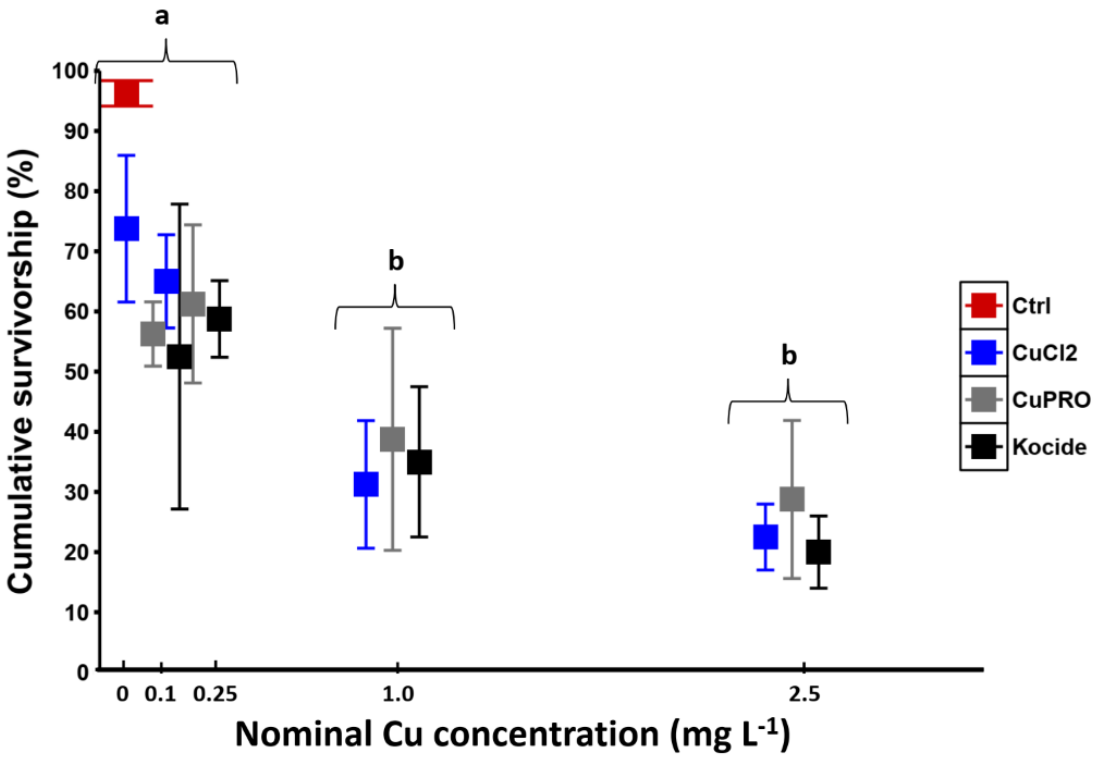
a
b
b
100
90
80
70
60
50
40
30
20
10
0
Cumulative survivorship (%)
0
0.1
0.25
1.0
2.5
Nominal Cu concentration (mg L-1)
Ctrl
CuCl2
CuPRO
Kocide

Figure 3.

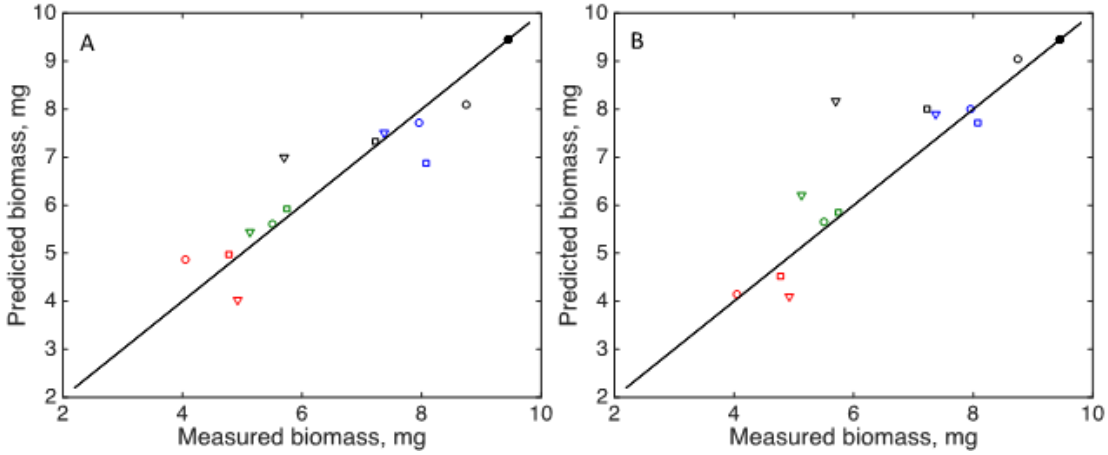

Figure 4.

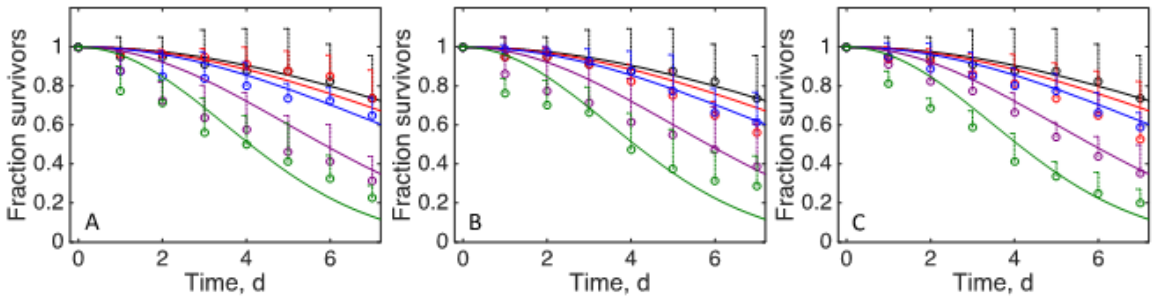

Figure 5.

1.7. Appendix. Supporting Information

Table S1. Summary characterization of the commercial Cu nanopesticides used in this study (adapted from Adeleye et al., 2014; Conway et al., 2015; Lin et al., 2015).

			Cu nanopesticides	
Physicochemical characterizations	**Technique**	**unit**	**Kocide**	**CuPRO**
Primary size	TEM	nm	~ 50-1000	~10
Phase and structure	XRD		orthorhombic $Cu(OH)_2$, impurities	orthorhombic $Cu(OH)_2$, impurities
Shape/morphology	TEM		irregular	irregular
Size in DI H_2O	HT-DLS	nm	1397 ± 143	889 ± 156
Zeta potential in DI H_2O	ZetaPALS	mV	-53.8 ± 0.7	-45.1 ± 0.8
Size in H buffer (w/alginate)	HT-DLS	nm	1172 ± 104	953 ± 88
Zeta potential in H buffer (w/alginate)	ZetaPALS	mV	-19.9 ± 0.8	-22.9 ± 0.6
Purity[a]	ICP-OES	wt %	39.9 ± 1.4	47.1 ± 2.6

[a] Purity refers to weight percentage of each main component (i.e., $Cu(OH)_2$ in Kocide and CuPRO).

Table S2. Concentrations of dissolved, nanosized, and bulk forms of Cu (mg L^{-1}) measured in the microcosms of *Leptocheirus plumulosus* of each sampling day (1, 4 and 7) for each Cu compound $CuCl_2$, CuPRO and Kocide (0.25 and 2.5 mg Cu L^{-1}), and seawater controls (0 mg L^{-1}).

	[Cu]	Day 1			Day 4			Day 7		
	(mg L^{-1})	Dissolved	Nano	Bulk	Dissolved	Nano	Bulk	Dissolved	Nano	Bulk
$CuCl_2$	0	0.006	0.000	0.000	0.001	0.001	0.000	0.002	0.001	0.000
	0.25	0.184	0.029	0.000	0.179	0.023	0.000	0.174	0.034	0.000
	2.5	0.743	0.152	0.236	0.830	0.043	0.002	0.748	0.100	0.000
CuPRO	0	0.006	0.000	0.000	0.001	0.001	0.000	0.002	0.001	0.000
	0.25	0.074	0.020	0.000	0.085	0.022	0.024	0.090	0.025	0.000
	2.5	0.290	0.082	0.008	0.373	0.086	0.275	0.376	0.096	0.190
Kocide	0	0.006	0.000	0.000	0.001	0.001	0.000	0.002	0.001	0.000
	0.25	0.066	0.027	0.000	0.077	0.030	0.000	0.083	0.041	0.000
	2.5	0.215	0.192	0.089	0.235	0.217	0.445	0.259	0.217	0.315

Table S3. Results of a two-way ANOVA for dissolved Cu concentration data (mg L^{-1}) detected in the amphipods microcosms after 24 hours. The treatments were three different Cu-based compounds: $CuCl_2$, representing conventional pesticides, and CuPRO and Kocide ($Cu(OH)_2$), as commercial nanopesticides, and natural seawater controls. The nominal concentrations were 0.25 and 2.5 mg Cu L^{-1}, and 0 mg Cu L^{-1}. All solutions were prepared with filtered (0.45µm) natural seawater diluted (nanopure water) to salinity 20, pH 7.9 (± 0.2), at a constant 20 (± 1.1) Celsius degree. More detailed physicochemical water parameters are found in the Material and methods section.

Source	*df*	SS	*MS*	*F-value*	P-value
Treatments (T)	3	0.54	0.18	114.03	$p < 0.0001$
Concentrations (C)	1	0.43	0.43	270.08	$p < 0.0001$
T x C	2	0.14	0.07	45.79	$p < 0.0001$
Residuals	14	0.02	0.00		
Total	20	1.14	0.68		
Model R-squared: 0.98					

Note — *df* = Degree of freedom, SS = Sum squares, MS = Mean squares.

Table S4. Results of a two-way ANOVA for nanoparticle Cu concentration data (mg L^{-1}) detected in the amphipods microcosms after 24 hours. The treatments were three different Cu-based compounds: $CuCl_2$, representing conventional pesticides, and CuPRO and Kocide ($Cu(OH)_2$), as commercial nanopesticides, and natural seawater controls. The nominal concentrations were 0.25 and 2.5 mg Cu L^{-1}, and 0 mg Cu L^{-1}. All solutions were prepared with filtered (0.45µm) natural seawater diluted (nanopure water) to salinity 20, pH 7.9 (± 0.2), at a constant 20 (± 1.1) Celsius degree. More detailed physicochemical water parameters are found in the Material and methods section.

Source	*df*	SS	*MS*	*F-value*	P-value
Treatments (T)	3	0.03	0.01	43.95	$p < 0.0001$
Concentrations (C)	1	0.06	0.06	294.70	$p < 0.0001$
T x C	2	0.01	0.00	18.97	$p < 0.001$
Residuals	14	0.00	0.00		
Total	20	0.10	0.08		
Model R-squared: 0.97					

Note — *df* = Degree of freedom, SS = Sum squares, MS = Mean squares.

Table S5. Results of a two-way ANOVA for total Cu uptake data (mg L^{-1}) measured in all remaining alive amphipods at the end of the exposure experimental period of 7 days. The treatments were three different Cu-based compounds: $CuCl_2$, representing conventional pesticides, and CuPRO and Kocide ($Cu(OH)_2$), as commercial nanopesticides, and natural seawater controls. The nominal concentrations were 0.1, 0.25, 1.0 and 2.5 mg Cu L^{-1}, and 0 mg Cu L^{-1}. All organisms were rinsed with EDTA 0.1M solution in order to account for internal Cu only. More detailed uptake procedures are found in the Material and methods section.

Source	*df*	SS	*MS*	*F-value*	P-value
Treatments (T)	3	105,56	35,19	15.00	$p < 0.0001$
Concentrations (C)	3	187,73	62,58	26.68	$p < 0.0001$
T x C	6	28,65	4,78	2.04	$p > 0.05$
Residuals	39	91,46	2,35		
Total	51	413,40	104,88		
Model R-squared: 0.78					

Note — *df* = Degree of freedom, SS = Sum squares, MS = Mean squares.

Table S6. Results of a two-way ANOVA for cumulative survival data (%) of the amphipods at the end of the exposure experimental period of 7 days. Survival was accounted every day. The treatments were three different Cu-based compounds: $CuCl_2$, representing conventional pesticides, and CuPRO and Kocide ($Cu(OH)_2$), as commercial nanopesticides, plus natural seawater controls. The nominal concentrations were 0.1, 0.25, 1.0 and 2.5 mg Cu L^{-1}, and 0 mg Cu L^{-1}.

Source	*df*	SS	*MS*	*F-value*	P-value
Treatments (T)	3	0.99	0.33	15.96	$p < 0.0001$
Concentrations (C)	3	1.30	0.43	20.79	$p < 0.0001$
T x C	6	0.10	0.02	0.82	$p > 0.05$
Residuals	39	0.81	0.02		
Total	51	3.20	0.80		
Model R-squared: 0.75					

Note — *df* = Degree of freedom, SS = Sum squares, MS = Mean squares.

Table S7: Mean (95 % C.I.) length (mm) of dead organisms and of surviving organisms in microcosms exposed to conventional Cu pesticide ($CuCl_2$), commercial Cu nanopesticides (kocide and cupro), and seawater controls, as a function of nominal Cu concentrations 0, 0.1, 0.25, 1, and 2.5 mg L^{-1} at the end of the experiment. N = 4 replicate microcosms per treatment.

Nominal Cu concentration (mg L^{-1})	**Dead organisms**			**Surviving organisms**		
	Length (mm)					
	$CuCl_2$	CuPRO	Kocide	$CuCl_2$	CuPRO	Kocide
0	6.06 ± 0.43	6.06 ± 0.43	6.06 ± 0.43	5.77 ± 0.92	5.77 ± 0.92	5.77 ± 0.92
0.1	5.73 ± 0.54	5.90 ± 0.26	5.65 ± 0.72	5.66 ± 0.74	5.76 ± 0.67	5.57 ± 0.77
0.25	5.43 ± 0.34	5.90 ± 0.76	5.90 ± 0.68	5.30 ± 0.85	5.80 ± 0.1	5.50 ± 0.85
1	5.35 ± 0.52	5.60 ± 0.60	5.88 ± 0.64	5.62 ± 0.1	5.72 ± 0.92	5.66 ± 0.87
2.5	4.92 ± 0.79	5.63 ± 0.88	5.87 ± 0.68	5.53 ± 0.67	5.69 ± 0.78	5.64 ± 0.87

Initial length (at day 0): 5.15 ± 0.90 mm.

Table S8: Mean (95 % C.I.) biomass (mg) of surviving organisms in microcosms exposed to conventional Cu pesticide ($CuCl_2$), commercial Cu nanopesticides (Kocide and CuPRO), and seawater controls, as a function of nominal Cu concentrations 0, 0.1, 0.25, 1, and 2.5 mg L^{-1} at the end of the experiment. N = 4 replicate microcosms per treatment.

	Biomass (mg)		
Nominal Cu concentrations (mg L^{-1})	**$CuCl_2$**	**CuPRO**	**Kocide**
0	0.63 ± 0.13	0.63 ± 0.13	0.63 ± 0.13
0.1	0.54 ± 0.13	0.59 ± 0.12	0.50 ± 0.13
0.25	0.55 ± 0.05	0.57 ± 0.06	0.51 ± 0.04
1	0.50 ± 0.11	0.49 ± 0.15	0.50 ± 0.18
2.5	0.45 ± 0.19	0.47 ± 0.12	0.42 ± 0.19

Initial biomass (at day 0): 0.59 ± 0.10 mg.

Table S9: Mean (95 % C.I.) motility (mm) of amphipods in microcosms exposed to conventional Cu pesticide ($CuCl_2$), commercial Cu nanopesticides (Kocide and CuPRO), and seawater controls, as a function of nominal Cu concentrations 0, 0.1, 0.25, 1, and 2.5 mg L^{-1} at the end of the experiment. N = 4 replicate microcosms per treatment.

	Motility (mm)		
Nominal Cu concentrations (mg L^{-1})	**$CuCl_2$**	**CuPRO**	**Kocide**
0	20.03 ± 11.51	20.03 ± 11.51	20.03 ± 11.51
0.1	31.22 ± 15.52	21.78 ± 9.30	24.87 ± 12.69
0.25	32.42 ± 16.13	35.45 ± 14.45	21.70 ± 6.94
1	12.77 ± 5.62	22.27 ± 10.03	29.96 ± 15.01
2.5	23.62 ± 7.96	18.31 ± 1.45	17.36 ± 21.11

Initial motility (at day 0): 24.18 ± 10.10 mm.

Corpse Removal Dynamics

A phenomenological function was fitted to measurements of the cumulative amount of dead biomass that was daily manually removed from the containers, W_r. It was assumed that those discrete removal events could be approximated with a continuous process. The function is

$$W_r = W_{rm}\left(1 - e^{-\gamma t}\right) \quad \text{(S1)}$$

in which W_{rm} and γ are parameters. Figure S1 shows fits of Equation S1 to data of the cumulative amount of dead biomass removed from the experiments; Table S10 lists the parameter values with standard errors as estimated with nonlinear least squares. In three treatments the data showed an insufficient curvilinearity for parameter estimation; in those cases, some data were omitted or extra weighted in the fitting procedure, as indicated in the comment's column of Table S10.

Differentiation of Equation S1 with respect to time yields the time-dependent removal rate of dead biomass,

$$\frac{dW_r}{dt} = E = \gamma W_{rm} e^{-\gamma t} \quad \text{(S2)}$$

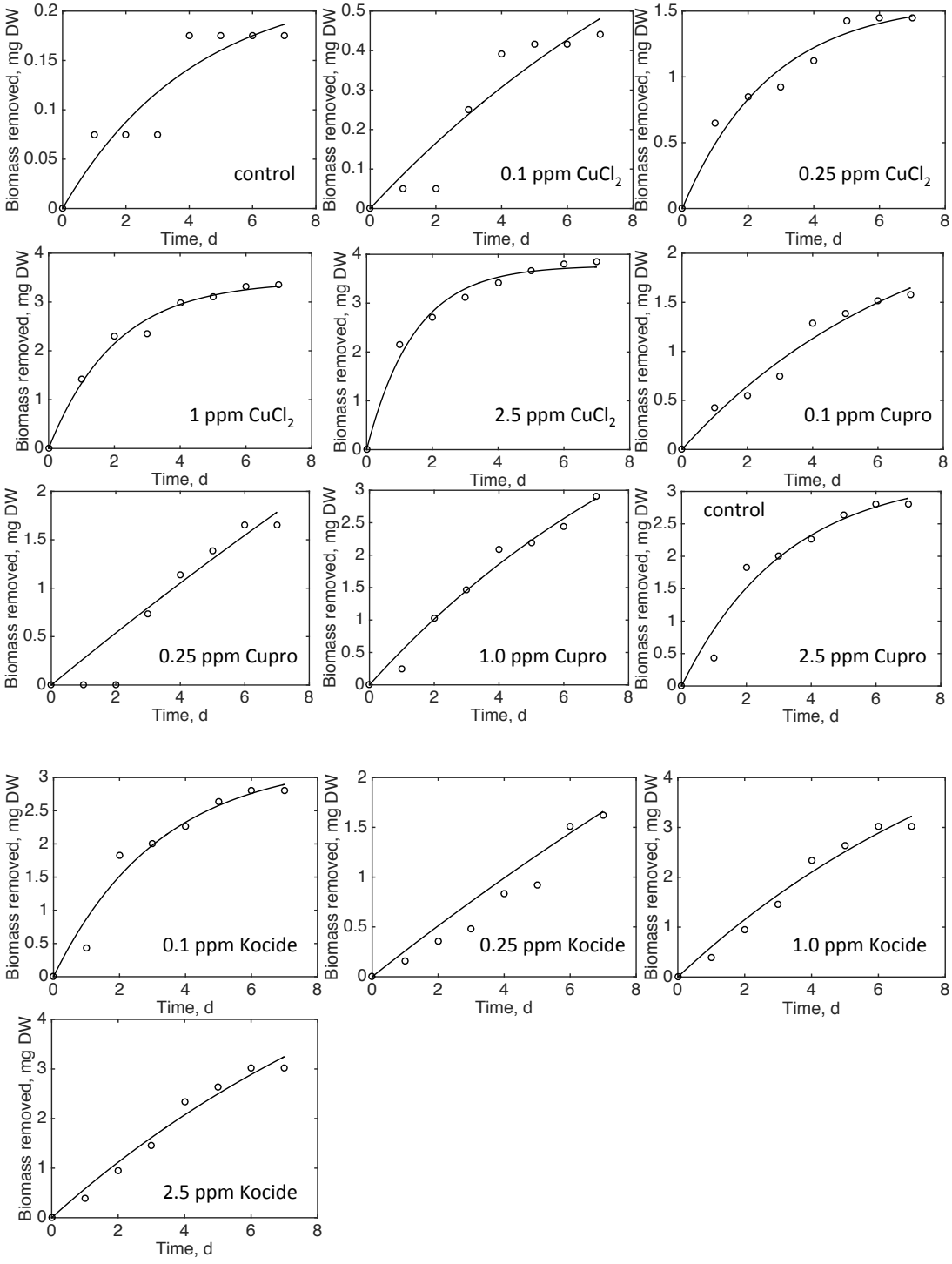

Figure S1. Fits of biomass removal model (curve, Equation S1) fitted to data of cumulative dead biomass removal (open circles). Parameter estimates are in Table S9.

Table S10. Dead biomass removal parameter estimation.

	[Cu] (mg L^{-1})	(day^{-1})		(mg)		Comments
		Estimate	SE	Estimate	SE	
Control	0	0.241	0.116	0.229	0.058	
$CuCl_2$	0.1	0.079	0.091	1.131	1.040	
$CuCl_2$	0.25	0.376	0.074	1.572	0.123	
$CuCl_2$	1	0.493	0.052	3.430	0.119	
$CuCl_2$	2.5	0.691	0.069	3.770	0.094	
CuPRO	0.1	0.140	0.050	2.638	0.642	
CuPRO	0.25	0.022	0.059	12.769	32.794	Data day 2 excluded
CuPRO	1	0.091	0.040	6.096	2.092	
CuPRO	2.5	0.311	0.069	3.265	0.331	
Kocide	0.1	0.071	0.078	3.678	3.291	
Kocide	0.25	0.030	0.051	8.650	12.998	Data day 6 and 7 weighted 8x
Kocide	1	0.035	0.045	11.205	13.161	Data day 1 excluded
Kocide	2.5	0.080	0.044	7.595	3.352	

Table S11. Log likelihood values of data fitted to biomass decline model.

	All data	$CuCl_2$	CuPRO	Kocide
Dose Metric: Nominal Concentration, $M = C$				
C_{0r} and C_{Kr} free	-158.88	-50.42	-51.85	-52.41
$C_{0r} = 0$, C_{Kr} free	-160.59	-50.44	-51.91	-54.44
$C_{0r} = 0$, $C_{Kr} = 1.27$	-160.59	-50.47	-51.93	-54.44
Dose Metric: Body Burden, $M = c$				
c_{0r} and c_{Kr} free	-158.20	-50.50	-52.22	-51.05
$c_{0r} = 148.6$, c_{Kr} free	-158.20	-51.16	-52.36	-51.34
$c_{0r} = 148.6$, $c_{Kr} = 145.4$	-158.20	-51.18	-52.36	-51.35

Table S12. Log likelihood values of data fitted to survival model.

	All data	$CuCl_2$	CuPRO	Kocide
Dose Metric: Nominal Concentration, $M = C$				
$C_{0\dagger}$ and $C_{K\dagger}$ free	-90.67	-32.48	-33.13	-33.92
$C_{0\dagger} = 0$, $C_{K\dagger}$ free	-90.83	-32.49	-33.22	-34.02
$C_{0\dagger} = 0$, $C_{K\dagger} = 0.44$	-90.83	-32.49	-33.25	-34.05
Dose Metric: Body Burden, $M = c$				
$c_{0\dagger}$ and $c_{K\dagger}$ free	-91.42	-32.65	-33.30	-33.88
$c_{0\dagger} = 188.0$, $c_{K\dagger}$ free	-91.42	-33.05	-33.30	-33.88
$c_{0\dagger} = 188.0$, $c_{K\dagger} = 45.4$	-91.42	-33.13	-33.30	-33.93

References

Adeleye, A. S., Conway, J. R., Perez, T., Rutten, P., & Keller, A. A. (2014). Influence of extracellular polymeric substances on the long-term fate, dissolution, and speciation of copper-based nanoparticles. *Environmental Science and Technology*. https://doi.org/10.1021/es5033426

Conway, J. R., Adeleye, A. S., Gardea-Torresdey, J., & Keller, A. A. (2015). Aggregation, dissolution, and transformation of copper nanoparticles in natural waters. *Environmental Science and Technology*, *49*(5), 2749–2756. https://doi.org/10.1021/es504918q

Lin, S., Taylor, A. A., Ji, Z., Chang, C. H., Kinsinger, N. M., Ueng, W., … Nel, A. E. (2015). Understanding the transformation, speciation, and hazard potential of copper particles in a model septic tank system using zebrafish to monitor the effluent. *ACS Nano*, *9*(2), 2038–2048. https://doi.org/10.1021/nn507216f

Chapter 2. Aging of copper nanoparticles in the marine environment regulates toxicity to phytoplankton

This work will be submitted for publication. Target journal: Environmental Science & Management.

Key words: Engineered nanomaterials; environmental conditions; aging; copper nanoparticles; marine phytoplankton; ecotoxicity.

2.1. Abstract

Environmental conditions in aquatic ecosystems, including water chemistry, hydrology, and disturbance, as well as biotic interactions, can transform or "age" toxic chemicals, making them more or less bioavailable and toxic. Chemical aging occurs through processes such as hydrolysis, precipitation, complexation, speciation, adsorption, redox, and dissolution. The extent of aging can vary considerably within a water body as a function of light, temperature, and other factors; or between water bodies, such as a river that flows through an estuary into the ocean, due to changes in salinity and organic matter content. We tested whether exposure to estuarine water for different time periods (0, 1, 2, 3, 4, and 15 weeks) aged copper nanoparticles (nano-Cu; single dose of 20 mg L^{-1}) and influenced their uptake and toxicity to marine phytoplankton, organisms critical to coastal marine and estuarine ecosystems. Changes in the morphology and average size of nano-Cu aged in stock solutions were initially rapid and drastic, characterized by intensive aggregation, followed by a decrease in particle size due to Cu dissolution. Dissolution was slowest at 15 weeks of aging when particles were highly oxidized and formed complex Cu structures. Cu particles aged from 0-15 weeks then introduced into algal cultures further dissolved, thus indicating that algal-derived organic matter and ionic strength play important roles in controlling Cu bioavailability. Dissolution of Cu in algal cultures increased threefold after 15-weeks of aging, by which time the re-aggregated nanoparticles developed highly intricate Cu crystalline-like structures formed by complexation with phytoplankton-derived organic matter. Toxicity to phytoplankton decreased significantly as a function of particle aging from 0 to 4 weeks but increased substantially at 15 weeks, a pattern driven ostensibly by Cu ion dissolution. Results indicate that the transformation, fate, and toxicity of nano-Cu in marine

ecosystems are influenced by ionic strength, but also chemical aging controlled, at least in part, by organic matter produced by micro-organisms.

2.2. Introduction

Human activities threaten global ecosystems, their functioning, and the services that they provide. Threats include contamination of aquatic ecosystems by anthropogenic chemicals, which can cause serious ecological problems, and that are expanding in their diversity as we accelerate the rate at which we produce new materials, many with poorly understood biological impacts[1–3]. This is especially true for nanomaterials that are produced for ever-expanding applications, ranging from medicines, foods, electronics, and fertilizers, as well as pesticides and myriad protective coatings[4,5]. Many of these materials, including nanoparticle-based marine paints, are designed specifically to release toxic compounds, such as copper (Cu) and zinc (Zn), into the environment to repel or kill micro-organisms.

The fate, transport, and toxicity of nanomaterials released into the environment are the subject of much research over the past decade[4,6,7], with a great deal of information having been produced on nanomaterial fate and transport[8–10], transformation as function of environmental conditions, and toxicity to a wide of area of organisms in terrestrial and aquatic ecosystems. For example, temperature, pH, ionic strength, salinity, alkalinity, natural organic matter concentrations, and hydrodynamics can trigger chemical process that modify the bioavailability, uptake, and toxicity of pollutants, including those nano-sized[4,5,11,12]. Two paradigms that emerge from recent research are that (1) the down-sizing of metal containing nanomaterials can enhance their toxicity due to faster dissolution rates, and (2) environmentally-induced aggregation and complexation of nano-metals can increase functional particle size thereby reducing metal ion dissolution and toxicity[8,9].

Aquatic ecotoxicological research has made much progress in assessing the impacts of nanoparticles (NPs) mainly through studies of their pristine form in freshwater solutions. In turn, most studies have focused on freshwater species[13–16] and relatively few on

marine/estuarine organisms[17,18]. Unique NPs properties and environmental conditions interact in different ways to impact aquatic ecosystems, but ecological risk assessment and the potential for an adverse outcome under environmentally realistic conditions has rarely been examined. Likewise, only a few studies have focused on prolonged exposure periods and on how fast aging occurs relative to toxicity assessment in marine and estuarine organisms[19–21].

A suite of metal/metal oxide (M/MO) ENMs (i.e., Cu [23,24], Ag[25,26], and Zn [27,28]) are toxic to aquatic organisms mainly because they release ions that have the capacity to cross biological cell membranes, stimulate production of Reactive Oxygen Species (ROS) leading to oxidative stress, and damage mitochondrial, DNA, protein, and membranes[29–31]. For example, silver nanoparticles (Ag NPs), when aged in crude wastewater samples (CWs) for up to eight weeks, declined in toxicity to the bacteria *Pseudomonas putida* with time because the concentration and exposure to free Ag ions declined. However, Ag NPs showed steady dissolution rates when aged in final effluent (FWs), thus causing toxicity regardless aging. Unfortunately, there are still crucial gaps in knowledge and published material related to the aging process[32,19,33] (see Supplemental Information). Aging is an important aspect of the nanoparticle life cycle analysis as it gives an understanding of how transformations of a nanoparticle are affected by time. Predominantly the focus on research to date has been on pristine materials. However, most ENMs react in ways that change their behavior and physicochemical properties over time. Therefore, aged NPs no longer have the same characteristics as their pristine counterparts[33].

Copper (Cu) is an essential element for aquatic organisms, but also a heavy metal used in engineered nanomaterials (ENMs) that is toxic to many organisms in relatively low concentrations of ionic Cu. Aging influences the rate of metal-ion dissolution, hence plays an

important role in controlling toxicity to aquatic organisms[22]. Here we explore how aging in the marine environment can alter copper nanoparticles (nano-Cu) and influence their bioavailability and toxicity to marine phytoplankton, organisms that critical to coastal areas and estuarine ecosystems.

2.3. Methods

ENMs and aging media

Nanosized copper (nano-Cu) was obtained from US Research Nanomaterials (Houston, TX). The primary particle size of the engineered nanomaterial (ENM) was determined using a FEI Titan 300 kV FEG transmission electron microscopy (TEM) equipped with an Oxford INCA x-sight probe for energy-dispersive X-ray spectroscopy (EDS) for elemental composition. The morphology of pristine nano-Cu was determined using FEI XL30 Sirion scanning electron microscopy (SEM) equipped with an EDAX APOLLO X probe for EDS. The average initial hydrodynamic diameter (HDD), particle size distribution, and zeta (ζ) potential of the ENM in deionized (DI) water (Barnstead Nanopure diamond) with 2 mM phosphate buffer (pH 8), and nanoparticle aging media were determined using a Malvern Zetasizer ZS90 (Malvern, UK)[34]. Additional characterizations for the ENM were reported previously[35]. Artificial seawater (pH 8.1) was made according to Kester and collaborators[36], and its composition is shown in Table S1.

Transformation of nano-Cu during aging

20 mg Cu L^{-1} of the ENM was aged in sterilized artificial seawater in conditions simulating the surface of natural marine waters (14:10 h Light : Dark photoperiod, 100 μmol m^{-2} s^{-1}, 20°C). To disperse the nanoparticles, the suspensions were sonicated in a water-bath

for 1 h (CPX8800H, Branson Ultrasonics, Danbury, CT). Aging was done in sterilized 1 L Erlenmeyer flasks for 0, 1, 2, 3, 4, and 15 weeks (one flask per aging time) after which they were exposed to the marine phytoplankton *Dunaliella tertiolecta*. Nanoparticles in stock solutions were analyzed for different Cu size fractions (dissolved, nano, and bulk) prior to and after exposing phytoplankton to understand how particles transformed as a function of the organic matrices produced by phytoplankton.

The dissolved fraction of Cu was determined by ultrafiltration with Millipore Amicon Ultra-4 3 kDa centrifugal filter tubes (maximum pore size ~2 nm). The nano fraction (loosely defined in this study as the fraction between 2 nm and 200 nm) was derived by filtering out particles larger than 200 nm (Target 0.2 µm PVDF syringe filter, Fisher Scientific) while accounting for the dissolved fraction left in the filtrate. The bulk fraction was determined via mass balance as follows: Total Cu – (dissolved Cu + nano-Cu).

The different fractions were digested with 7 % trace-metal grade nitric acid (Fisher Scientific) and analyzed via ICP-AES (iCAP 6300, Thermo Scientific). Further speciation and complexation of Cu were estimated using Visual MINTEQ 3.0, which was downloaded from http://vminteq.lwr.kth.se/ and used without modification[35]. Nano-Cu was input as finite solids based on their copper content and the Cu ions were derived from the composition of the artificial seawater. Additional TEM analyses of aged nano-Cu were done using the FEI Titan.

Physicochemical kinetics of nano-Cu

Nano-Cu stock solutions were diluted to concentrations of 0, 0.01, 0.1, 0.5, 1, 5, 10, and 20 mg L^{-1}, hereafter referred to as “nominal Cu concentrations”. Dissolution of nano-Cu was quantified by measuring the amount of Cu^{2+} ions present in the 0, 0.1, 1, 10, and 20 mg L^{-1}

nominal Cu concentrations, and hereafter referred to as "dissolved Cu concentration". Variability of the dissolution rate of Cu particles with increasing nominal Cu concentration at different levels of aging was evaluated using a semi-parametric regression approach based on generalized linear mixed-effect models (GLMMs) and penalized-splines[37]. The resulting dissolution curves (Figure S1) were used to estimate the dissolved Cu concentrations for the solutions for which Cu^{2+} ions were not directly measured, i.e. nominal concentrations of 0.01, 0.5, and 5 mg L^{-1}.

Exposure of aged nano-Cu to *Dunaliella tertiolecta*

Marine phytoplankton *D. tertiolecta* (Chlorophyceae: Chlamydomonadales) was cultured in 80 mL of L/2 media without silicate in artificial seawater, pH 8.1, salinity 35, at 20 °C, under cool fluorescent lights (100 μmol m^{-2} s^{-1}) with 14:10 h Light : Dark photoperiod. All experiments were performed with exponentially growing cultures at ~ 15 x 10^3 cells mL^{-1} and cell densities were determined using a microscope and a hematocytometer. Algal culturing was continually shaken throughout the bioassay using a rotary shaker at 120 rpm. At the end of each aging period, marine phytoplankton cells were exposed to concentrations of 0, 0.01, 0.1, 0.5, 1, 5, 10, and 20 mg Cu L^{-1} for 5 days.

Intracellular Cu uptake in marine phytoplankton

The potential for Cu uptake by the cells was determined using a modified method from Levy and collaborators[38]. Algal cells were sampled at the end of the experiment (5 days) using three replicate flasks per treatment, and centrifuged for 4 min (RC 5B Plus, Sorvall, CT) at 2,500 rpm. Concentrated algal cells were then rinsed in seawater, centrifuged again, and washed in EDTA solution for 20 min (0.01 M EDTA, 0.1 M KH_2PO_4/ K_2HPO_4 buffer

pH 6, salinity adjusted to 35 ‰), followed by centrifugation as described above. Final pellets were then rinsed in seawater, centrifuged, and digested in 1 mL concentrated trace-metal grade HNO_3 overnight (Fisher Scientific). Digested samples were diluted to 7 % nitric acid and saved for intracellular ICP-MS Cu fraction analysis (iCAP 6300, Thermo Scientific). Additional aliquots were removed from algal cultures (exposed to 0, 0.1, 1, 10, and 20 mg Cu L^{-1}) after 1, 3, and 5 days and analyzed for dissolved Cu fraction (< 2 nm) and nano-Cu fraction (2 nm < Cu < 200 nm). *D. tertiolecta* cultures were exponential in all performed experiments, and all intracellular Cu uptake data were normalized by number of cells.

Toxicity tests

Population growth rate coefficients

Cells were counted at the beginning and at the end of each experiment to test the influence of Cu nanoparticle aging on phytoplankton population growth rate coefficient. For phytoplankton growth rate coefficient analysis, 1 mL of each treatment flask was taken daily, and cell densities were obtained using a fluorometer (Trilogy, Turner Designs), converting the fluorescence measurements into number of cells, previously calibrated with a standard curve made with Turner Designs Liquid Primary Chlorophyll a Standards. Growth rates (μ, d^{-1}) were estimated using linear regression over natural logarithm transformed cell densities against time[37], and can be described by:

$$\mu = \ln (n2 / n1) / (t2 - t1)$$

where n1 and n2 is the number of cells in time 1 and time 2. Variability in the logarithmic growth rate coefficient of phytoplankton populations with increasingly dissolved Cu concentration at different levels of aging was characterized using semi-parametric regressions[37] (Figure S2). All experiments were performed with exponentially growing

cultures of *D. tertiolecta*, and all growth rate coefficient data were normalized by number of cells.

Reactive oxygen species (ROS)

Cell toxicity can be assessed through quantifying an excess of reactive oxygen species (ROS)[39]. Molecular probes are useful ROS indicators, including singlet oxygen, superoxide, hydroxyl radical and various peroxide and hydroperoxides. High intracellular ROS levels can quickly cause cellular oxidative damage and eventually cell death[40]. To test the influence of aging on the production of ROS, we used the carboxy-2',7'-dichloro-dihydro-fluorescein diacetate (CM-H_2DCFDA) probe, purchased in dried aliquots of 50 µg from Invitrogen Molecular Probe (Eugene, OR, USA). At the end of the experiment (5 days), marine phytoplankton cells were seeded on black 96-well plates and incubated with a final concentration of 4 µg mL^{-1} of CM-H_2DCFDA probe (dissolved in anhydrous dimethyl sulfoxide, DMSO, Fisher Scientific), under dark conditions at 20 °C, for 45 min.

Immediately after the incubation period, both biotic and abiotic fluorescence were measured at 485 nm (excitation) and 530 nm (emission) wavelengths using a microplate reader (Synergy H1, BioTek). All assays were performed using three replicate flasks per treatment, each comprising no less than four replicates. All ROS data were normalized by number of cells. The relative ROS level (%) was calculated by the mean fluorescence intensity of treated samples compared to the mean fluorescence intensity of untreated samples[41,42].

Statistical analyses

To test differences between the mean responses of marine phytoplankton after the exposure to aged nano-Cu, separate two-way ANOVAs were used to test whether the mean total dissolved Cu concentration (mg L^{-1}), intracellular Cu uptake, and nano-Cu toxicity in marine phytoplankton cultures responded to aging (weeks), nominal Cu concentration (mg L^{-1}) treatments, and their interaction. Prior to ANOVA, all data were square root transformed and tested for equality of variances using Levene's test. Transformed data passed subsequent Levene's tests for homogeneity of variances ($P > 0.05$). Differences between specific treatments were determined with Tukey's honestly significant difference (HSD) post hoc tests ($P < 0.01$). All statistical analyses and graphics were conducted in R (R Development Core Team) and Excel.

2.4. Results

Characterization of ENMs

TEM analysis of pristine, dry powder nano-Cu revealed that the primary particles were 30 nm to 100 nm in size, but most of the Cu particles were aggregated (between 500 nm and 1000 nm in diameter) (Figure S3 a and b). EDS analyses showed that the elemental composition of nano-Cu was 82.46 % Cu by weight (Figure S3 c), which agrees well with ICP-AES analyses (83.3 wt. %)[35]. The purity of nano-Cu was therefore considered to be 83 % for our study. As expected, the nano-Cu aggregated in aqueous phase despite ultrasonication for 1 h.

The average hydrodynamic diameter (HDD) of the particle in DI water (with 2 mM pH 8 phosphate buffer) was 2326 ± 163.4 nm. Aggregation of nano-Cu can be attributed to low surface charge as indicated by ζ potential of -21.2 ± 0.8 mV in DI. The particles were also aggregated in aging stock solutions (HDD = 3549 ± 604.3 nm), with only a small fraction

remaining below 100 nm (Figure S4). The nano-Cu was almost neutral in charge (ζ potential = -2.89 ± 0.90) due to the relatively high salinity of the aging stock solutions.

Transformation of nano-Cu during aging

Aging stock solutions (20 mg nano-Cu L^{-1}) were thoroughly mixed prior to sampling but aggregation led to heterogeneous distribution of Cu in the aging stocks, which led to the detection of bulk Cu at levels below the nominal 20 mg L^{-1} concentration in all aged stocks solutions (Table S2). The morphology of the nano-Cu was clearly transformed over time, especially of nano-Cu aged in stock solutions over the 15-week period (Figure 1). Although particle sizes appeared to decrease over time, due to dissolution, individual Cu particles were only visible when nano-Cu was aged for a few hours, after which micron-sized clusters (possibly made up of small-sized particles) were observed. Energy-dispersive X-ray Spectroscopy (EDS) analyses (Figure S5) showed that for nano-Cu aged in seawater Cu typically accounted for less than 40 wt. % of the aggregates, which also contained sodium, magnesium, aluminum, sulfur, chlorine, potassium, and calcium.

In addition to aggregation, dissolution of nano-Cu in the aged stocks was observed. About 4 % of the total Cu detected in the stocks was in dissolved form within 2 h of aging but the dissolved fraction decreased over time to less than 0.1 % at 15 weeks (Table S2). Dissolution of Cu in seawater media is typically driven by complexation with chloride ions (Cl^-) to form soluble or insoluble copper species[35]. Concentration of Cl^- was 530 mM in the artificial seawater thus helping to explain the relatively rapid dissolution of nano-Cu within 2 h of aging. Dissolved Cu species in seawater, therefore, are typically short-lived due to the precipitation of dissolved ions as complexes like $CuCl_2$, $Cu_2Cl(OH)_3$, CuO, and $Cu(OH)_2$[43], which helps explain the change in morphology and elemental composition of nano-Cu aged

for 15 weeks in saltwater systems (Figure 1 B and Figure S5). Complexation also explains the decrease, over time, of dissolved Cu in the aging stocks (Table S2). The Visual MINTEQ model predicted that the most abundant Cu species at equilibrium formed from aging the nanoparticles in seawater was $CuCl_2^-$, a complexed copper species (Table S3).

Fate of aged nano-Cu in phytoplankton cultures

Nanosized Cu was either non-detectable in the algal cultures or generally in very low concentrations (< 0.17 mg L^{-1}) (Table S4). This is not surprising as very low levels of nanosized Cu were present in aging stock solutions due to particle aggregation (Table S2). More so, further aggregation of the particles was expected to occur in the algal cultures, especially heteroaggregation with phytoplankton cells[10,44,45].

In addition to (hetero)aggregation, further dissolution of particles (nanosized and bulk) occurred in all treatments upon the introduction of the aged stock solutions into algal cultures. This is probably due to Cu particles binding to the algae-derived natural organic matter (NOM), which was previously shown to increase dissolution of nano-Cu by our group[35]. However, the dissolution was much higher in culture treatments that were exposed to aged nano-Cu than the treatments that were exposed to pristine nano-Cu (0 wk). For example, the dissolved Cu concentration measured in the 0 wk aging stock solution was 0.8 mg L^{-1} (Table S2) and increased to only 0.9 mg L^{-1} after 24 hours in their respective phytoplankton cultures (Table S4). In contrast, the dissolved Cu concentration measured in the 15 wk aging stock was 0.01 mg L^{-1} (Table S2) and rapidly increased to 0.28 mg L^{-1} after 24 hours in their respective phytoplankton cultures (Table S4).

Cu dissolution in algal cultures was also examined during the exposure time of 5 days. In cultures exposed to nano-Cu without aging (0 wk), Cu dissolution barely changed within the

5-day exposure time, and there were no differences in total dissolved Cu concentration between day 1 and day 5 across all nominal Cu concentrations (Tukey's HSD, $P > 0.05$; Figure 2). For instance, in treatments with nano-Cu without aging (0 wk) at nominal Cu concentration of 0.1 mg L^{-1}, dissolved Cu accounted for 95 % at day 1, and 85 % at day 5, of total Cu. At a nominal Cu concentration of 10 mg L^{-1}, dissolved Cu accounted for the same amount of 9 % of total Cu detected at day 1 and at day 5. Mean total dissolved Cu concentration in phytoplankton cultures exposed to nano-Cu without aging varied with nominal Cu concentration (0, 0.1, 1, 10, and 20 mg L^{-1}) and exposure day (day 1 and day 5), as noted by a significant two-way interaction in the 0 wk aging treatment ANOVA (2-way ANOVA; Concentration x Day; $F_{4,20} = 7.1$; $P < 0.0001$; Table S5). However, the two-way interaction explained less than 1 % of the total variation in the experiment. In contrast, nominal Cu concentration explained more than 99 % of the response among treatments.

By contrast, Cu dissolution accelerated within the 5-day exposure time in cultures exposed to aged nano-Cu, with a higher difference from day 1 compared to day 5 in the algal cultures exposed to nano-Cu aged for 15 weeks (Tukey's HSD, $P < 0.01$; Figure 2). For nano-Cu aged for 15 weeks at nominal Cu concentration of 0.1 mg L^{-1}, dissolved Cu increased from 11 % to 45 % (detected after 1 and 5 days respectively) of total Cu, and at a nominal Cu concentration of 10 mg L^{-1}, dissolved Cu increased from 2 % to 6 % of total Cu (detected after 1 and 5 days respectively). The significant two-way interaction of nominal Cu concentration and exposure day in treatments with nano-Cu aged for 15 weeks (2-way ANOVA; Concentration x Day; $F_{4,20} = 759.2$; $P < 0.0001$; Table S6) explained 12 % of the total variation. Total dissolved Cu concentration rapidly increased from day 1 to day 5 (Tukey's HSD, $P < 0.01$; Figure 2), but this factor explained only ~ 18 % of the total variation among treatments. In contrast, nominal Cu concentration explained 71 % of

response among treatments. There was also a significant two-way interaction of nominal Cu concentration and exposure day in the 3 wk (2-way ANOVA; Concentration x Day; $F_{4,20}$ = 33.6; $P < 0.0001$; < 1 % of variation; Table S7) and 4 wk (2-way ANOVA; Concentration x Day; $F_{4,20}$ = 191.2; $P < 0.0001$; 9 % of variation; Table S8) aging treatments.

Intracellular Cu uptake in marine phytoplankton

Considering that nanoparticle uptake can depend on cell density[46], *D. tertiolecta* population growth rates were exponential in all performed experiments. All uptake data is presented as Cu μg cells^{-1}x10^6. The accumulation of Cu in marine phytoplankton cells was detected in all experimental treatments and generally varied with aging and nominal Cu concentration (Figure 3). In the seawater controls, intracellular Cu concentrations were very similar to that of low levels of nominal Cu concentration treatments (< 100 ppb) across all aging periods (Tukey's HSD, $P > 0.05$; Figure 3). The two-way ANOVA explained much of the variation in mean total Cu uptake in the experiment (adjusted $r^2 = 0.97$), while the variation among treatments was similarly explained by nominal Cu concentrations (34 %) and aging (28 %).

There was a significant two-way interaction of nominal Cu concentration and aging treatment (2-way ANOVA; Concentration x Aging; $F_{12,20}$ = 50.93; $P < 0.0001$; 37 % of variation; Table S9) that was driven by (1) an increase in Cu uptake with increasing nominal Cu concentration (Tukey's HSD, $P < 0.01$), and (2) higher Cu uptake in the cultures exposed with nano-Cu aged for 15 weeks than in those with smaller aging periods (Figure 3).

Toxicity of aged nano-Cu in marine phytoplankton

Population growth rate coefficient

Toxicity, assessed by a decrease in the phytoplankton growth rate coefficient (μ, d^{-1}), generally increased with increasing nominal Cu concentration in all aging treatments (Tukey's HSD, $P < 0.01$; Figure 4). The decrease in growth rate coefficient was more dramatic in culture treatments exposed to the 0 wk aging treatment (pristine nano-Cu). The ANOVA model explained most of the total variation in growth rate coefficient (adjusted $r^2 = 0.94$), and nominal Cu concentration explained the greatest amount of variation among treatments (42 %). A significant two-way interaction of nominal Cu concentration and aging periods (2-way ANOVA; Concentration x Aging; $F_{12,40} = 53.4$; $P < 0.0001$; Table S10) explained only 22 % of the variation while aging explained 34 %.

Phytoplankton population growth rate coefficients generally increased with aging period. The growth rate coefficient was highest in the 4 wk aging treatment in all nominal Cu concentrations (Tukey's HSD, $P < 0.01$; Figure 4), with growth rate coefficients of 0.97, 0.93, and 0.88 at nominal Cu concentrations of 5, 10, and 20 mg L^{-1}, respectively. However, growth rate coefficient in the 15 wk aging treatment decreased, showing growth rate coefficients of 0.92, 0.75, and 0.68 at nominal Cu concentrations 5, 10, and 20 mg L^{-1}, respectively (Tukey's HSD, $P < 0.01$).

Reactive oxygen species (ROS)

To measure the intracellular total ROS production in *D. tertiolecta* in response to an aging process of nano-Cu in marine ecosystems, the DCFH-DA assay was used, as DCF fluorescence values indicate an increase in intracellular total ROS. Mean total ROS production varied with nominal Cu concentration and aging treatment, as signified by a significant two-way interaction in the ANOVA (2-way ANOVA; Concentration x Aging; $F_{10,630} = 52.5$; $P < 0.0001$; Table S11). The model explained only 45 % of the

variation among treatments (adjusted model $r^2 = 0.45$), and the two-way interaction explained 18 % of the total variation in the experiment. Total generation of ROS declined with increasing aging period, but increased with increasing nominal Cu concentration, and this factor explained 42 % of the total variation among treatments. Aging also explained 18 % of response among treatments (Figure 5).

Mean total intracellular ROS was much higher in the 0 wk aging treatment when compared to those that were exposed to aged nano-Cu. A higher level of ROS in the highest nominal Cu concentration, compared to all treatments, was found when marine phytoplankton cultures were exposed to nano-Cu without aging (Tukey's HSD, $P < 0.01$; Figure 5). ROS production was also generally high in algal cultures exposed to 20 mg L^{-1} (Tukey's HSD, $P < 0.01$). There was no difference among ROS generation in the lowest nominal Cu concentration in which the toxicity was relatively low. This pattern was observed repeatedly for the other toxic responses (see Cu uptake, and growth rate).

ROS production showed relatively low fluorescence for all nominal Cu concentrations in phytoplankton cultures exposed to nano-Cu aged for 15 wk, in contrast to Cu uptake and growth rates results. This finding suggests that the induction of cell death by nano-Cu is not always mediated by the generation of ROS[35]. Nevertheless, algal cultures exposed to nano-Cu aged for 15 wk still generated higher ROS levels in the two highest nominal Cu concentrations of 10 and 20 mg L^{-1}, relative to the controls (Tukey's HSD, $P < 0.01$). The different aging periods tested in this study induced similar intracellular ROS formation in phytoplankton, indicating that aged nano-Cu does not play an important role in cellular oxidative damage. The 3 wk aging treatment was not accounted for in the ROS analyses due to contamination of cultures.

2.5. Discussion

Physicochemical transformations of copper nanoparticles caused by chemical aging in seawater regulated toxicity to phytoplankton in our experiment. As the period of aging increased so did the transformations, even in the aggregates of Cu particles. For example, sedimentation of the Cu aggregates is likely to occur in aqueous solutions and may have contributed for the heterogeneous distribution of Cu in all aging stocks. This emphasizes the need for caution in using nanoparticle release modeling results for predicting exposures as ENMs (especially those with low stability) can form "hot-spots" (e.g., in sediments) rather than distribute homogeneously in aquatic systems. Nevertheless, the nanometer range of primary particles size in our experiments could be newly formed $CuCl_2$ NPs[47].

Complexation and aggregation occur in aquatic systems but are influenced by the availability of anions and organic materials. Consequently, the proportion of freely dissolved Cu (i.e., Cu^+ and Cu^{2+}), which are the most toxic Cu species for phytoplankton[48], is expected to be small in saltwater ecosystems. However, Cu dissolution may also occur due to additional complexation, recrystallization of dissolved ions, or from large-sized particles that are mainly composed of aggregated nanosized particles held together by van der Waals attraction[49], which is in good agreement with the smaller-sized particles that we observed in our longest aging period.

In the surface coastal waters, processes that might be involved in the transformations of Cu particles after aging under environmental conditions for over 100 days are (1) oxidation, given by the reaction of dissolved oxygen, mediated by protons and other components in the liquid phase, (2) dissolution, as a result of Cu ions derived from the oxidation of nano-Cu (zero valence), and (3) complexation, due to the positively charged free Cu ions, which has a strong tendency to associate with negatively charged ions in seawater to achieve a stable

state. For instance, the inorganic anionic binders present in seawater, including chloride (Cl^-), sulfate (SO_4^{2-}), hydroxide (OH^-) and carbonate (CO_3^{2-}), compete for association with cationic metals. Chloride complexation, however, is the main expected reaction in seawater[50].

In aquatic organisms, the mechanisms of toxicity caused by NPs greatly vary and are hotly debated, yet some studies have indicated that exposure period, cell type, and growth conditions play a significant role in the induction of nanomaterial cytotoxicity[34]. For example, an uptake of Cu may not generate toxicity; it will depend on several factors, including intracellular solubility and the type and phase of the cell[34]. Cellular uptake is also affected by the external morphology, size and surface charge of the NP, which directly influences cell absorption, as the size of the contact area is directly proportional to the biocompatibility[41,51].

Intracellular ROS production in *D. tertiolecta* detected in our experiment was probably influenced by the transformation pathways (e.g. adsorption) of the Cu particles, which may have decreased the toxic effects and persistence of aged nano-Cu in the seawater system, and by the ability of aquatic organisms to scavenge ROS production by defense mechanisms. The amount and the chemical compositions of organic matter in the cultures may also have influenced the formation and detection of oxidative stress in the cells as the generation of ROS strongly depends on the molecular size of NOM[52,53]. However, environmental stress, including toxicant bioavailability[54] and exposure, may interfere in these mechanisms and even induce to a disruption of cellular homeostasis that lastly may lead to cell death[55,56].

It is important to note that throughout our experimental the same ambient conditions were maintained for all aging treatments and all phytoplankton cultures. The environmental factors have a paramount effect on the behavior and transformations of NPs, and differences

between these factors are the main cause of inconsistent experimental results[57]. For instance, high IS in aquatic systems reduces NPs electrostatic repulsion and increases aggregation processes; also, the effect of salinity is higher in low than in high concentration of NPs. Therefore, the different behavior, transformations, and toxicity of nano-Cu in our experiment were driven mainly by the extent of the aging period rather than the water properties (e.g., IS, and salinity), or NPs properties (e.g., size, and surface charge), as our environmental factors (IS, salinity, pH, temperature, light, DO, and NP concentration), and nano-Cu properties (size, shape, surface area, and nano-Cu concentration) were initially the same.

Our results stress the importance of the time at which a released NP will remain in marine/estuarine surface waters. For instance, the physicochemical transformations of exposure to nano-Cu aged at or below 28 days in seawater decreased the most toxic Cu species by aggregation and complexation processes over time. In turn, sedimentation and deposition of the large-sized Cu particles are expected to occur as the following processes, which may favor the subsequent depletion of Cu in the surface waters[4]. This pattern may appear to be nearly linear, and a more pronounced nonlinear response may not be expected at exposure periods higher than 30 days. Therefore, physicochemical transformations can mitigate the behavior, fate, and toxicity of nano-Cu that might be aging in seawater ecosystems, by (1) further facilitating their dissolution and bioavailability, and by (2) exposing toxic Cu ions to the pelagic organisms, as shown in the experiments of this study. In fact, aging reduced toxicity in its initial stages, as dissolution declined, then increased as the particles became physically complexed, a process that led to additional dissolution.

2.6. References

1. Newbold, T. *et al.* Global effects of land use on local terrestrial biodiversity. *Nature* **520**, 45–50 (2015).
2. Galloway, T. S., Cole, M. & Lewis, C. Interactions of microplastic debris throughout the marine ecosystem. *Nat. Ecol. Evol.* **1**, 0116 (2017).
3. Lenihan, H. S., Peterson, C. H., Miller, R. J., Kayal, M. & Potoski, M. Biotic disturbance mitigates effects of multiple stressors in a marine benthic community. *Ecosphere* **9**, e02314 (2018).
4. Garner, K. L. & Keller, A. A. Emerging patterns for engineered nanomaterials in the environment: a review of fate and toxicity studies. *J. Nanoparticle Res.* **16**, (2014).
5. Klaine, S. J. *et al.* Nanomaterials in the environment: Behavior, fate, bioavailability, and effects. *Environ. Toxicol. Chem.* **27**, 1825–1851 (2008).
6. Nel, A. *et al.* Nanomaterial toxicity testing in the 21st century: use of a predictive toxicological approach and high-throughput screening. *Acc. Chem. Res.* **46**, 607–621 (2013).
7. Service, R. F. Nanotechnology Grows Up. *Science* **304**, 1732–1734 (2004).
8. Keller, A. A. *et al.* Comparative environmental fate and toxicity of copper nanomaterials. *NanoImpact* **7**, 28–40 (2017).
9. Garner, K. L., Suh, S. & Keller, A. A. Assessing the Risk of Engineered Nanomaterials in the Environment: Development and Application of the nanoFate Model. *Environ. Sci. Technol.* **51**, 5541–5551 (2017).
10. Adeleye, A. S. *et al.* Influence of Phytoplankton on Fate and Effects of Modified Zerovalent Iron Nanoparticles. *Environ. Sci. Technol.* **50**, 5597–5605 (2016).
11. Scheufele, D. A. *et al.* Scientists worry about some risks more than the public. *Nat. Nanotechnol.* **2**, 732–734 (2007).

12. Keller, A. A. *et al.* Stability and Aggregation of Metal Oxide Nanoparticles in Natural Aqueous Matrices. *Environ. Sci. Technol.* **44**, 1962–1967 (2010).
13. Książyk, M., Asztemborska, M., Stęborowski, R. & Bystrzejewska-Piotrowska, G. Toxic Effect of Silver and Platinum Nanoparticles Toward the Freshwater Microalga Pseudokirchneriella subcapitata. *Bull. Environ. Contam. Toxicol.* **94**, 554–558 (2015).
14. Keller, A. A., Garner, K., Miller, R. J. & Lenihan, H. S. Toxicity of Nano-Zero Valent Iron to Freshwater and Marine Organisms. *PLoS ONE* **7**, e43983 (2012).
15. Xiao, Y., Peijnenburg, W. J. G. M., Chen, G. & Vijver, M. G. Impact of water chemistry on the particle-specific toxicity of copper nanoparticles to Daphnia magna. *Sci. Total Environ.* **610**–**611**, 1329–1335 (2018).
16. Croteau, M.-N., Misra, S. K., Luoma, S. N. & Valsami-Jones, E. Bioaccumulation and Toxicity of CuO Nanoparticles by a Freshwater Invertebrate after Waterborne and Dietborne Exposures. *Environ. Sci. Technol.* **48**, 10929–10937 (2014).
17. Peng, C. *et al.* Behavior and Potential Impacts of Metal-Based Engineered Nanoparticles in Aquatic Environments. *Nanomaterials* **7**, 21 (2017).
18. Su, Y. *et al.* Impact of ageing on the fate of molybdate-zerovalent iron nanohybrid and its subsequent effect on cyanobacteria (Microcystis aeruginosa) growth in aqueous media. *Water Res.* **140**, 135–147 (2018).
19. Valsami-Jones, E. & Lynch, I. How safe are nanomaterials? *Science* **350**, 388–389 (2015).
20. Holden, P. A. *et al.* Considerations of Environmentally Relevant Test Conditions for Improved Evaluation of Ecological Hazards of Engineered Nanomaterials. *Environ. Sci. Technol.* **50**, 6124–6145 (2016).

21. Amde, M., Liu, J.-F., Tan, Z.-Q. & Bekana, D. Transformation and bioavailability of metal oxide nanoparticles in aquatic and terrestrial environments. A review. *Environ. Pollut. Barking Essex 1987* **230**, 250–267 (2017).
22. Mouneyrac, C., Syberg, K. & Selck, H. Ecotoxicological Risk of Nanomaterials. in *Aquatic Ecotoxicology* 417–440 (Elsevier, 2015). doi:10.1016/B978-0-12-800949-9.00017-6
23. Golobič, M. *et al.* Upon Exposure to Cu Nanoparticles, Accumulation of Copper in the Isopod Porcellio scaber Is Due to the Dissolved Cu Ions Inside the Digestive Tract. *Environ. Sci. Technol.* **46**, 12112–12119 (2012).
24. Bao, S., Lu, Q., Fang, T., Dai, H. & Zhang, C. Assessment of the Toxicity of CuO Nanoparticles by Using Saccharomyces cerevisiae Mutants with Multiple Genes Deleted. *Appl Env. Microbiol* **81**, 8098–8107 (2015).
25. Miao, A.-J. *et al.* The algal toxicity of silver engineered nanoparticles and detoxification by exopolymeric substances. *Environ. Pollut. Barking Essex 1987* **157**, 3034–3041 (2009).
26. Beer, C., Foldbjerg, R., Hayashi, Y., Sutherland, D. S. & Autrup, H. Toxicity of silver nanoparticles - nanoparticle or silver ion? *Toxicol. Lett.* **208**, 286–292 (2012).
27. Miller, R. J. *et al.* Impacts of Metal Oxide Nanoparticles on Marine Phytoplankton. *Environ. Sci. Technol.* **44**, 7329–7334 (2010).
28. Wong, S. W. Y., Leung, P. T. Y., Djurisić, A. B. & Leung, K. M. Y. Toxicities of nano zinc oxide to five marine organisms: influences of aggregate size and ion solubility. *Anal. Bioanal. Chem.* **396**, 609–618 (2010).

29. Horst, A. M., Vukanti, R., Priester, J. H. & Holden, P. A. An assessment of fluorescence- and absorbance-based assays to study metal-oxide nanoparticle ROS production and effects on bacterial membranes. *Small Weinh. Bergstr. Ger.* **9**, 1753–1764 (2013).

30. Manke, A., Wang, L. & Rojanasakul, Y. Mechanisms of Nanoparticle-Induced Oxidative Stress and Toxicity. *BioMed Research International* (2013). doi:10.1155/2013/942916

31. Siddiqui, M. A. *et al.* Molybdenum nanoparticles-induced cytotoxicity, oxidative stress, G2/M arrest, and DNA damage in mouse skin fibroblast cells (L929). *Colloids Surf. B Biointerfaces* **125**, 73–81 (2015).

32. Mallevre, F. *et al.* Toxicity Testing of Pristine and Aged Silver Nanoparticles in Real Wastewaters Using Bioluminescent Pseudomonas putida. *Nanomater. Basel Switz.* **6**, (2016).

33. Mitrano, D. M. & Nowack, B. The need for a life-cycle based aging paradigm for nanomaterials: importance of real-world test systems to identify realistic particle transformations. *Nanotechnology* **28**, 072001 (2017).

34. Adeleye, A. S. & Keller, A. A. Long-term colloidal stability and metal leaching of single wall carbon nanotubes: Effect of temperature and extracellular polymeric substances. **49**, 236–250 (2014).

35. Adeleye, A. S., Conway, J. R., Perez, T., Rutten, P. & Keller, A. A. Influence of Extracellular Polymeric Substances on the Long-Term Fate, Dissolution, and Speciation of Copper-Based Nanoparticles. *Environ. Sci. Technol.* **48**, 12561–12568 (2014).

36. Kester, D. R., Duedall, I. W., Connors, D. N. & Pytkowicz, R. M. Preparation of Artificial Seawater1. *Limnol. Oceanogr.* **12**, 176–179 (1967).

37. Ruppert, D., Wand, M. P. & Carroll, R. J. Semiparametric Regression by David Ruppert. *Cambridge Core* (2003). doi:10.1017/CBO9780511755453

38. Levy, J. *et al.* Uptake and internalisation of copper by three marine microalgae: comparison of copper-sensitive and copper-tolerant species. *Fac. Sci. - Pap. Arch.* 82–93 (2008). doi:10.1016/j.aquatox.2008.06.003

39. Kohen, R. & Nyska, A. Invited Review: Oxidation of Biological Systems: Oxidative Stress Phenomena, Antioxidants, Redox Reactions, and Methods for Their Quantification. *Toxicol. Pathol.* **30**, 620–650 (2002).

40. Bulcke, F., Thiel, K. & Dringen, R. Uptake and toxicity of copper oxide nanoparticles in cultured primary brain astrocytes. *Nanotoxicology* **8**, 775–785 (2014).

41. Fu, P. P., Xia, Q., Hwang, H.-M., Ray, P. C. & Yu, H. Mechanisms of nanotoxicity: generation of reactive oxygen species. *J. Food Drug Anal.* **22**, 64–75 (2014).

42. Hong, Y. *et al.* Gramine-induced growth inhibition, oxidative damage and antioxidant responses in freshwater cyanobacterium Microcystis aeruginosa. *Aquat. Toxicol.* **91**, 262–269 (2009).

43. Conway, J. R., Adeleye, A. S., Gardea-Torresdey, J. & Keller, A. A. Aggregation, Dissolution, and Transformation of Copper Nanoparticles in Natural Waters. *Environ. Sci. Technol.* **49**, 2749–2756 (2015).

44. Ma, S., Zhou, K., Yang, K. & Lin, D. Heteroagglomeration of Oxide Nanoparticles with Algal Cells: Effects of Particle Type, Ionic Strength and pH. *Environ. Sci. Technol.* **49**, 932–939 (2015).

45. Wang, H., Adeleye, A. S., Huang, Y., Li, F. & Keller, A. A. Heteroaggregation of nanoparticles with biocolloids and geocolloids. *Adv. Colloid Interface Sci.* **226**, 24–36 (2015).

46. Kim, J. A., Åberg, C., Salvati, A. & Dawson, K. A. Role of cell cycle on the cellular uptake and dilution of nanoparticles in a cell population. *Nat. Nanotechnol.* **7**, 62–68 (2011).

47. Murdock, R. C., Braydich-Stolle, L., Schrand, A. M., Schlager, J. J. & Hussain, S. M. Characterization of Nanomaterial Dispersion in Solution Prior to In Vitro Exposure Using Dynamic Light Scattering Technique. *Toxicol. Sci.* **101**, 239–253 (2008).

48. Sunda, W. The relationship between cupric ion activity and the toxicity of copper to phytoplankton. (Massachusetts Institute of Technology and Woods Hole Oceanographic Institution, 1975). doi:10.1575/1912/1275

49. Adeleye, A. S., Pokhrel, S., Mädler, L. & Keller, A. A. Influence of nanoparticle doping on the colloidal stability and toxicity of copper oxide nanoparticles in synthetic and natural waters. *Water Res.* **132**, 12–22 (2018).

50. Kiaune, L. & Singhasemanon, N. Pesticidal copper (I) oxide: environmental fate and aquatic toxicity. *Rev. Environ. Contam. Toxicol.* **213**, 1–26 (2011).

51. Deng, J. & Gao, C. Recent advances in interactions of designed nanoparticles and cells with respect to cellular uptake, intracellular fate, degradation and cytotoxicity. *Nanotechnology* **27**, 412002 (2016).

52. Yang, X. *et al.* Interactions between algal (AOM) and natural organic matter (NOM): Impacts on their photodegradation in surface waters. *Environ. Pollut. Barking Essex 1987* **242**, 1185–1197 (2018).

53. McKay, G., Couch, K. D., Mezyk, S. P. & Rosario-Ortiz, F. L. Investigation of the Coupled Effects of Molecular Weight and Charge-Transfer Interactions on the Optical and Photochemical Properties of Dissolved Organic Matter. *Environ. Sci. Technol.* **50**, 8093–8102 (2016).

54. Navarro, E. *et al.* Environmental behavior and ecotoxicity of engineered nanoparticles to algae, plants, and fungi. *Ecotoxicol. Lond. Engl.* **17**, 372–386 (2008).

55. Knauert, S. & Knauer, K. THE ROLE OF REACTIVE OXYGEN SPECIES IN COPPER TOXICITY TO TWO FRESHWATER GREEN ALGAE(1). *J. Phycol.* **44**, 311–319 (2008).

56. Sharma, P., Jha, A. B., Dubey, R. S. & Pessarakli, M. Reactive Oxygen Species, Oxidative Damage, and Antioxidative Defense Mechanism in Plants under Stressful Conditions. *Journal of Botany* (2012). doi:10.1155/2012/217037

57. Salieri, B. *et al.* Does the exposure mode to ENPs influence their toxicity to aquatic species? A case study with TiO2 nanoparticles and Daphnia magna. *Environ. Sci. Pollut. Res.* **22**, 5050–5058 (2015).

List of captions

Figure 1. Transmission electron micrographs (TEM) of nano-Cu transformed after aging in the stock solutions (20 mg L^{-1}) in artificial seawater under environmental conditions: (A) represents nano-Cu without aging (pristine), and (B) reperesents nano-Cu aged for up to 15 weeks (scale bar = 100 nm). 103

Figure 2. Mean (95 % C.I.) total dissolved Cu concentration (mg L^{-1}) of all phytoplankton cultures at day 1 and day 5 as a function of nominal Cu concentration (mg L^{-1}) and aging period (weeks). N = 3 replicate culture flasks per treatment. Results of a Tukey's Honestly Significant Difference (HSD) post hoc test are provided above each bar (* at $P < 0.01$)..... 104

Figure 3. Mean (95 % C.I.) intracellular copper uptake (μg $cell^{-1}x10^6$) of all phytoplankton cultures at day 5 as a function of nominal Cu concentration (mg L^{-1}) and aging period (weeks). N = 3 replicate culture flasks per treatment. Results of a Tukey's Honestly Significant Difference (HSD) post hoc test are provided above each bar (A>B>C, etc., at $P < 0.01$). 105

Figure 4. Mean (95 % C.I.) growth rate coefficient (μ, d^{-1}) of all phytoplankton cultures at day 5 as a function of nominal Cu concentration (mg L^{-1}) and aging period (weeks). N = 3 replicate culture flasks per treatment. Results of a Tukey's Honestly Significant Difference (HSD) post hoc test are provided above each bar (A>B>C, etc., at $P < 0.01$). 106

Figure 5. Mean (95% C.I.) total ROS level (%) of all phytoplankton cultures at day 5 as a function of nominal Cu concentration (mg L^{-1}) and aging period (weeks). N = 3 replicate culture flasks per treatment. Results of a Tukey's Honestly Significant Difference (HSD) post hoc test are provided above each bar (A>B>C, etc., at $P < 0.01$)..... 107

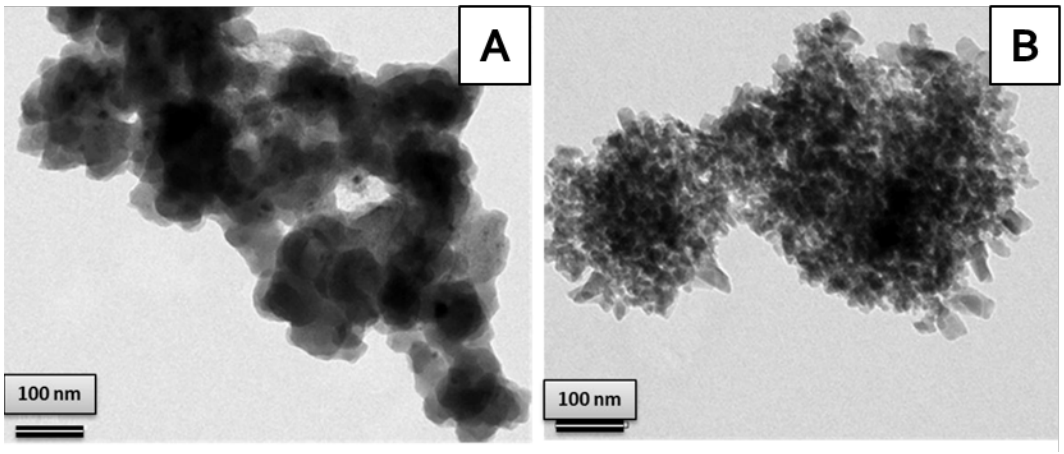

Figure 1.

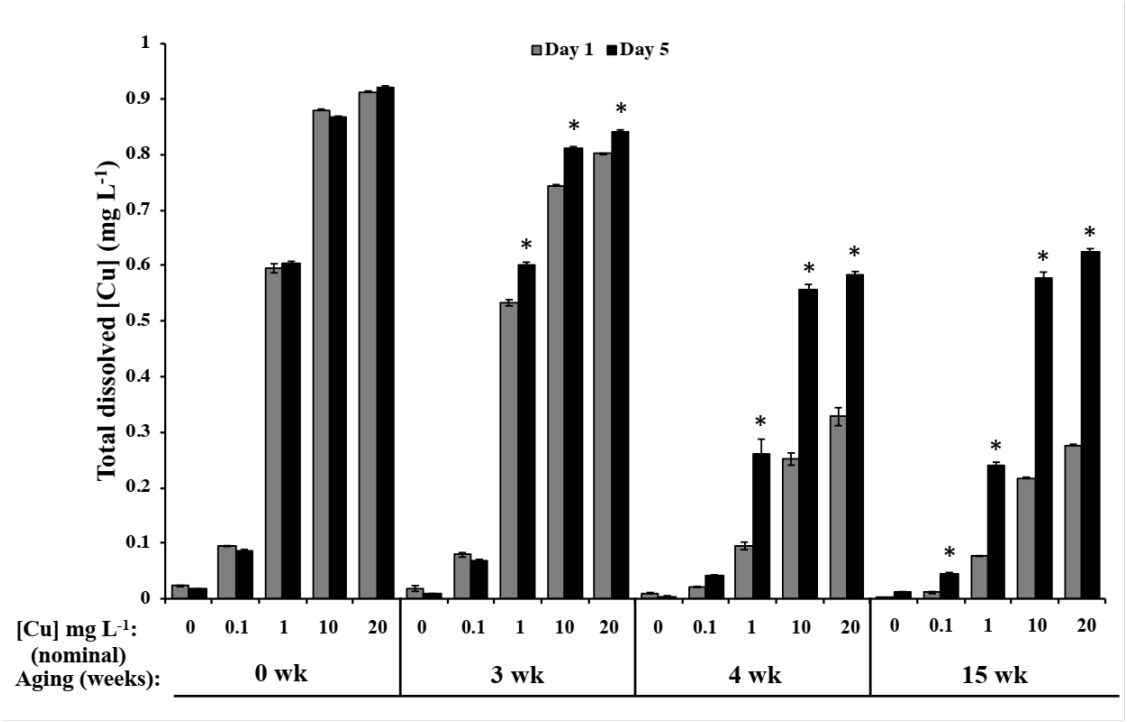
Day 1
Day 5
Total dissolved [Cu] (mg L-1)
1
0.9
0.8
0.7
0.6
0.5
0.4
0.3
0.2
0.1
0
[Cu] mg L-1: (nominal)
0 0.1 1 10 20 0 0.1 1 10 20 0 0.1 1 10 20 0 0.1 1 10 20
Aging (weeks):
0 wk
3 wk
4 wk
15 wk

Figure 2.

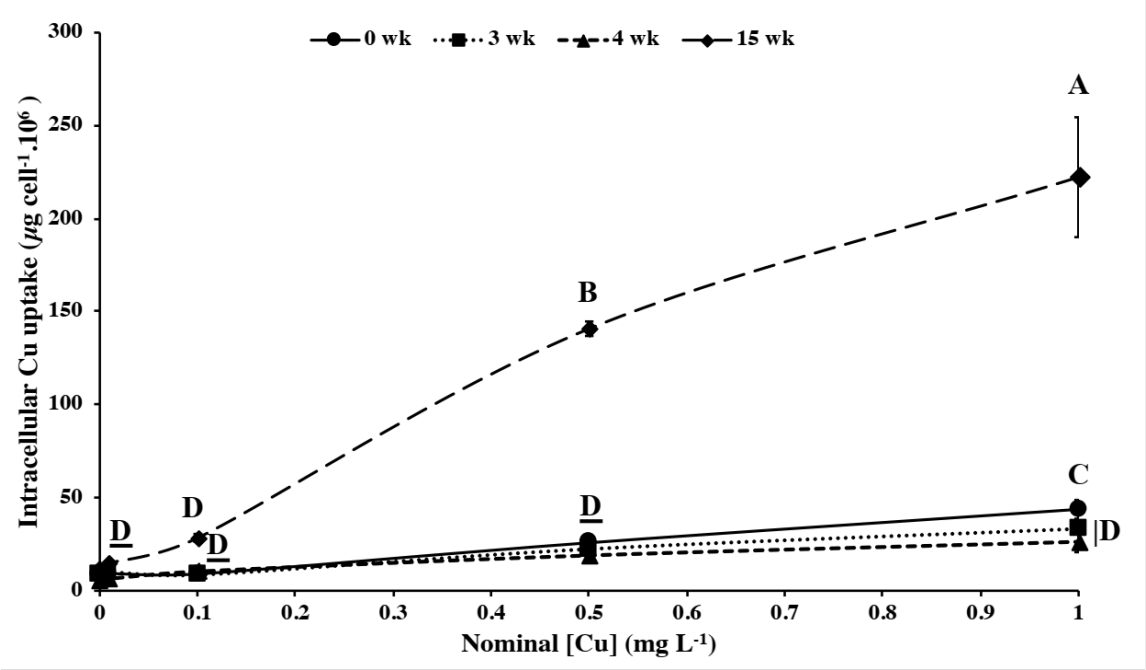
0 wk
3 wk
4 wk
15 wk
Intracellular Cu uptake (µg cell-1.10⁶)
Nominal [Cu] (mg L-1)
300
250
200
150
100
50
0
0
0.1
0.2
0.3
0.4
0.5
0.6
0.7
0.8
0.9
1
A
B
C
D
D
D
D
|D

Figure 3.

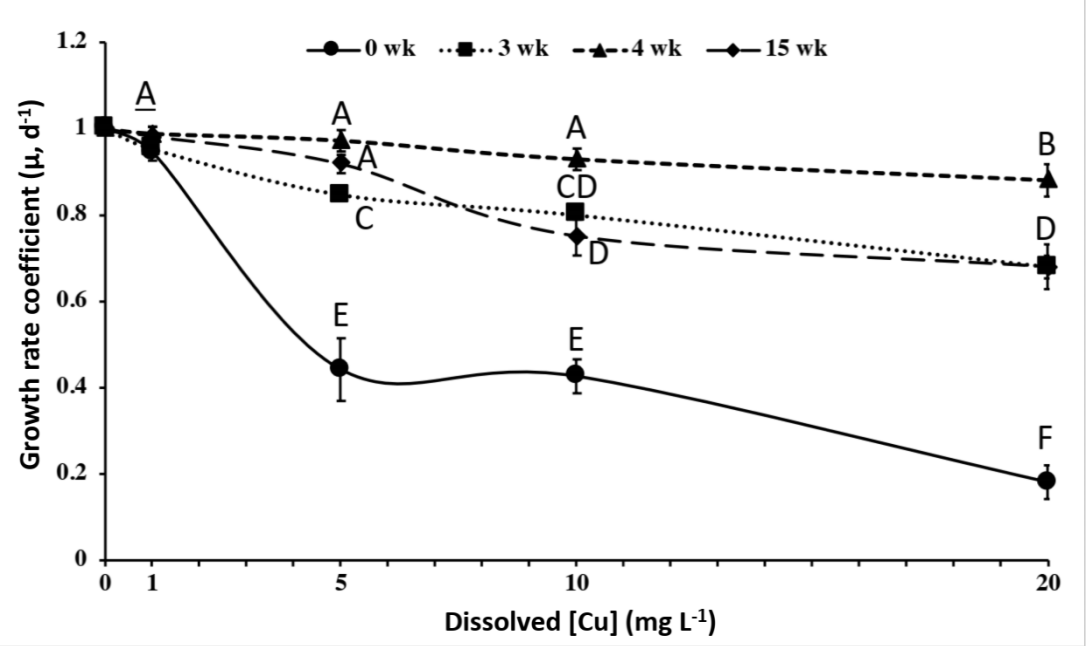
0 wk
3 wk
4 wk
15 wk
Growth rate coefficient (μ, d-1)
Dissolved [Cu] (mg L-1)
1.2
1
0.8
0.6
0.4
0.2
0
0
1
5
10
20
A
A
A
B
A
CD
C
D
D
E
E
F

Figure 4.

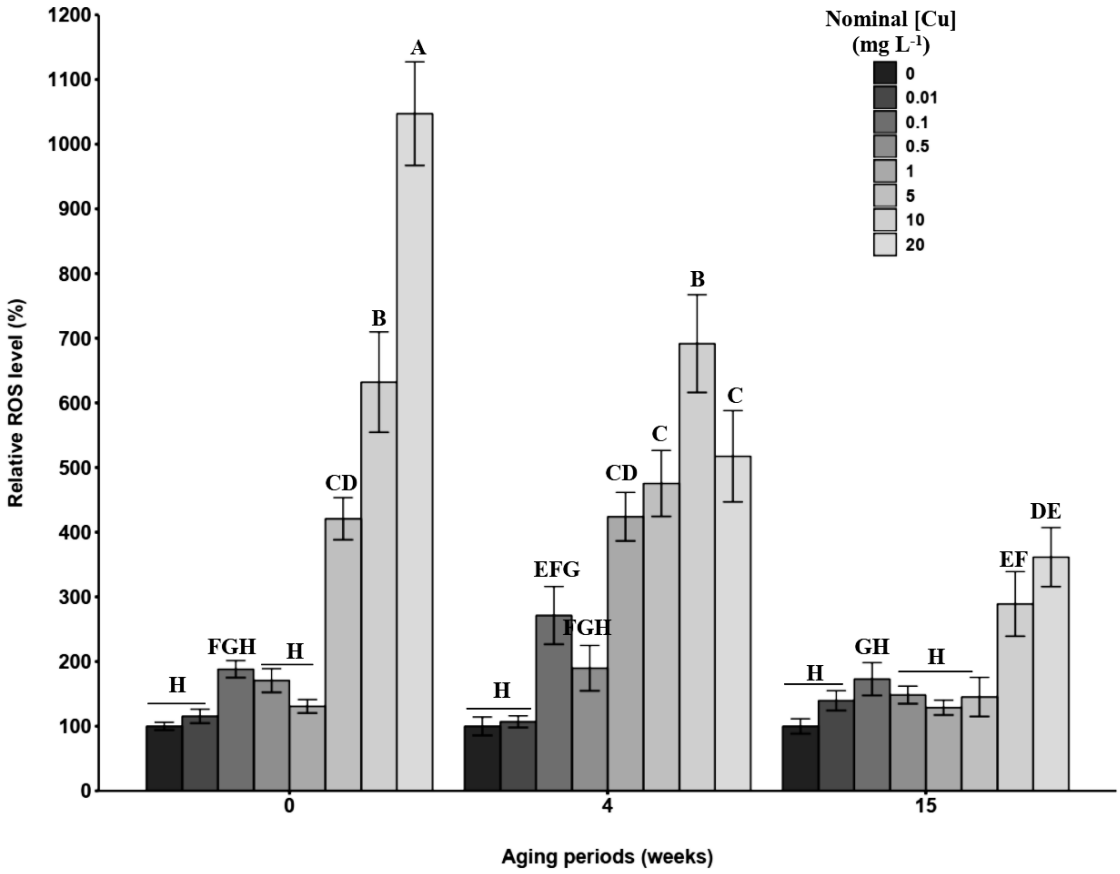
Nominal [Cu]
(mg L-1)
0
0.01
0.1
0.5
1
5
10
20
Relative ROS level (%)
1200
1100
1000
900
800
700
600
500
400
300
200
100
0
H
FGH
H
CD
B
A
H
EFG
FGH
CD
C
B
C
H
GH
H
EF
DE
0
4
15
Aging periods (weeks)

Figure 5.

2.7. Appendix. Supporting Information

Aging studies

This section provides a literature review that compiles examples of the impacts of metal/metal oxide nanoparticles (M/MO NPs) which underwent aging in aquatic systems, relating the tested ambient conditions with their respective environmental exposure scenarios. The following sequences of M/MO NPs are presented here: copper (Cu NPs), silver (Ag NPs), zinc oxide (ZnO NPs), cerium oxide (CeO_2 NPs), titanium dioxide (TiO_2 NPs), molybdate-zerovalent iron nanohybrid (Mo-NZVI), and zerovalent iron (NZVI). Further studies using aging procedures can be found in the recent review by Nowack and Mitrano (2018)[1].

Copper (Cu NPs)[2]

In this particular study the authors did not age the Cu NPs in aqueous media. Instead, powder forms of newly purchased Cu NPs and CuO NPs and an old batch of Cu NPs that had been stored (aged) in the laboratory at 20 °C, under ambient conditions since their purchase date in 2006, was treated as the aging process. However, the aged Cu NPs in powder form were assessed in aqueous media, and to the best of our knowledge, this is the only study that has compared the aqueous behavior of Cu NPs from aged to pristine (newly purchased). The aim of this study was to assess the mobility of Cu-based NPs through dissolution and deaggregation processes in the presence and absence of organic acids, as a function of pH. The three tested Cu NPs solutions (1 g Cu NP L^{-1}) were mixed with concentrations of 0, 0.1, 1, and 10 mM of citric acid and oxalic acid, at pH 3, 7, and 11, and placed on a circular rotator for 24 h in dark conditions. The results showed that the aged Cu NPs acted as binding ligands under ambient conditions, and then experienced an increase in average particle size and a shift in size distribution. The resulting aged particles also differed in composition from

new Cu and CuO NPs. The presence of organic acids inhibited the formation of paratacamite and the Cu metal was converted into Cu_2O for both the new and aged Cu NPs.

This study considered the aging of Cu NPs in powder form prior to exposure to aquatic systems. While valuable insights into the impacts of nanoparticle aging during storage were obtained, information on how the physicochemical characteristics and reactivity of nanomaterials changes when aged directly into aquatic systems remained unassessed. The most relevant aging process would be based on ENMs released from products, which then move through environmental systems[1]. For example, TiO_2 NPs released from paint or cosmetic products and Cu NPs released from antifouling paints or nanopesticides, are likely to age directly in the receiving media[3]. The stability of the NP in a powder state is dependent on its composition [4], and the aging process during storage would therefore differ greatly from an aging process in a complex matrix such as an aquatic system.

Considering the low expected levels of NPs entering the environment[5], high concentrations of 1 g NPs L^{-1} would be physically and chemically different from those formed under more natural processes[6]. The realistic exposure scenario would also be altered if the aged NPs were altered prior to exposure. Even a minor alteration can trigger a major transformation, which may influence or even mitigate the true impact of the aging process of a NP[7]. In this study, for example, the aging conditions of the Cu NP powder were different from the conditions of the solutions that were further analyzed (e.g., dark, rotational conditions). Finally, ecotoxicity tests were not performed to compare the aged NPs to pristine NPs.

Silver (Ag NPs)[8]

In this study, the impacts of chloride ions on NPs undergoing an aging process were assessed. The authors aged polyvinylpyrrolidone-coated Ag NPs (PVP-Ag NPs) in solutions

with > 8 mg L^{-1} of dissolved oxygen (DO), in the presence of three different NaCl concentrations (0.5, 0.1, and 0.01 M) and in DI water, for 12 days in an orbital shaker (100 rpm/min), in the dark at room temperature. The resulting AgCl was used to assess the toxic responses to the *E. coli* bacteria. The authors found that the dissolution of Ag NPs varied with Ag speciation, which was determined by the amount of Ag and Cl^- in the media. For instance, there was a higher dissolution rate in the solutions with a high Cl/Ag ratio than in the DI water control. In solutions with a lower Cl/Ag ratio, however, the dissolution rate of the Ag NPs was slower than the Ag NPs in DI water. The authors indicated that the reaction of the Ag NP surfaces with chloride ions occurred in the first 2 h and that the high Cl/Ag ratio formed more $AgCl_x^{(x-1)-}$ soluble species than solid AgCl.

Initial oxidation of the aged Ag NP surfaces formed soluble Ag species more quickly than the dissolution rate in the DI water system. The effects of *E. coli* on the aged Ag NPs showed an inhibition in growth as a function of Cl^- concentration. For instance, the highest growth inhibition occurred with Ag ions in DI water, followed by Ag NPs in DI water, 0.5 M NaCl, 0.1 M NaCl, and 0.01 M NaCl. The authors suggested that Ag toxicity is due to exposure to soluble species of Ag rather than the effect of Ag NPs and described the importance of the presence of inorganic ligands (Cl^-) when interpreting toxicity data.

For this study, the utilization of DI water as the aging media did not represent natural aquatic systems as it did not consider the natural composition of the aquatic system. The components of such a system would play an important role in the kinetics of the NPs in the environment[9]. A total aging period of less than 30 days would not be enough for some NPs, including Ag NPs, due to their slow dissolution in aqueous media. This is especially true for coated-NPs, the stability of which is improved by chemical synthesis[10]. Again, the aging conditions differed from the exposure conditions. Such differences should be avoided, as NPs

can easily change in response to minor modifications. Also, the omission of natural environmental characteristics, including light/dark cycles and different external stimulations (e.g., shaking speed and intensity) can strongly impact the results of the aged and non-aged NPs even under similar conditions of aging and exposure[7].

Zinc oxide (ZnO NPs)[11]

The freshwater green microalga *Chlorella vulgaris* was used as a model system to determine the ecological impact of aged ZnO NPs. Stock solutions were prepared by suspending 1 g ZnO NPs (20 nm) in 1 L of ultrapure water followed by a 20 min sonication (300 W) and the maintaining of the final solutions at 20 °C for 0, 30, 60, 90, 120, 160 and 210 days. The shapes of the NPs varied. For example, the SEM images did not identify differences between the pristine and the aged ZnO NPs, while the TEM images revealed a sheet-like shape for the ZnO NPs aged for 90 days. This transformation was confirmed by XRD spectroscopy, which showed $Zn_5(OH)_6(CO3)_2$ with some of the ZnO NPs in the aged sample, while a typical wurtzite phase was found for the pristine sample. The sedimentation rate of the pristine ZnO NPs was higher than the aged ZnO NPs.

The specific growth rate after a 20-day exposure period showed different toxicities based on the concentrations and aging periods. For instance, at concentrations of 10 mg L^{-1}, all the aged treatments (ZnO-30 days, ZnO-120 days and ZnO-210 days) showed similar and higher toxicity to microalgae than the pristine sample. However, at 50 mg L^{-1}, the culture exposed to ZnO NPs aged for 30 days displayed the maximum growth inhibition among all the treatments. Results of cell membrane integrity, changes of photosynthesis activity, and the chlorophyll (a) contents of *C. vulgaris* were similar to the highest ZnO NPs' concentration (50 mg L^{-1}), revealing the higher toxicity of the ZnO NPs aged for 30 days in comparison with the other treatments. This higher toxicity during the early aging stage was ascribed to

the gradual increase of released zinc ions from 48 h to 30 days, followed by a steady and a slight reduction in the amount of zinc ions in samples of ZnO NPs aged for longer.

Similar to the aforementioned observations, the pristine and the aged ZnO NPs tested underwent different procedures in the exposure and aging periods. For instance, the cultures were incubated at 26 °C, under artificial lighting (60 μE m^{-2} s^{-1}) with a 16:8 h Light : Dark photoperiod and were shaken three to four times per day. However, the only ambient condition described for the aging process was temperature, which was 20 °C. Furthermore, it is not clear whether the aged stock solutions were sonicated before and/or after the aging period. The stock solutions were aged in ultrapure water and were further diluted with microalgae culture BG11 medium.

Cerium oxide (CeO_2 NPs)[12]

This study assessed the ecotoxicity of non-aged and aged CeO_2 NPs to *Pseudokirchneriella subcapitata* freshwater microalgae. A commercially available CeO_2 NPs (10 nm) suspended in water (248 g L^{-1}), composed of a ceria core coated with a triammonium citrate layer, was diluted in algal growth medium (OECD, 2011) to achieve a stock suspension of 31.25 mg L^{-1}, which was then aged for three and thirty days at 20 °C under magnetic stirring (300 rpm) and artificial lighting (4000-5000 lux). The aged suspensions were diluted to obtain a range of concentrations (from 0.2 to 25 mg CeO_2 L^{-1}) and were then inoculated for microalgae cells in the exponential growth phase. However, all the tests were conducted under different conditions to the aging procedure (e.g., at 22 °C under artificial lighting of 5000-6000 lux). The total exposure period was also relatively short (72 h of incubation). Results of the size distribution of the CeO_2 NPs from the aged suspensions (aged for 3 and 30 days) was similar to those from the non-aged suspension. For instance, the particles were mainly clustered in clusters with weakly-bound particles. In the first 24 h, the

results revealed stable suspensions, followed by a rapid increase in particle size (580 nm after 28 h). At the end of the 3- and 30-day aging period, large particle size distribution was reported (from 7 to 10 mm). Accordingly, even though ecotoxicity to the freshwater microalgae exhibited a clear concentration-response relationship, the EC_x (10, 20, and 50) values calculated for these experiments cannot be regarded as biologically different. The EC_{50} values were 5.6, 4.1, and 6.2 mg L^{-1}, after exposure to non-aged, 3- and 30-day aged suspensions, respectively.

As already mentioned, the procedures used for the aging and exposure conditions were different, and therefore did not represent the natural ecosystem. The amount of light, for example, is an important determinant of NP transformation[13]. This is also true for the high concentrations chosen for the aging process.

Titanium dioxide (TiO_2 NPs) [14]

This work studied the toxic effects of dietary exposure to aged TiO_2 NPs (T-Lite™) used in sunscreen cream on *D. magna*. The aging procedure consisted of stirring commercial TiO_2 NPs in ultrapure water (2:5 ratio) for 48 h under artificial lighting (400 W). After the aging period, 100 mg L^{-1} of the aged stock solution, composed of residues of nanomaterials (RNM) and hereafter referred to as "aged TiO_2 RNM", was used without further treatment for exposure to daphnia and algae. The algae culture *Pseudokirchneriella subcapitata* was inoculated in the medium with nominal concentrations of 0.01, 0.1, 1 and 10 mg aged TiO_2 RNM L^{-1} plus a control, at pH 7.4-7.6, for 3 days, at 21 °C, continuous aeration and lighting at 15 W. At the end of this period (3 days), contaminated algae were used to feed *D. magna* in a 21-day chronic bioassay, using natural water with a total hardness of 200 mg $CaCO_3$ L^{-1}, pH 7.8-8.2, conductivity of 600 mS cm^{-1}, at 22 °C and with a 16:8 h Light : Dark photoperiod.

The overall results from the chronic exposure of daphnia to aged TiO_2 RNM carried by food did not affect mortality but resulted in a reduction in growth and reproduction due partially to digestive physiology modification. For this study, the same considerations reported for the CeO_2 NPs[14] study were observed.

Molybdate-zerovalent iron (Mo-NZVI) nanohybrid [16]

In this study, the release of metal-NZVI nanohybrid into a river was simulated by aging the Mo-NZVI nanohybrid (500 mg NZVI L^{-1} and 20 mg Mo(VI) L^{-1}) for 30 days in solutions prepared in deoxygenated deionized water (DDIW). The aged solutions were then transferred into modified river water (90 % raw river water and 10 % BG-11 medium), containing cyanobacteria, for another 30 days, on a shaking table (250 rpm) at 25 °C. The effects of Mo-NZVI hybrid on the growth and the chlorophyll a (Chl a) of cyanobacteria (*Microcystis aeruginosa*) was assessed. Freshly prepared NZVI was stored in 100 % ethanol. The removal performance of NZVI for Mo (VI) and the transformation of NZVI were monitored during the 30 days exposure period. Results showed that the aging period played an important role in the chemical stabilization of the Mo-NZVI hybrid, and common groundwater ions retarded the stabilizing process, indicating that significant remobilization of Mo (VI) from the hybrid may occur after exposure to water bodies. The aged Mo-NZVI hybrid inhibited the growth of *M. aeruginosa*, but in the presence of HPO_4 2/CO_3 ^{2}, hybrid stabilization was retarded, and aging did not affect cyanobacteria growth. In contrast, low levels of Mo (VI) ions stimulated cyanobacteria growth.

Our observations regarding this study are similar to those previously made. It is crucial to provide a clear and detailed information of the aging procedure adopted for each study. Here, little information is provided about the chosen procedure for the aging treatments, which makes comparison with the exposure conditions difficult. It appears that the aged stock

solutions were prepared in deoxygenated deionized water, and the final aged suspensions was only added into the cyanobacteria media at the end of the total exposure aging period (30 days). However, the likelihood that an NP will age in DI water is very low and does not represent a natural environmental condition. The transformations that occurred during aging will therefore not occur in any realistic aquatic ecosystem. After aging in the DI water, however, the suspensions were aged again, but this time in an environmental realistic media (river). The collected river water was filtered to avoid experimental interferences, but again this filtration somewhat reduces or even eliminates the realism of the natural conditions.

Zerovalent Iron (NZVI) [17]

In this work, nanoscale zerovalent iron (NZVI) particles were studied. A total of 10 g L^{-1} were aged for a period of 1 month and 6 months in nanopure DI water containing 10 mN of common groundwater anion solutions (NO^{3-}, SO_4^{2-}, HCO^{3-}, HPO_4^{2-}, and Cl^-). The aging suspensions were kept in 60 mL bottles which were rotated end-over-end, at 22 °C. Results from suspensions with 1 month of aging showed that the dissolved anions inhibited the oxidation of the NZVI to varying degrees, and the oxidized particles remained predominantly a binary phase system containing Fe0 and Fe_3O_4. Suspensions aged for 6 months, however, showed similar oxidation states to one another, regardless of the anion used, except nitrate. The NZVI surface was passivated by nitrate and resulted in the same mineral and Fe0 content as the fresh NZVI after 6 months of aging.

Of all the studies reviewed, this presented the closest conditions to the aquatic environment. However, it also presented the highest aged concentration of the NPs (10 g NZVI L^{-1}), and ecotoxicity tests were not performed to compare the aged to pristine NPs.

Realistic scenario approach

The role of ecotoxicity assays of aged NPs was recently reviewed [39]. The authors state that further procedures should be carried out with the final aged suspensions to obtain a better understanding of the aged NP itself [39]. For example, the authors argued it is necessary to separate the released particles from the dissolved components to determine if an effect is caused by the nanomaterial or by any of the other components of the test solution [39]. The authors further state that the aged particles can be isolated by purification through repeated washing or dialysis, or by performing control assays with filtrates to separate the effect of the dissolved metals from that of the particles.

The aim of separating the particles from the mixture of dissolved ions through a purification process is appropriate for the production of aged NPs for further testing procedures. However, the transformation process that provided the NPs with a new 'environmental identity' may be lost or changed through any further procedure. Consequently, three important issues remain unclear: the behavior of the NPs in the environment, the link to this new environmental identity, and the effect on toxicity [14].

The behavior and transformations of NPs are mostly unpredictable, and several studies have found differences even in similar experimental setups [41]. This is due to the colloidal complexity of NPs and to their physical and chemical forms. Both are dependent on their surroundings, making the control and manipulation of a NP extremely fragile, and a process that may initiate both biotic and abiotic transformations [42]. As a consequence, the simplest assessment may change the physicochemical properties of the NPs, making analysis susceptible to artifacts [43]. Even storage conditions and time may affect compositional or physical characteristics [40].

There is increasing awareness of the potential for interference when performing assays with NPs. There are a number of reports of the modifications of NPs due to filtration,

repeated washing or dialysis, including phase transition [44] and an increased size and aggregation process[45]. For example, centrifugal filtration may cause the particles to stick to the filter, leading to important losses. In contrast, with dialysis the colloidal nature of all NPs resulted in incompatibility for purification and aggregation occurred [44, 45]. Therefore, to prioritize environmental relevance in the hazard assessment of NPs, further procedures with aged NPs should be carefully implemented through analytical techniques that introduce minimal artifacts to the new physicochemical properties of the aged NPs.

Table S1. Artificial seawater (pH 8.1) used for aging of nano-Cu, according to Kester and collaborators[19], and composition.

Nutrient	Concentration (g L^{-1})
NaCl	23
Na_2SO_4	4
KCl	0.7
KBr	0.1
H_3BO_3	30
$MgCl_2.6H_2O$	10.8
$CaCl_2.2H_2O$	1.5
$SrCl_2$	20
$NaHCO_3$	0.172

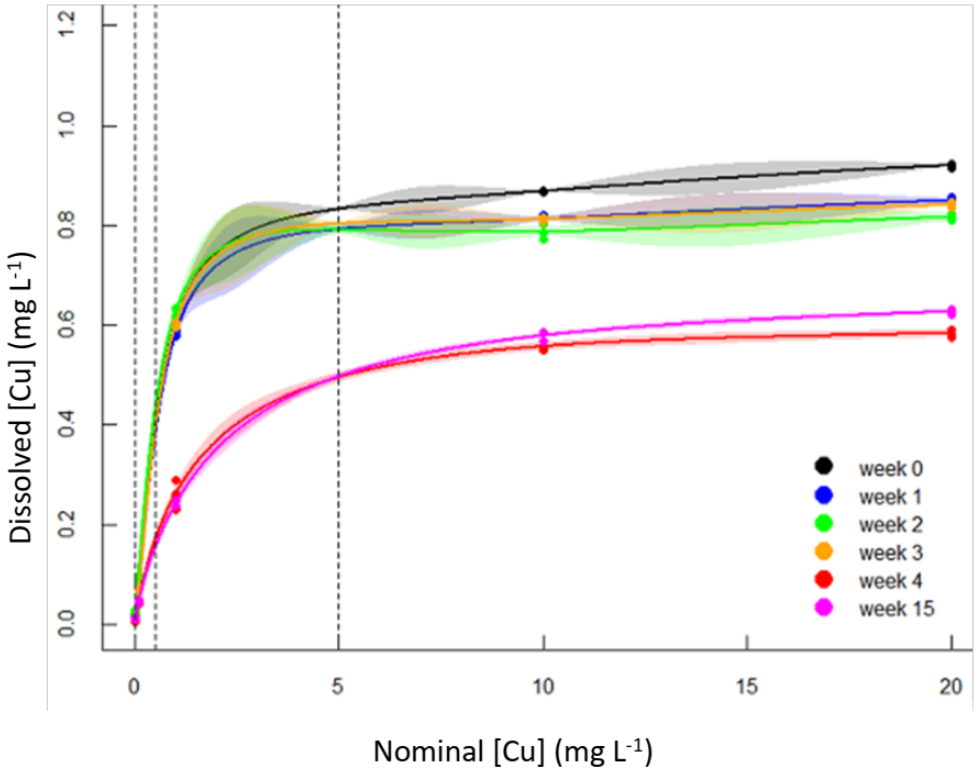

Figure S1. Variation in dissolved Cu concentrations (mg L^{-1}) measured in phytoplankton cultures as a function of nominal Cu concentrations (mg L^{-1}) over the experimental aging periods (weeks). Dots represent Cu concentrations (n=3). Lines and shading represent mean (95 % C.I.) estimated Cu concentrations from semi-parametric regressions (detailed in the experimental section of this paper). Dashed lines represent nominal Cu concentrations (0.01, 0.5, and 5) where the corresponding estimated dissolved Cu concentrations were not measured from the solutions but taken from the curves.

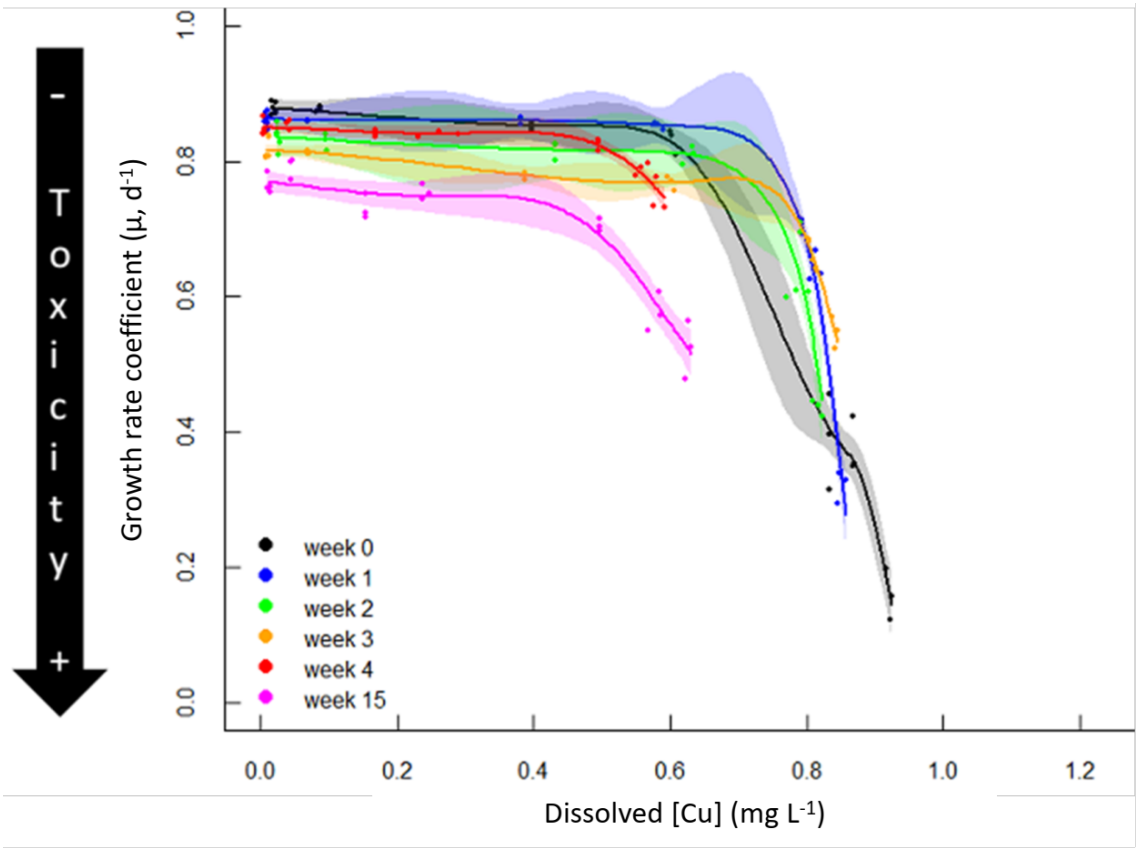

Figure S2. Growth rate coefficient of marine phytoplankton microcosms as a function of dissolved Cu concentrations (mg L^{-1}) over the experimental aging periods (weeks). Dots represent Cu concentrations (n=3). Lines and shading represent mean (95% C.I.) estimated Cu concentrations from semi-parametric regressions (detailed in the experimental section of this paper).

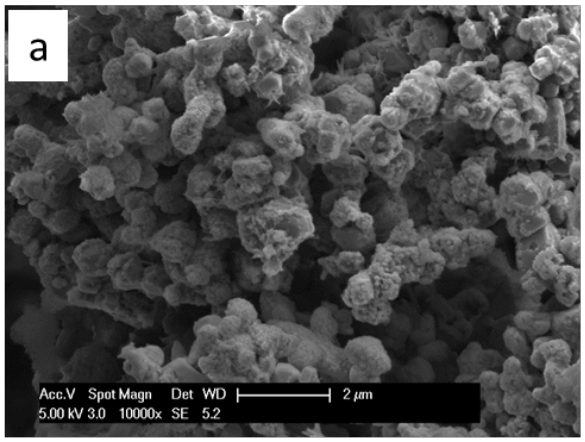

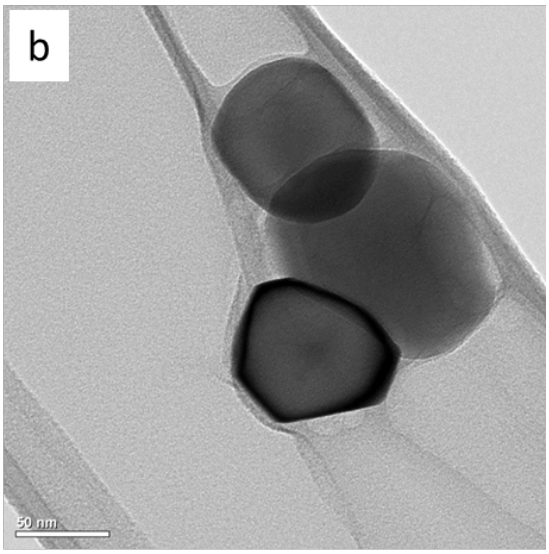

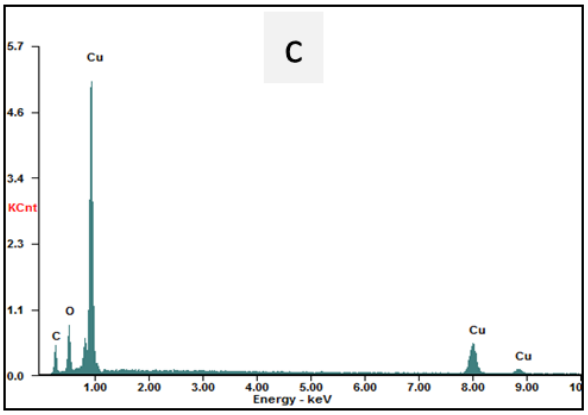

Element	Weight %	Atomic %
C	10.46	33.35
O	7.08	16.95
Cu	82.46	49.69
	100	100

Figure S3. Characterization of the nanoparticle used in this study: (a) Scanning and (b) transmission electron micrographs of nanosized copper (nano-Cu), (c) EDS spectrum of nano-Cu, with elemental composition shown in the table.

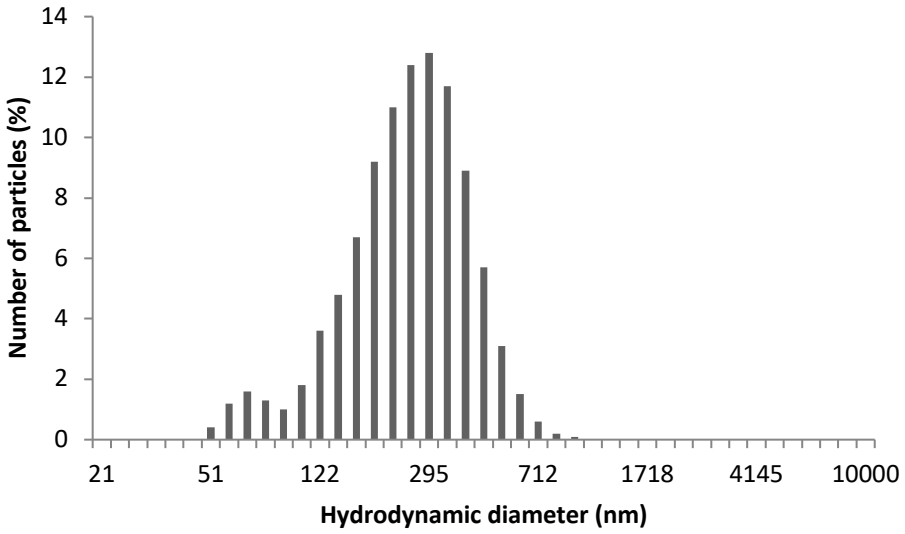

Figure S4. The size distribution of the particles in aging stocks (20 mg Cu L^{-1}) collected over 1 h, showing particle aggregation, with a small fraction remaining below 100 nm.

Table S2. Concentrations of different copper fractions detected in nano-Cu (20 mg L^{-1}) stock solutions without aging (pristine) and aged (up to 15 weeks) in artificial seawater under environmental conditions.

Aging periods (weeks)	Cu speciation	Cu concentrations (mg L^{-1})
0	**Dissolved**	0.8
	Nano	0.2
	Bulk	17.5
1	**Dissolved**	0.6
	Nano	0.1
	Bulk	16.6
2	**Dissolved**	0.8
	Nano	0.0
	Bulk	17.2
3	**Dissolved**	0.53
	Nano	0.1
	Bulk	17.2
4	**Dissolved**	0.03
	Nano	0.1
	Bulk	16.2
15	**Dissolved**	0.01
	Nano	0.0
	Bulk	15.7

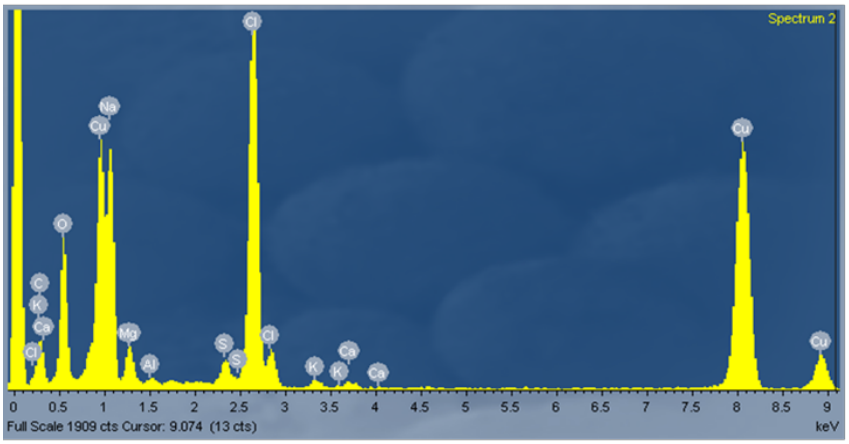

Element	Weight%
C	15.65
O	16.3
Na	15.28
Mg	2.16
Al	0.32
S	1.27
Cl	21.71
K	0.45
Ca	0.31
Cu	26.55

Figure S5. Energy-dispersive X-ray Spectroscopy (EDS) of nano-Cu aged in seawater over the 15 wk period, showing elemental composition by weight.

Table S3. Abundance (%) of Cu species at equilibrium in artificial seawater predicted by Visual MINTEQ.

Cu species	Abundance (%)
Cu^{+}	-
CuCl (aq)	0.7
$CuCl_2^{-}$	82
$CuCl_3^{2-}$	17
Cu^{2+}	-
CuBr (aq)	0.0

Table S4. Concentrations of dissolved and nanosized Cu (mg Cu L^{-1}) detected in cultures of *Dunaliella tertiolecta* exposed nano-Cu previously aged for different periods in artificial seawater. ND = not detected.

Aging time (wk)	[Cu] (mg/L)	Day 1		Day 3		Day 5	
		Dissolved	Nano	Dissolved	Nano	Dissolved	Nano
0	0	0.023	0.022	0.023	ND	0.017	ND
	0.1	0.095	0.000	0.100	0.008	0.085	0.000
	1	0.595	0.001	0.476	0.162	0.603	0.008
	10	0.881	0.007	0.884	ND	0.868	0.010
	20	0.914	0.035	0.924	0.019	0.920	0.008
1	0	0.010	0.002	0.006	ND	0.009	ND
	0.1	0.121	ND	0.075	0.001	0.069	ND
	1	0.569	0.020	0.587	0.026	0.583	0.009
	10	0.799	0.006	0.818	0.134	0.812	0.010
	20	0.843	0.007	0.842	0.019	0.850	0.003
2	0	0.028	0.002	0.027	ND	0.027	0.004
	0.1	0.086	0.001	0.098	0.002	0.096	0.003
	1	0.368	ND	0.554	0.002	0.628	0.014
	10	0.689	ND	0.788	0.002	0.786	0.019
	20	0.788	0.022	0.825	ND	0.816	0.012
3	0	0.018	ND	0.015	0.004	0.009	ND
	0.1	0.079	0.002	0.080	0.005	0.070	0.001
	1	0.533	0.010	0.610	ND	0.601	0.009
	10	0.745	0.021	0.819	ND	0.812	0.026
	20	0.801	0.024	0.848	ND	0.841	0.012
4	0	0.010	ND	0.009	0.014	0.005	0.006
	0.1	0.021	ND	0.034	0.000	0.042	0.003
	1	0.095	0.002	0.174	0.007	0.261	0.011
	10	0.252	ND	0.454	0.036	0.558	0.015
	20	0.328	ND	0.536	0.016	0.582	0.021
15	0	0.000	0.000	0.014	ND	0.012	0.000
	0.1	0.011	ND	0.034	0.001	0.045	ND
	1	0.077	ND	0.177	0.002	0.240	0.000
	10	0.218	ND	0.434	0.012	0.579	0.003
	20	0.277	ND	0.538	0.025	0.626	0.007

Table S5. Results of two-way ANOVA for dissolved Cu concentration data (mg L^{-1}) detected in the phytoplankton cultures with 0 wk aging treatment. There were five different nominal Cu concentrations (mg L^{-1}): 0, 0.1, 1, 10, and 20 mg L^{-1}. The exposure times were day 1 and day 5. More detailed characteristics of aging media and cultures are found in the Methods section.

Source	*df*	SS	*MS*	*F-value*	P-value
Concentration (C)	4	4.33	1.08	56670.4	$p < 0.0001$
Day (D)	1	0.00	0.00	2.9	$p > 0.05$
C x D	4	0.00	0.00	7.1	$p < 0.0001$
Residuals	20	0.00	0.00		
Total	29	4.33	1.08		
Model R-squared:	1.00				

Note — *df* = Degree of freedom, SS = Sum squares, MS = Mean squares.

Table S6. Results of two-way ANOVA for dissolved Cu concentration data (mg L^{-1}) detected in the phytoplankton cultures with 15 wk aging treatment. There were five different nominal Cu concentrations (mg L^{-1}): 0, 0.1, 1, 10, and 20 mg L^{-1}. The exposure times were day 1 and day 5. More detailed characteristics of aging media and cultures are found in the Methods section.

Source	*df*	SS	*MS*	*F-value*	P-value
Concentration (C)	4	1.03	0.26	4674.4	$p < 0.0001$
Day (D)	1	0.25	0.25	4617.0	$p < 0.0001$
C x D	4	0.17	0.04	759.2	$p < 0.0001$
Residuals	20	0.00	0.00		
Total	29	1.45	0.55		
Model R-squared:	0.99				

Note — *df* = Degree of freedom, SS = Sum squares, MS = Mean squares.

Table S7. Results of two-way ANOVA for dissolved Cu concentration data (mg L^{-1}) detected in the phytoplankton cultures with 3 wk aging treatment. There were five different nominal Cu concentrations (mg L^{-1}): 0, 0.1, 1, 10, and 20 mg L^{-1}. The exposure times were day 1 and day 5. More detailed characteristics of aging media and cultures are found in the Methods section.

Source	*df*	SS	*MS*	*F-value*	P-value
Concentration (C)	4	3.55	0.89	13197.2	$p < 0.0001$
Day (D)	1	0.01	0.01	107.9	$p < 0.0001$
C x D	4	0.01	0.00	33.6	$p < 0.0001$
Residuals	20	0.00	0.00		
Total	29	3.56	0.90		
Model R-squared:	0.90				

Note — *df* = Degree of freedom, SS = Sum squares, MS = Mean squares.

Table S8. Results of two-way ANOVA for dissolved Cu concentration data (mg L^{-1}) detected in the phytoplankton cultures with 4 wk aging treatment. There were five different nominal Cu concentrations (mg L^{-1}): 0, 0.1, 1, 10, and 20 mg L^{-1}. The exposure times were day 1 and day 5. More detailed characteristics of aging media and cultures are found in the Methods section.

Source	*df*	SS	*MS*	*F-value*	P-value
Concentration (C)	4	1.03	0.26	1716.2	$p < 0.0001$
Day (D)	1	0.16	0.16	1096.5	$p < 0.0001$
C x D	4	0.11	0.03	191.2	$p < 0.0001$
Residuals	20	0.00	0.00		
Total	29	1.31	0.45		
Model R-squared:	0.97				

Note — *df* = Degree of freedom, SS = Sum squares, MS = Mean squares.

Table S9. Results of two-way ANOVA for Cu uptake data presented as Cu µg cells^{-1} x 10^6 and normalized by number of cells. There were four different aging periods: 0 wk, 3 wk, 4 wk, and 15 wk. The nominal Cu concentrations were: 0, 0.01, 0.1, 0.5, and 1 mg L^{-1}. More detailed uptake procedures are found in the Methods section.

Source	*df*	SS	*MS*	*F-value*	P-value
Aging (A)	3	14506	3627	139.63	$p < 0.0001$
Concentration (C)	4	12161	4054	156.07	$p < 0.0001$
A x C	12	15873	1323	50.93	$p < 0.0001$
Residuals	20	519	26		
Total	39	43059	9030		
Model R-squared: 0.97					

Note — *df* = Degree of freedom, SS = Sum squares, MS = Mean squares.

Table S10. Results of two-way ANOVA for phytoplankton population growth rate coefficient (μ, d^{-1}) data normalized by number of cells. There were four different aging periods: 0 wk, 3 wk, 4 wk, and 15 wk. The nominal Cu concentrations were: 0, 1, 5, 10, and 20 mg L^{-1}. More detailed growth rate coefficient procedures are found in the Methods section.

Source	*df*	SS	*MS*	*F-value*	P-value
Aging (A)	3	1.3	0.3	307.7	$p < 0.0001$
Concentration (C)	4	1.1	0.4	328.7	$p < 0.0001$
A x C	12	0.7	0.1	53.4	$p < 0.0001$
Residuals	40	0.0	0.0		
Total	59	3.1	0.7		
Model R-squared:	0.94				

Note — *df* = Degree of freedom, SS = Sum squares, MS = Mean squares.

Table S11. Results of two-way ANOVA for intracellular reactive oxygen species (ROS) production data normalized by number of cells. There were four different aging periods: 0 wk, 4 wk, and 15 wk. The nominal Cu concentrations were: 0, 0.01, 0.1, 0.5, 1, 5, 10, and 20 mg L^{-1}. More detailed intracellular ROS assay procedures are found in the Methods section.

Source	*df*	SS	*MS*	*F-value*	P-value
Aging (A)	2	1.4×10^{5}	6.9×10^{6}	260.3	$p < 0.0001$
Concentration (C)	5	3.2×10^{5}	6.4×10^{6}	241.9	$p < 0.0001$
A x C	10	1.4×10^{5}	1.4×10^{6}	52.5	$p < 0.0001$
Residuals	630	1.7×10^{5}	2.6×10^{8}		
Total	647	7.6×10^{5}	1.5×10^{5}		
Model R-squared: 0.45					

Note — *df* = Degree of freedom, SS = Sum squares, MS = Mean squares.

References

1. Nowack, B. & Mitrano, D. M. Procedures for the production and use of synthetically aged and product released nanomaterials for further environmental and ecotoxicity testing. *NanoImpact* **10**, 70–80 (2018).
2. Mudunkotuwa, I. A., Pettibone, J. M. & Grassian, V. H. Environmental implications of nanoparticle aging in the processing and fate of copper-based nanomaterials. *Environmental Science and Technology* **46**, 7001–7010 (2012).
3. Keller, A. A. *et al.* Comparative environmental fate and toxicity of copper nanomaterials. *NanoImpact* **7**, 28–40 (2017).
4. Lipiäinen, T., Peltoniemi, M., Räikkönen, H. & Juppo, A. Spray-dried amorphous isomalt and melibiose, two potential protein-stabilizing excipients. *International Journal of Pharmaceutics* **510**, 311–322 (2016).
5. Garner, K. L., Suh, S. & Keller, A. A. Assessing the Risk of Engineered Nanomaterials in the Environment: Development and Application of the nanoFate Model. *Environmental Science and Technology* **51**, 5541–5551 (2017).
6. Mouneyrac, C., Syberg, K. & Selck, H. Ecotoxicological Risk of Nanomaterials. in *Aquatic Ecotoxicology* 417–440 (Elsevier, 2015). doi:10.1016/B978-0-12-800949-9.00017-6
7. von der Kammer, F. *et al.* Analysis of engineered nanomaterials in complex matrices (environment and biota): General considerations and conceptual case studies. *Environmental Toxicology and Chemistry* **31**, 32–49 (2012).
8. Levard, C. C. *et al.* Effect of Chloride on the Dissolution Rate of Silver Nanoparticles and Toxicity to E. coli. (2013). doi:10.1021/es400396f

9. Conway, J. R., Adeleye, A. S., Gardea-Torresdey, J. & Keller, A. A. Aggregation, dissolution, and transformation of copper nanoparticles in natural waters. *Environmental Science and Technology* **49**, 2749–2756 (2015).
10. Abramenko, N. B. *et al.* Ecotoxicity of different-shaped silver nanoparticles: Case of zebrafish embryos. *Journal of Hazardous Materials* **347**, 89–94 (2018).
11. Zhang, H., Huang, Q., Xu, A. & Wu, L. Spectroscopic probe to contribution of physicochemical transformations in the toxicity of aged ZnO NPs to Chlorella vulgaris: new insight into the variation of toxicity of ZnO NPs under aging process. *Nanotoxicology* **10**, 1177–1187 (2016).
12. Manier, N., Bado-Nilles, A., Delalain, P., Aguerre-Chariol, O. & Pandard, P. Ecotoxicity of non-aged and aged CeO 2 nanomaterials towards freshwater microalgae. *Environmental Pollution* **180**, 63–70 (2013).
13. Klaine, S. J. *et al.* NANOMATERIALS IN THE ENVIRONMENT: BEHAVIOR, FATE, BIOAVAILABILITY, AND EFFECTS. *Environmental Toxicology and Chemistry* (2008). doi:10.1897/08-090.1
14. Fouqueray, M. *et al.* Effects of aged TiO 2 nanomaterial from sunscreen on Daphnia magna exposed by dietary route. *Environmental Pollution* **163**, 55–61 (2012).
15. Carpenter, S. R. *et al.* NONPOINT POLLUTION OF SURFACE WATERS WITH PHOSPHORUS AND NITROGEN. *Ecological Applications* **8**, 559–568 (1998).
16. Su, Y. *et al.* Impact of ageing on the fate of molybdate-zerovalent iron nanohybrid and its subsequent effect on cyanobacteria (Microcystis aeruginosa) growth in aqueous media. *Water Research* **140**, 135–147 (2018).

17. Reinsch, B., Forsberg, B., Penn, R. L. E. E. & Kim, C. S. Chemical Transformations during Aging of Zerovalent Iron Nanoparticles in the Presence of Common Groundwater Dissolved Constituents. *Environ. Sci. ...* 3455–3461 (2010).
18. Holden, P. A. *et al.* Considerations of Environmentally Relevant Test Conditions for Improved Evaluation of Ecological Hazards of Engineered Nanomaterials. *Environ. Sci. Technol.* **50**, 6124–6145 (2016).
19. Kester, Dana R., Duedall, Iver W., Connors, Donald N., Pytkowicz, R. M. PREPARATION OF ARTIFICIAL SEAWATER. 176–178 (1967).

Chapter 3. Aging in freshwater increases copper nanoparticle toxicity to marine phytoplankton.

This work will be submitted for publication. Target journal: Scientific Reports.

Key words: Nanomaterials; nanoparticles; ecotoxicity; environmental conditions; aquatic ecosystems.

3.1. Abstract

The fate, behavior, and toxicity of engineered nanomaterials (ENMs) is influenced by environmental conditions, and interaction between the environment and the chemical properties of a nanomaterial. Aquatic ecosystems are an important sink for ENMs released into the environment, especially those materials that are released by accident or on purpose into wastewater treatment systems, point and non-point source runoff, of the atmosphere. Understanding how ENMs transform chemically in their passage through aqueous media to aquatic ecosystem sinks, such as estuaries, is important to assess environmental risks of nanotechnology. I tested whether the chemical transformations of copper nanoparticles (Cu NPs), experienced as the particles aged in freshwater over different periods of time, influence their toxicity to phytoplankton (*Dunaliella tertiolecta*). Specifically, I examined the aging of Cu NPs in a mesocosm system designed to mimic the passage of material through a freshwater riverine system over a period of days-weeks, and the subsequent toxicity the aged NPs had on coastal marine phytoplankton. Aging enhanced the bioavailability of the toxic Cu species and thus increased toxicity to marine phytoplankton populations. The relatively slow rate of morphological changes observed in Cu NPs facilitated an increase in total dissolved Cu availability (mg L^{-1}) over time. Further dissolution through Cu aging occurred in phytoplankton cultures, leading to a substantial increase in total intracellular Cu uptake and toxicity. The results of the experiment indicate that Cu NPs aged in freshwater systems are toxic to *D. tertiolecta* and that Cu toxicity primarily results from ion rather than nanoparticle exposure.

3.2. Introduction

A major challenge for ecotoxicologists is predicting how natural environmental conditions modify anthropogenic contaminants, including complex engineered materials, thereby enhancing or decreasing their toxicity to humans and other organisms[1]. Many engineered nanomaterials (ENMs), especially nanoparticles (NPs), interact with and change through environmental exposure, thereby influencing their fate, transport, and toxicity[2]. This is especially true in aquatic ecosystems, through which materials can pass rapidly over long distances, and within which they are exposed to and potentially modified by a wide variety of complex environmental matrices[3–5]. Freshwater (FW) ecosystems, mainly rivers and streams, act important natural conduits for many anthropogenic chemicals, including ENMs that eventually can accumulate in coastal estuaries and lagoons[6]. Assessing the ecological risks of ENMs that pass through FW ecosystems to eventually settle in coastal aquatic ecosystems presents a suite of challenging, management-relevant scenarios for researchers focused on the environmental implications and impacts of nanotechnology.

Copper nanoparticles (Cu NPs) are expected to enter natural aquatic environments in ever-increasing amounts[5,7,8]. FW ecosystems are particularly at risk, in part because studies of ENM chemistry suggest transport through rivers and streams provide major routes of passage to downstream estuaries; and low ionic strength (IS) in FW increases ENM stability (i.e., the capacity to remain suspended in water), thereby reducing the probability that the materials are sequestered through deposition and sedimentation[9]. The ecological risk of stable ENMs, including Cu NPs, suspended for different periods of time in FW is not well understood, especially because the materials can transform chemically, or "age". Cu is an essential trace metal for aquatic organisms but is also highly toxic, even at very low concentrations (ppb levels)[10–13]. Mechanisms of toxicity include interference with

osmoregulation due to enzyme inhibition, the reduction of total antioxidant capacity, and increased intracellular ROS production[14,15]. Biological injuries are caused primarily by free Cu cations, usually in the Cu^{+2} form, that are made bioavailable through dissolution but potentially also made less bioavailable through complexation with organic matter and salts. The process of chemical aging in Cu NPs, and their potential eventual toxicity to organisms, therefore depends heavily on the degree to which free Cu ions are made available through dissolution or bound up in complex inorganic or organic matrices.

It is reasonable to predict that the length of time Cu NPs pass through a FW ecosystem, after being released into the environment, influences their potential bioavailability and toxicity to organisms once they reach coastal marine ecosystems. Nevertheless, ecological rick assessments of ENMs to date have largely ignored realistic environmental scenarios[1,5,16,17], such as flowing down river, and as a result we do not adequately understand how realistic fate and transport processes influence NP toxicity, or more generally the ecological risks NPs pose when released into the environment[1,5]. Research of ENM toxicity has focused mainly on the responses of organisms to freshly prepared pristine materials[5,18], while only a few have addressed the toxicity of nanoparticles which have been transformed or "aged" under realistic environmental conditions[16,19,20].

Here I tested whether Cu NPs aged in freshwater for different time periods (days-weeks) impacted the coastal marine phytoplankton species, *Dunaliella tertiolecta*. A mesocosm freshwater system was designed to mimic the aging of the materials over different time periods as they flowed down river to coastal marine ecosystems. Marine phytoplankton were used as a model population as they are holopelagic organisms that support significant and vital components of the productivity and biodiversity of the ocean[21]. Pelagic ecosystems are also heavily exploited, receiving several anthropogenic contaminants, including Cu NPs[5,22].

The fate and transport processes of pristine Cu NPs in freshwater are well known[23,24]. We also know the that the growth rate coefficient of phytoplankton populations can decline in the presence of Cu particles[11,25], while Cu uptake[25] and intracellular ROS generation increases[11]. To address the general question of how aging in FW influences the toxicity of coastal marine phytoplankton, I addressed the following hypotheses: (1) Aging of Cu NPs in FW increase their uptake in *D. tertiolecta*; (2) that aging increases the relative toxicity of Cu NPs, in terms of phytoplankton population growth rate coefficients; and, (3) that toxicity increased with ROS production by phytoplankton cells. These hypotheses were tested using descriptive two-way ANOVA models to quantitatively describe the exposure dose and time dependence of aging, Cu speciation, intracellular Cu uptake, growth rate and intracellular ROS production, factors which provide useful information for assaying the risk of this emerging contaminant for marine ecosystems, under environmentally realistic conditions.

3.3. Methods

The hypotheses were tested using an experimental scenario that was designed to mimic the transport and behavior of Cu NPs moving down a freshwater river. The NPs were aged over different time periods (days-weeks) and were then mixed (i.e. transformed) in saltwater.

Cu NPs characterization

Cu NPs were obtained from US Research Nanomaterials (Houston, TX). Primary particle size measurements were conducted with a transmission electron microscopy or TEM (FEI Titan 300 kV FEG with an Oxford INCA x-sight probe for energy-dispersive X-ray spectroscopy or EDS). Morphology was analyzed by scanning electron microscopy or SEM (FEI XL30 Sirion equipped with an EDAX APOLLO X probe for EDS). The average initial

hydrodynamic diameter (HDD), particle size distribution, and zeta (ζ) potential of the Cu NPs were measured on a Malvern Instruments Zetasizer Nano-ZS90 instrument (Malvern, UK) in solutions of deionized (DI) water (Barnstead Nanopure diamond) with 2 mM phosphate buffer (pH 8) and in the aging media (simulated freshwater)[26]. Additional characterizations of the Cu NPs have been previously reported[23].

Stock solution preparation (aging media) and behavior of Cu NPs during aging

Simulated freshwater media (pH 7.3) were produced in accordance with EPA method 1003.0[27]. EDTA was not added to the media to avoid affecting the dissolved metal measurements. The composition of freshwater is shown in Table S1. Stock solutions were created by adding a single dose of 20 mg-Cu NPs L^{-1} to simulated sterilized freshwater, followed by sonication in a water-bath for 1 h (CPX8800H, Branson Ultrasonics, Danbury, CT), to assure the NPs were optimally dispersed so that the aging treatments were uniformly dosed. Cu NPs stock solutions were then aged for 0, 1, 2, 3, 4, and 15 weeks (one flask per aging period) under conditions simulating the surface of natural freshwater ecosystems, as follows: 14:10 h Light : Dark photoperiod, 80–120 µmol m^{-2} s^{-1}, at a temperature of 20 °C, and constantly mixed at 120 rotations per min on a rotary shaker (New Brunswick Scientific Co., NJ, USA).

Prior to the phytoplankton experiments described below, aged Cu NPs from all the stock solutions (20 mg-Cu L^{-1} aged for 0, 1, 2, 3, 4, and 15 wk in simulated freshwater) were analyzed for the dissolved, nanosized and bulk fractions, and assessed as described in a previous study by our group (Vignardi et al., 2019 in prep). Further DLS (Malvern Zetasizer ZS90) and TEM (FEI Titan) measurements were conducted to evaluate the size distribution, state of dispersion, and zeta potential of the aged Cu NPs. As well as the behavior and

transformations of the aged Cu NPs indicated above, the unmodified Visual MINTEQ 3.0 model[23] was used to estimate subsequent Cu speciation and complexation in the aging stock solutions at equilibrium. The concentration of Cu NPs was input as finite solids based on their pristine copper content; the components of the simulated freshwater and seawater media therefore yielded the Cu ions detected in the experiment.

Cell culture and exposure of aged Cu NPs to *Dunaliella tertiolecta*

Marine phytoplankton cultures of *Dunaliella tertiolecta* (Chlorophyceae: Chlamydomonadales) were obtained from the Provasoli-Guillard National Center for Culture of Marine Phytoplankton (Bigelow Laboratory for Ocean Sciences, West Boothbay Harbor, Maine, USA). Culture cells were maintained in standard media (f/2) without silicate[28] in artificial seawater made from sterilized deionized (DI) water (Barnstead Nanopure diamond), pH 8.1, with 35‰ salinity[29]. The composition of artificial seawater is shown in Table S2.

To obtain the inoculant for the experiments, the algae were incubated in 125 mL polycarbonate flasks with a media volume of 80 mL, under the same conditions for all the aged Cu NPs stock solutions (14:10 h Light : Dark cycles, 80–120 µmol m^{-2} s^{-1}, at 20 °C, constantly mixed on a rotary shaker at 120 rpm) until log phase growth occurred. The cell numbers were counted every day with a Neubauer hemocytometer (Reichert, 120 Buffalo NY) at 200 × magnification, and with a fluorometer (Trilogy, Turner Designs) by converting the fluorescence measurements into the number of cells, calibrated with a standard curve.

At the end of each aging period, the pH and the salinity of each freshwater aged stock solution was adjusted to 8.1 and 35 ‰, respectively, by adding and mixing the same salts used to prepare the artificial seawater[29] for the marine phytoplankton cultures. Phytoplankton culture flasks inoculated with ~ 15 x 10^3 cells mL^{-1} in 3 replicates were then exposed to the

adjusted aged stock solutions diluted to Cu concentrations of 0, 0.01, 0.1, 0.5, 1, 5, 10, and 20 mg L^{-1}, hereafter referred to as the "nominal Cu concentrations".

The phytoplankton were exposed to the aged Cu NPs for five days. The cell densities were monitored every day by sampling 1 mL of each replicate treatment. Additional aliquots of 10 mL were removed from cultures exposed to nominal Cu concentrations of 0, 0.1, 1, 10, and 20 mg-Cu L^{-1} after 1, 3, and 5 days to determine the dissolved Cu fraction and the nano Cu fraction in the cultures exposed to the Cu NPs previously aged in simulated freshwater media.

The dissolution of the Cu NPs was quantified by measuring the amount of ionic Cu (Cu^{+1}, Cu^{+2}) present in the nominal Cu concentrations of 0, 0.1, 1, 10, and 20 mg L^{-1}, hereafter referred to as the "dissolved Cu concentrations". A semi-parametric regression approach based on generalized linear mixed-effect models (GLMMs) and penalized-splines[30] was used to evaluate the variability of the Cu dissolution rate with increasing nominal Cu concentrations at different stages of aging. The dissolved Cu concentrations for the solutions for which the Cu ions were not directly measured, i.e. the nominal Cu concentrations of 0.01, 0.5, and 5 mg L^{-1}, were estimated using the dissolution curves obtained from the semi-parametric regression statistical analyses (Figure S1).

All the exposed phytoplankton culture flasks were kept under the same ambient conditions as the freshwater aging stocks throughout the experiment. These include culture medium, temperature, light cycle, light intensity, and rotatory shaking. Other than the differing water compositions of the media, freshwater and seawater, a consistent exposure scenario was maintained, so that these factors did not adversely affect Cu NPs transformation during aging.

Cu uptake in phytoplankton cells

Intracellular Cu uptake in the marine phytoplankton was detected using the method described by Levy and collaborators[31], with modifications. Aliquots of 5 mL from each replicate were placed in 15 mL polypropylene centrifuge tubes, and the algal cells were concentrated via centrifugation for 4 min at 2,500 rpm (RC 5B Plus, Sorvall, CT). The intact algal cells (pellet) were rinsed with 5 mL seawater, centrifuged again, and washed in EDTA solution for 20 min (0.01 M EDTA, 0.1 M KH_2PO_4/ K_2HPO_4 buffer pH 6, salinity adjusted to 35 ‰). The washed samples were centrifuged, the supernatant was subsequently discharged and the pellet was rinsed again using 5 mL of seawater, following which centrifugation was performed as described above. The final pellet was digested overnight in 1 mL of concentrated trace-metal grade HNO_3 (Fisher Scientific). Digested final samples were diluted to 7% nitric acid and analyzed using ICP-AES (iCAP 6300, Thermo Scientific). Uptake analysis was carried out at the end of the experiment (5 days) using three replicate flasks per treatment and a seawater control. The *D. tertiolecta* cultures were exponential growth in all the experiments performed. All the intracellular Cu uptake data were normalized by cell number.

Phytoplankton population growth rate coefficients

The phytoplankton growth rate coefficient (μ, d^{-1}) was estimated using linear regression over natural logarithm transformed cell densities against time, such as $\ln(N_2/N_1)/(t_2-t_1)$, where N_1 and N_2 are the cell concentrations on two consecutive days, and t_1 and t_2 are time 1 and time 2, respectively[32]. The phytoplankton cell densities of each treatment were measured by sampling a 1 mL aliquot from each replicate which was then analyzed with a hemocytometer or fluorometer. Fluorescence was converted to chlorophyll a concentration

(μg L^{-1}) using a standard curve made with Turner Designs Liquid Primary Chlorophyll a Standards. All experiments were performed with exponentially growing cultures of *D. tertiolecta*, and all the growth rate coefficient data were normalized by cell number.

Cellular reactive oxygen species (ROS)

The effects of the aged Cu NPs on ROS levels were investigated using the general oxidative stress indicator dichlorofluorescein (CM-H_2DCFDA), purchased in dried aliquots of 50 μg from Invitrogen Molecular Probe (Eugene, OR, USA). This free radical sensor for ROS in marine phytoplankton cells is a chloromethyl derivative of H_2DCFDA and exhibits excellent retention in live cells. Prior to starting the incubation (~ 30 minutes before) the probe aliquots were dissolved in 50 μL of anhydrous dimethyl sulfoxide (DMSO, Fisher Scientific). Meanwhile, aliquots of 250 μL from each phytoplankton culture treatment were loaded into black 96-well plates, and incubated for 45 min at 20°C, in the dark, with a final concentration of 4 μg mL^{-1} of CM-H_2DCFDA. The probe diffuses into the cells and its acetate and thiol-reactive chloromethyl groups react with intracellular esterase, glutathione, and other thiols, producing a fluorescent adduct generated by subsequent oxidation inside the cells[33].

The generation of ROS was determined both biotically and abiotically, at 485 nm (excitation) and 530 nm (emission) wavelengths in a microplate reader (Synergy H1, BioTek). All the assays were performed at the end of the experiment (5 days) using three replicate flasks per treatment and controls including seawater + Cu concentrations of 1, 10, and 20 mg L^{-1} (no algae), and seawater + algae (no copper). The values given in the graphs were blank-corrected fluorescence intensity units (FIU). Each experiment was repeated four times to account for the inherent variability between replicates. The dye concentration and

staining time were optimized with a positive control (five increasing concentrations from 0 to 200 mg L^{-1} of H_2O_2 standards solutions) with a sodium phosphate buffer (25 mM, pH 7.2) before running the test samples, to give the best signal-to-background ratio (data not shown). All the ROS data were normalized by cell number, and the ROS levels generated for each treatment were calculated by comparing the mean differences between the aged Cu NPs exposed treatments and their respective controls, as follow:

Relative ROS level (%) = 1 + (Mean DCF fluorescence $_{[\text{aged Cu NPs-treated}]}$ − Mean DCF fluorescence $_{[\text{Control}]}$) / Mean DCF fluorescence $_{[\text{Control}]}$ × 100[34].

Statistical analyses

To assess the differences between the mean responses of the marine phytoplankton after exposure to aged nano-Cu in freshwater media, separate two-way ANOVAs were used to test whether the mean total Cu uptake, mean population growth rate coefficients, and mean total ROS production responded to the aging period (0, 3, and 15 wk) and nominal Cu concentration (0, 0.01, 0.1, 0.5, 1, 5, 10, and 20 mg L^{-1}) of the treatments, and the interaction between them. Prior to ANOVA, all data were square root transformed and tested for heterogeneity of variance using Levene's test. The transformed data passed the subsequent Levene's testing for homogeneity of variance ($P > 0.05$). Differences between the specific treatments were determined with Tukey's honestly significant difference (HSD) post hoc tests ($P < 0.01$). All statistical analyses were conducted in R (R Development Core Team, 2018) and Excel.

3.4. Results

Cu NPs characterization

The Cu NPs were highly aggregated (between 500 nm and 1000 nm in diameter) in their pristine, dry powder states. The primary particle size of the Cu NPs, however, ranged from 30 - 100 nm, as shown by TEM analysis (Figure S2 a and b). The surface chemical composition of Cu NPs was calculated at 82.46 % Cu by weight via EDS analysis (Figure S2), and 83.3 wt. % via ICP-AES analysis. The purity of the Cu NPs used in this study was therefore taken as 83 % for the aging and exposure experiments. The major impurities were calculated at 10.46 % C, and 7.08 % O by weight calculated via EDS analysis.

Cu NPs size distribution, or the particle size in solution, analyzed via dynamic light scattering (DLS), revealed particles with a large hydrodynamic diameter (HDD) of 2326 ± 163.4 nm in the DI water (with 2 mM phosphate buffer, pH 8). Aggregation of the Cu NPs also occurred in all freshwater aging stock solutions (Figure S3), demonstrating high particle polydispersity (HDD = 2782 ± 477.6 nm). The surface charge of Cu NPs was low (ζ potential of -21.2 ± 0.8 mV) in the DI water, but the relatively low salinity of the freshwater aging stock solutions caused some charge screening, leading to a ζ potential of -15.7 ± 0.2 mV.

Behavior of Cu NPs during aging in freshwater stock solutions

The transformation of the aged stock solutions of 20 mg-Cu NPs L^{-1} in the simulated freshwater ecosystem was similar across all the aging periods (Figure 1). Aggregation of the Cu NPs was high in all the aging media tested. In terms of size, bulk Cu was identified as the most abundant Cu species, irrespective of the aging media. The mean total bulk Cu concentration was 18.93 in the 0 wk aging treatment, 24.02 in the 3 wk aging treatment, and 19.10 mg L^{-1} in the 15 wk aging treatment (Table S3).

The changes in the morphology of the Cu NPs aged in freshwater over the 15 wk period was consistent across the treatments (Figure 1). Nanosized Cu particles (forming aggregates)

were seen in all the freshwater aging stock solutions, although the particle size appeared to decrease over time, probably due to dissolution. EDS analysis (Figure S2) showed that Cu NPs aged in freshwater adsorbed small amounts (< 1 %) of chlorine and phosphorus (probably as chloride and phosphate, respectively) from the media.

Dissolution of Cu NPs in the aged stocks was also observed. For instance, the dissolved Cu species, which initially represented less than 1 % of the total Cu detected in the 0 wk freshwater aged stock, had doubled in concentration after the 15 wk. The concentration of chloride ions (Cl^-) in the simulated freshwater used in this study was only 0.19 mM, thus helping to explain the increased dissolution and the relatively slow change in the morphology and elemental composition of the Cu NPs in freshwater systems (Figure 1 and Figure S4). The Visual MINTEQ modeling prediction (Table S4) indicated that the most abundant Cu species formed from aging Cu NPs in freshwater was free Cu^+ (85.7 %) at equilibrium.

Behavior of aged Cu NPs in marine phytoplankton cultures

The concentrations of nanosized forms of Cu in the algal cultures were mostly non-detectable (Tables S5) probably due to particle dissolution and aggregation in the aging stocks. The mean total dissolved Cu concentration (mg L^{-1}) varied depending on the aging period (0, 3, and 15 wk) and media type (aged stocks vs. algal cultures at Day 1 and algal cultures at Day 5), indicated by a significant two-way interaction in the ANOVA testing (2-way ANOVA; Aging x Media type; $F_{4,18} = 1050.6$; $P < 0.0001$; Table S6). The total amount of dissolved Cu increased slowly with aging, and rapidly from aged stocks and algal cultures at D1 (Tukey's HSD test, $P < 0.01$; Figure 2). It is possible that this increase is related to the slow dissolution and transformation of the Cu NPs in the freshwater aging media, mainly due to the lower quantities of Cu-binders, which gives the solution more stability[35,36]. In contrast,

the mean total dissolved Cu from the algal cultures declined slowly from Day 1 to Day 5 across the aging periods of 0 wk and 3 wk (Tukey's HSD test, $P < 0.01$), but there were no differences between the total dissolved Cu concentration from the algal cultures at Day 1 and Day 5 in the 15 wk aging treatment. This outcome may be due to the complexation of the Cu with the components of the seawater, and (hetero)aggregation with the phytoplankton cells, especially in the 15 wk treatment, caused by greater dissolved Cu input from the 15 wk aged stock than the 0 and 3 wk aged stocks (Table S3).

Cu uptake in phytoplankton cells

To allow the Cu uptake to the cells to be assessed, the *D. tertiolecta* population growth rates were exponential in all the experiments performed, and all the uptake data is presented as Cu μg cells^{-1}x10^{6}. The Cu uptake in the phytoplankton cells in the control treatments was very similar across all the aging period treatments (Tukey's HSD test, $P < 0.01$; Figure 3). The concentration of intracellular Cu uptake in the control treatments ranged from 0.99 to 1.01 in the 0 wk aging treatment, 0.96–1.04 in the 3 wk aging treatment, and 0.95–1.05 Cu μg cells^{-1}x10^{6} in the 15 wk aging treatment.

The ANOVA model explained the majority of the total variation in the Cu uptake (adjusted $r^2 = 0.98$), and the nominal Cu concentration explained the majority of the variation among treatments (45 %). A significant two-way interaction between aging period and nominal Cu concentration (2-way ANOVA; Aging x Concentration; $F_{8,15} = 76.4$; $P < 0.0001$; Table S7) explained 34 % of the variation, while aging explained 21 %. Cu uptake generally grew with increasing nominal concentrations of Cu and increasing aging (Tukey's HSD test, $P < 0.01$; Figure 3). For example, at a nominal Cu concentration of 0.1 mg L^{-1}, the mean total intracellular Cu uptake was 0.98 and 1.96 Cu μg cells^{-1}x10^{6} when the Cu NPs were aged for

the 0 wk and 15 wk, respectively. At a nominal Cu concentration of 1 mg L^{-1}, the mean total Cu concentration detected in the phytoplankton cells was 4.37 and 17.96 Cu µg $cells^{-1}x10^6$ when the Cu NPs were aged for the 0 wk and 15 wk, respectively (Figure 3). These observations suggest that (1) the Cu particles in the algal cultures were readily bioavailable for uptake by the phytoplankton cells, and (2) the increasing levels of dissolved Cu in the freshwater aging stocks resulted in a higher Cu uptake by the cells.

Phytoplankton population growth rate coefficients

The population growth rate coefficient (µ, day^{-1}) varied by aging period (0, 3, and 15 wk) and nominal Cu concentration (1, 5, 10, and 20 mg L^{-1}), as shown by a significant two-way interaction in ANOVA testing (2-way ANOVA; Aging x Concentration; $F_{8,30} = 117.7$; $P < 0.0001$; Table S8). The model explained 97 % of the variation among the treatments (adjusted model $r^2 = 0.97$), while two-way interaction explained only 6 % of the total variation in the experiment.

Growth rate coefficient declined with increasing nominal Cu concentrations and aging (Tukey's HSD test, $P < 0.01$; Figure 4). The toxicity of the aged Cu NPs was greatest in the highest nominal Cu concentration (20 mg L^{-1}) across all the aging periods (Tukey's HSD test, $P < 0.01$). The toxicity of the Cu NPs aged for the periods of 3 wk and 15 wk was also generally higher in the nominal Cu concentrations of 5 and 10 mg L^{-1} than in the 0 wk aging treatment, at the same nominal Cu concentrations (Tukey's HSD test, $P < 0.01$). The nominal Cu concentration explained 91 % of the total variation among treatments, while aging explained only 3 % of the response among treatments (Figure 4).

Cellular reactive oxygen species (ROS)

Cellular reactive oxygen species (ROS) generation was evaluated using DCFH-DA assay to assess marine phytoplankton cellular stress after exposure to the aged Cu NPs. ROS production in the control treatments (0 mg L^{-1}) was very similar to the lowest nominal Cu concentration (0.01 mg L^{-1}) across all the aging period treatments (Tukey's HSD test, $P < 0.01$; Figure 5). Excess ROS generation was greatest in the highest nominal Cu concentration (20 mg L^{-1}) across all the aging periods (Tukey's HSD test, $P < 0.01$).

ROS level production (%) varied with aging (0, 3, and 15 wk) and nominal Cu concentration (0, 0.01, 0.1, 0.5, 1, 5, 10, and 20 mg L^{-1}), as exhibited by significant two-way interaction in ANOVA testing (2-way ANOVA; Aging x Concentration; $F_{14,840} = 145.6$; $P < 0.0001$; Table S9). The model explained 71 % of the variation among the treatments (adjusted model $r^2 = 0.71$), while the two-way interaction explained 24 % of the total variation in the experiment. Generally, total ROS generation grew with increasing nominal Cu concentration, and this factor explained 58 % of the total variation among treatments. Aging explained only 8 % of response among the treatments (Figure 5). Overall, there were no obvious signs that Cu NPs, seawater components or other artifacts significantly influenced the results of the present study.

3.5. Discussion

The physicochemical transformations of the Cu NPs that occurred during the aging process were caused by the combined effects of the properties of the nanoparticles and the freshwater aging stock solutions. The more Cu NPs aged, the more toxic they became. After aging Cu NPs in freshwater systems for several days, slow morphological transformations and increased Cu dissolution rates were observed over time. These impacts resulted in increased Cu uptake by the phytoplankton cells and toxicity and suggest that the

phytoplankton populations were unable to combat the effects of the excess Cu ions, or meet these demands at the longest aging period, 15 wk. However, phytoplankton can tolerate lower concentrations of the NPs which were aged for longer periods of time, as the growth rates were higher for the lower nominal Cu concentrations than the high concentrations after the 3 wk and 15 wk periods of aging.

The differences between the dissolved Cu concentrations in the phytoplankton cultures at Day 1 and Day 5 in our experiment were most likely due to (1) the uptake of Cu by (the exponentially growing) algal cells, (2) the adsorption of Cu onto the algal cells[37], and (3) the binding of Cu by the organic materials released into the algal cultures by the cells[23]. The introduction of potentially more toxic Cu species coupled with initially higher levels of dissolved Cu in the 15 wk aging stock solution resulted in the Cu NPs aged for longer periods (up to 100 days) having a greater impact than those aged for shorter periods (< 30 days). These observations suggest that the toxicity of the Cu ions or Cu complexes aged in freshwater ecosystems potentially increases with the aging period, probably due to increased Cu dissolution over time, followed by increased Cu uptake by the phytoplankton cells.

The growth rate coefficients of the phytoplankton declined as a function of nominal Cu concentration and aging time period. However, this relationship was asymptotic for the low levels of nominal Cu concentrations of 0.01, 0.1, 0.5, and 1 mg L^{-1}. This suggests that low nominal Cu concentrations cannot reduce the growth rate coefficient further, either due to the physiological or biochemical utilization of Cu by the cells, including for the mediation of redox transformations[38], and/or that phytoplankton cells may have initiated protective responses to guarantee their survival[39].

The growth rate coefficients of high nominal concentrations of Cu at long aging periods did not follow this pattern. This difference agreed with the finding of a greater Cu uptake in

the high nominal Cu concentration (20 mg L^{-1}) and long aging period (15 wk), in comparison with the other treatments. A similar relationship was also found between intracellular ROS production as a function of phytoplankton growth rates. Reduced growth rates in the presence of aged Cu NPs, combined with increased Cu uptake and ROS production after exposure to high levels of dissolved Cu, suggest that the phytoplankton cells used energy that would normally be dedicated to sequestering excess metals to prevent toxicity[40] to instead detoxify Cu or repair damage resulting from high concentrations of toxic Cu ions. This combined effect of high ROS production and low growth rates may have increased the toxic effect of high levels of nominal Cu concentrations by also (1) damaging cellular compounds, including membranes and organelles, and/or (2) directly causing genotoxicity or cytotoxicity[39].

The speciation of Cu particles determined directly via inductively coupled mass atomic emission spectroscopy (ICP-MS) revealed high particle aggregation after all the aging periods, although all the aged stocks were mixed constantly by the rotatory shaker (120 rpm) throughout the experiment to mimic the surface of natural freshwater ecosystems. The aged stocks were also thoroughly mixed prior to sampling. The heterogeneous particle size distribution probably reduced stability, however, and led to the detection of bulk Cu (> 200 nm) at higher levels than the nominal Cu concentration under some conditions (e.g., Cu NPs aged for 3 wk; Table S3).

The aggregation of Cu NPs in this experiment can be attributed to a low surface charge, as indicated by the ζ potential. In the phytoplankton cultures (seawater), the aggregation of Cu NPs is likely to have occurred due to a greater ionic strength and higher pH than in freshwater aging stock solutions. It is also likely that the greater amount of natural organic matter (NOM) released from the cells in exponential growth in the algal cultures than in the

aged stocks contributed to Cu particle aggregation and/or heteroaggregation with the phytoplankton cells[28,41,42]. These observations suggest that the fate and transformations of the aged Cu NPs in aquatic ecosystems were strongly affected by the characteristics of the receiving media.

In addition to aggregation, dissolution of Cu NPs was also observed in the aged stock solutions (freshwater) and the algal cultures (seawater). Dissolved Cu species in seawater are typically short-lived due to the precipitation of dissolved ions to form Cu complexes[24]. Complexation also occurs in freshwater systems, but is limited by the amount of anions and organic materials available. Therefore, the proportion of free dissolved Cu (i.e., Cu^{+} and Cu^{2+}), which are the most toxic Cu species[43], is higher in freshwater than seawater systems.

Assuming the continuous input of Cu NPs, and the behavior and transformation of the NPs once released, helped to elucidate the impacts of the aging of Cu NPs as they flow down river to coastal marine ecosystems. The aging of Cu NPs in a freshwater system for different periods in this experiment did not affect the stability of the nanoparticles through the subsequent formation of insoluble Cu precipitates, even those aged for up to 100 days. Chemical processes, including disaggregation and decreased sedimentation, may therefore enhance the exposure of pelagic organisms to toxic Cu species[23,24,44]. In turn, the impacts of aged Cu NPs in this experiment generally enhanced the bioavailability of toxic Cu species, Cu uptake, and toxicity to marine phytoplankton, in comparison with pristine Cu NPs. The reduced population growth of the marine phytoplankton in this experiment suggest that phytoplankton productivity will be reduced in zones of contamination by Cu NPs previously aged in freshwater ecosystems.

The fate and behavior of Cu NPs are dynamic processes under environmental conditions that have proven difficult to predict. Likewise, the transport, transformation, and subsequent

accumulation of original or aged (i.e., transformed) NPs has yet to be systematically investigated as part of an ecotoxicological study[17,45,46].

3.6. References

1. Holden, P. A. *et al.* Considerations of Environmentally Relevant Test Conditions for Improved Evaluation of Ecological Hazards of Engineered Nanomaterials. *Environ. Sci. Technol.* **50**, 6124–6145 (2016).
2. Keller, A. A. *et al.* Stability and Aggregation of Metal Oxide Nanoparticles in Natural Aqueous Matrices. *Environ. Sci. Technol.* **44**, 1962–1967 (2010).
3. Peijnenburg, W. J. G. M. *et al.* A Review of the Properties and Processes Determining the Fate of Engineered Nanomaterials in the Aquatic Environment. *http://dx.doi.org/10.1080/10643389.2015.1010430* (2015). Available at: https://openaccess.leidenuniv.nl/handle/1887/51414. (Accessed: 25th February 2019)
4. Minetto, D., Volpi Ghirardini, A. & Libralato, G. Saltwater ecotoxicology of Ag, Au, CuO, TiO2, ZnO and C60 engineered nanoparticles: An overview. *Environ. Int.* **92**–**93**, 189–201 (2016).
5. Keller, A. A. *et al.* Comparative environmental fate and toxicity of copper nanomaterials. *NanoImpact* **7**, 28–40 (2017).
6. Nam, D.-H., Lee, B., Eom, I., Kim, P. & Yeo, M.-K. Uptake and bioaccumulation of titanium- and silver-nanoparticles in aquatic ecosystems. *Mol. Cell. Toxicol.* **10**, 9–17 (2014).
7. Adeleye, A. S., Oranu, E. A., Tao, M. & Keller, A. A. Release and detection of nanosized copper from a commercial antifouling paint. *Water Res.* **102**, 374–382 (2016).

8. Zhao, L., Huang, Y., Hannah-Bick, C., Fulton, A. N. & Keller, A. A. Application of metabolomics to assess the impact of Cu(OH) 2 nanopesticide on the nutritional value of lettuce (Lactuca sativa): Enhanced Cu intake and reduced antioxidants. *NanoImpact* **3**–**4**, 58–66 (2016).
9. Garner, K. L. & Keller, A. A. Emerging patterns for engineered nanomaterials in the environment: a review of fate and toxicity studies. *J. Nanoparticle Res.* **16**, (2014).
10. Wang, N. *et al.* Chronic toxicity of copper and ammonia to juvenile freshwater mussels (Unionidae). *Environ. Toxicol. Chem.* **26**, 2048–2056 (2007).
11. Miller, R. J. *et al.* Photosynthetic efficiency predicts toxic effects of metal nanomaterials in phytoplankton. *Aquat. Toxicol.* **183**, 85–93 (2017).
12. Hanna, S. K., Miller, R. J., Zhou, D., Keller, A. A. & Lenihan, H. S. Accumulation and toxicity of metal oxide nanoparticles in a soft-sediment estuarine amphipod. *Aquat. Toxicol.* **142**–**143**, 441–446 (2013).
13. Hanna, S. K., Miller, R. J. & Lenihan, H. S. Accumulation and Toxicity of Copper Oxide Engineered Nanoparticles in a Marine Mussel. *Nanomaterials* **4**, 535–547 (2014).
14. Lin, S. *et al.* Zebrafish High-Throughput Screening to Study the Impact of Dissolvable Metal Oxide Nanoparticles on the Hatching Enzyme, ZHE1. *Small* **9**, 1776–1785 (2013).
15. Torres-Duarte, C. *et al.* Developmental effects of two different copper oxide nanomaterials in sea urchin (Lytechinus pictus) embryos. **10**, 671–679 (2016).
16. Lowry, G. V. *et al.* Environmental occurrences, behavior, fate, and ecological effects of nanomaterials: an introduction to the special series. *J. Environ. Qual.* **39**, 1867–1874 (2010).
17. Bernhardt, E. S. *et al.* An Ecological Perspective on Nanomaterial Impacts in the Environment. *J. Environ. Qual.* **39**, 1954 (2010).

18. Xiao, Y., Peijnenburg, W. J. G. M., Chen, G. & Vijver, M. G. Impact of water chemistry on the particle-specific toxicity of copper nanoparticles to Daphnia magna. *Sci. Total Environ.* **610**–**611**, 1329–1335 (2018).

19. Mitrano, D. M. & Nowack, B. The need for a life-cycle based aging paradigm for nanomaterials: importance of real-world test systems to identify realistic particle transformations. *Nanotechnology* **28**, 072001 (2017).

20. Valsami-Jones, E. & Lynch, I. How safe are nanomaterials? *Science* **350**, 388–389 (2015).

21. Grantham, H. S. *et al.* Accommodating Dynamic Oceanographic Processes and Pelagic Biodiversity in Marine Conservation Planning. *PLOS ONE* **6**, e16552 (2011).

22. Lenihan, H. S., Peterson, C. H., Miller, R. J., Kayal, M. & Potoski, M. Biotic disturbance mitigates effects of multiple stressors in a marine benthic community. *Ecosphere* **9**, e02314 (2018).

23. Adeleye, A. S., Conway, J. R., Perez, T., Rutten, P. & Keller, A. A. Influence of extracellular polymeric substances on the long-term fate, dissolution, and speciation of copper-based nanoparticles. *Environ. Sci. Technol.* (2014). doi:10.1021/es5033426

24. Conway, J. R., Adeleye, A. S., Gardea-Torresdey, J. & Keller, A. A. Aggregation, Dissolution, and Transformation of Copper Nanoparticles in Natural Waters. *Environ. Sci. Technol.* **49**, 2749–2756 (2015).

25. Bielmyer-Fraser, G. K., Jarvis, T. A., Lenihan, H. S. & Miller, R. J. Cellular Partitioning of Nanoparticulate versus Dissolved Metals in Marine Phytoplankton. *Environ. Sci. Technol.* **48**, 13443–13450 (2014).

26. Adeleye, A. S. & Keller, A. A. Long-term colloidal stability and metal leaching of single wall carbon nanotubes: Effect of temperature and extracellular polymeric substances. *Water Res.* (2014). doi:10.1016/j.watres.2013.11.032

27. EPA, U. S. *Short-term Methods for Estimating the Chronic Toxicity of Effluents and Receiving Waters to Freshwater Organisms Fourth Edition*. (2002).

28. Ma, S., Zhou, K., Yang, K. & Lin, D. Heteroagglomeration of Oxide Nanoparticles with Algal Cells: Effects of Particle Type, Ionic Strength and pH. *Environ. Sci. Technol.* **49**, 932–939 (2015).

29. Kester, D. R., Duedall, I. W., Connors, D. N. & Pytkowicz, R. M. Preparation of Artificial Seawater1. *Limnol. Oceanogr.* **12**, 176–179 (1967).

30. Ruppert, D., Wand, M. P. & Carroll, R. J. Semiparametric Regression by David Ruppert. *Cambridge Core* (2003). doi:10.1017/CBO9780511755453

31. Levy, J. *et al.* Uptake and internalisation of copper by three marine microalgae: comparison of copper-sensitive and copper-tolerant species. *Fac. Sci. - Pap. Arch.* 82–93 (2008). doi:10.1016/j.aquatox.2008.06.003

32. Lürling, M. Effects of a surfactant (FFD-6) on Scenedesmus morphology and growth under different nutrient conditions. *Chemosphere* **62**, 1351–1358 (2006).

33. Fu, P. P., Xia, Q., Hwang, H.-M., Ray, P. C. & Yu, H. Mechanisms of nanotoxicity: generation of reactive oxygen species. *J. Food Drug Anal.* **22**, 64–75 (2014).

34. Hong, Y. *et al.* Gramine-induced growth inhibition, oxidative damage and antioxidant responses in freshwater cyanobacterium Microcystis aeruginosa. *Aquat. Toxicol.* **91**, 262–269 (2009).

35. Ates, M., Dugo, M. A., Demir, V., Arslan, Z. & Tchounwou, P. B. EFFECT OF COPPER OXIDE NANOPARTICLES TO SHEEPSHEAD MINNOW (CYPRINODON VARIEGATUS) AT DIFFERENT SALINITIES. 9

36. Ates, M., Arslan, Z., Demir, V., Daniels, J. & Farah, I. O. Accumulation and Toxicity of CuO and ZnO Nanoparticles through Waterborne and Dietary Exposure of Goldfish (Carassius auratus). *Environ. Toxicol.* **30**, 119–128 (2015).

37. Levy, J. L., Stauber, J. L. & Jolley, D. F. Sensitivity of marine microalgae to copper: The effect of biotic factors on copper adsorption and toxicity. *Sci. Total Environ.* **387**, 141–154 (2007).

38. Merchant, S. S. The Elements of Plant Micronutrients1. *Plant Physiol.* **154**, 512–515 (2010).

39. Roesslein, M., Hirsch, C., Kaiser, J.-P., Krug, H. & Wick, P. Comparability of in Vitro Tests for Bioactive Nanoparticles: A Common Assay to Detect Reactive Oxygen Species as an Example. *Int. J. Mol. Sci.* **14**, 24320–24337 (2013).

40. Finney, L. A. & O'Halloran, T. V. Transition Metal Speciation in the Cell: Insights from the Chemistry of Metal Ion Receptors. *Science* **300**, 931–936 (2003).

41. Adeleye, A. S., Conway, J. R., Perez, T., Rutten, P. & Keller, A. A. Influence of Extracellular Polymeric Substances on the Long-Term Fate, Dissolution, and Speciation of Copper-Based Nanoparticles. *Environ. Sci. Technol.* **48**, 12561–12568 (2014).

42. Wang, H., Adeleye, A. S., Huang, Y., Li, F. & Keller, A. A. Heteroaggregation of nanoparticles with biocolloids and geocolloids. *Adv. Colloid Interface Sci.* **226**, 24–36 (2015).

43. Sunda, W. The relationship between cupric ion activity and the toxicity of copper to phytoplankton. (Massachusetts Institute of Technology and Woods Hole Oceanographic Institution, 1975). doi:10.1575/1912/1275

44. Mudunkotuwa, I. A., Pettibone, J. M. & Grassian, V. H. Environmental Implications of Nanoparticle Aging in the Processing and Fate of Copper-Based Nanomaterials. *Environ. Sci. Technol.* **46**, 7001–7010 (2012).

45. Nowack, B. & Mitrano, D. M. Procedures for the production and use of synthetically aged and product released nanomaterials for further environmental and ecotoxicity testing. *NanoImpact* **10**, 70–80 (2018).

46. Mouneyrac, C., Syberg, K. & Selck, H. Ecotoxicological Risk of Nanomaterials. in *Aquatic Ecotoxicology* 417–440 (Elsevier, 2015). doi:10.1016/B978-0-12-800949-9.00017-6

List of captions

Figure 1. Transmission electron micrographs (TEM) of Cu NPs after aging in the freshwater stock solutions (20 mg L^{-1}): (0 wk), (3 wk), and (15 wk) represent Cu NPs aged for 0, 3, and 15 weeks, respectively (scale bar = 100 nm). 164

Figure 2. Mean (95 % C.I.) dissolved Cu concentration (mg L^{-1}) as a function of aged stocks (nominal Cu concentration of 20 mg L^{-1}), and phytoplankton cultures (nominal Cu concentration of 20 mg L^{-1}) at day 1, and day 5. Aging periods are 0, 3, and 15 wk. N = 3 replicate flasks per treatment. Results of a Tukey HSD post hoc test are provided above each bar (A > B > C, etc., at $P < 0.01$). 165

Figure 3. Mean (95 % C.I.) intracellular copper uptake (μg $cell^{-1}x10^6$) of all phytoplankton cultures at day 5 as a function of nominal Cu concentrations (mg L^{-1}) and aging periods (wk). N = 3 replicate culture flasks per treatment. Results of a Tukey's Honestly Significant Difference (HSD) post hoc test are provided above each bar (A > B > C, etc., at $P < 0.01$). D. tertiolecta cultures were exponential in all performed experiments. All intracellular Cu uptake data were normalized by cell number. 166

Figure 4. Mean (95 % C.I.) phytoplankton population growth rate (μ, d^{-1}) as a function of nominal Cu concentrations (mg L^{-1}) and aging periods (wk). N = 3 replicate culture flasks per treatment. Results of a Tukey's Honestly Significant Difference (HSD) post hoc test are provided above each bar (A > B > C, etc., at $P < 0.01$). D. tertiolecta population growth rates were exponential in all performed experiments. All growth rate data were normalized by cell number. 167

Figure 5. Mean (95 % C.I.) total intracellular ROS production level (%) as a function of nominal Cu concentration (mg L^{-1}) and aging periods (wk). N = 3 replicate culture flasks per treatment. Results of a Tukey's Honestly Significant Difference (HSD) post hoc test are

provided above each bar (A > B > C, etc., at P < 0.01). All relative DCF fluorescence data were normalized by cell number. 168

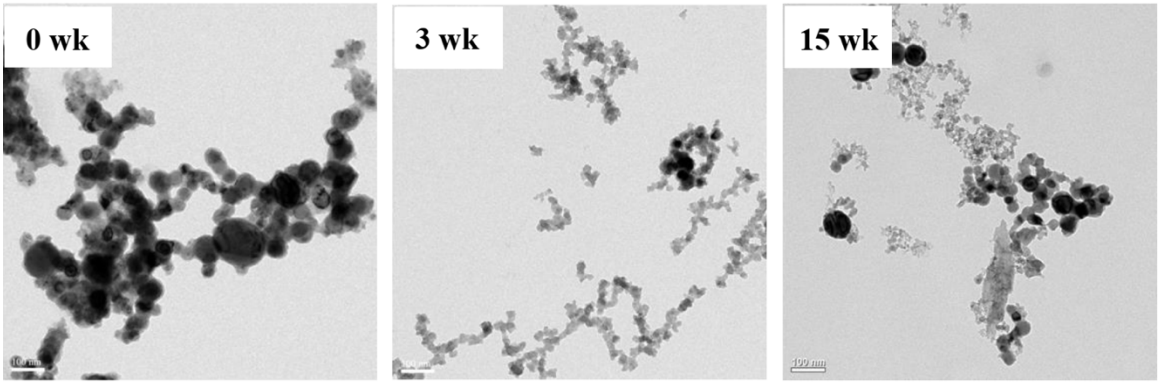

Figure 1.

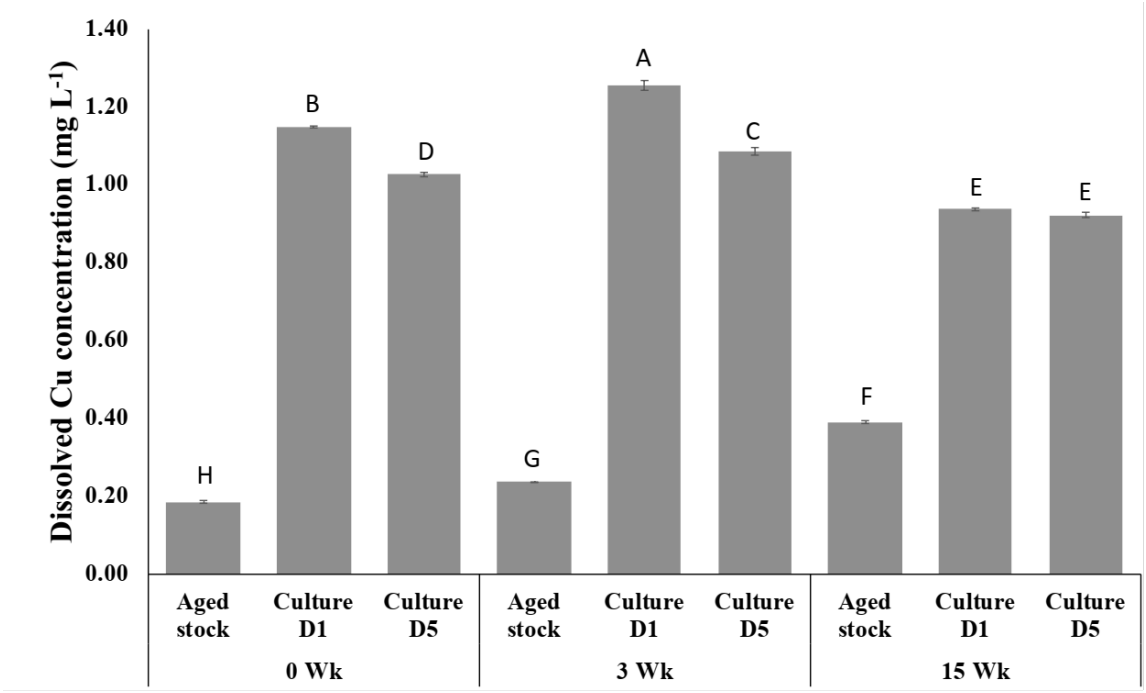
Dissolved Cu concentration (mg L-1)
1.40
1.20
1.00
0.80
0.60
0.40
0.20
0.00
H
B
D
G
A
C
F
E
E
Aged stock
Culture D1
Culture D5
Aged stock
Culture D1
Culture D5
Aged stock
Culture D1
Culture D5
0 Wk
3 Wk
15 Wk

Figure 2.

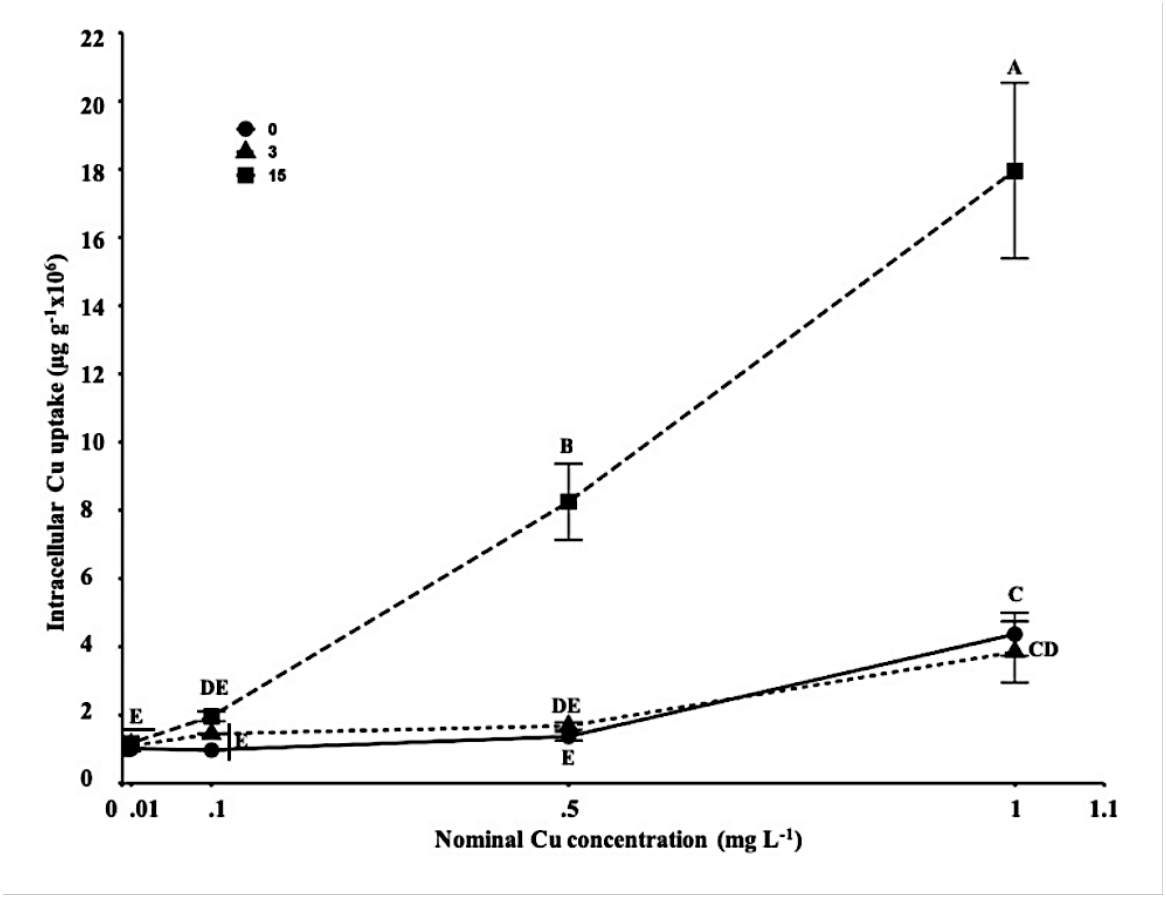
Intracellular Cu uptake (µg g-1x10⁶)
Nominal Cu concentration (mg L-1)
0
3
15
A
B
C
CD
DE
DE
E
E
E
0
2
4
6
8
10
12
14
16
18
20
22
0
.01
.1
.5
1
1.1

Figure 3.

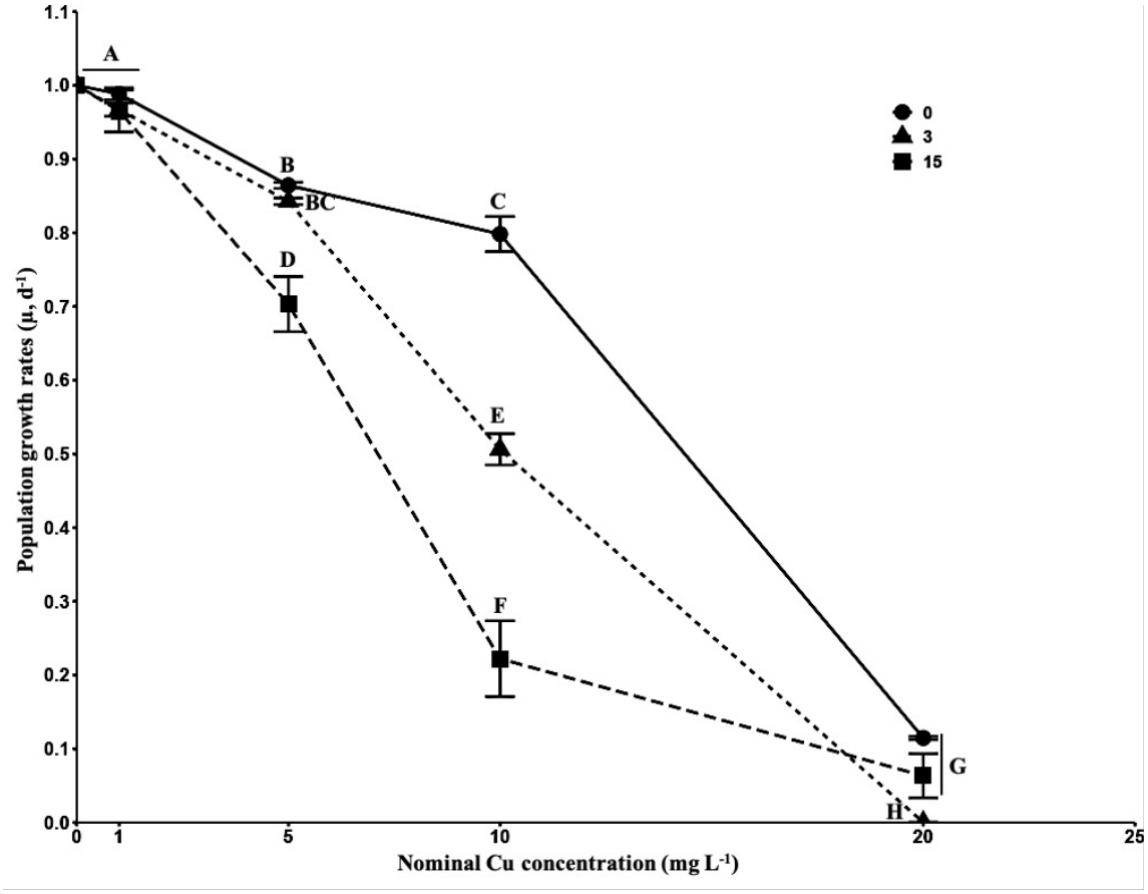
A
B
BC
C
D
E
F
G
H
0
3
15
Population growth rates (μ, d-1)
Nominal Cu concentration (mg L-1)
0.0
0.1
0.2
0.3
0.4
0.5
0.6
0.7
0.8
0.9
1.0
1.1
0
1
5
10
20
25

Figure 4.

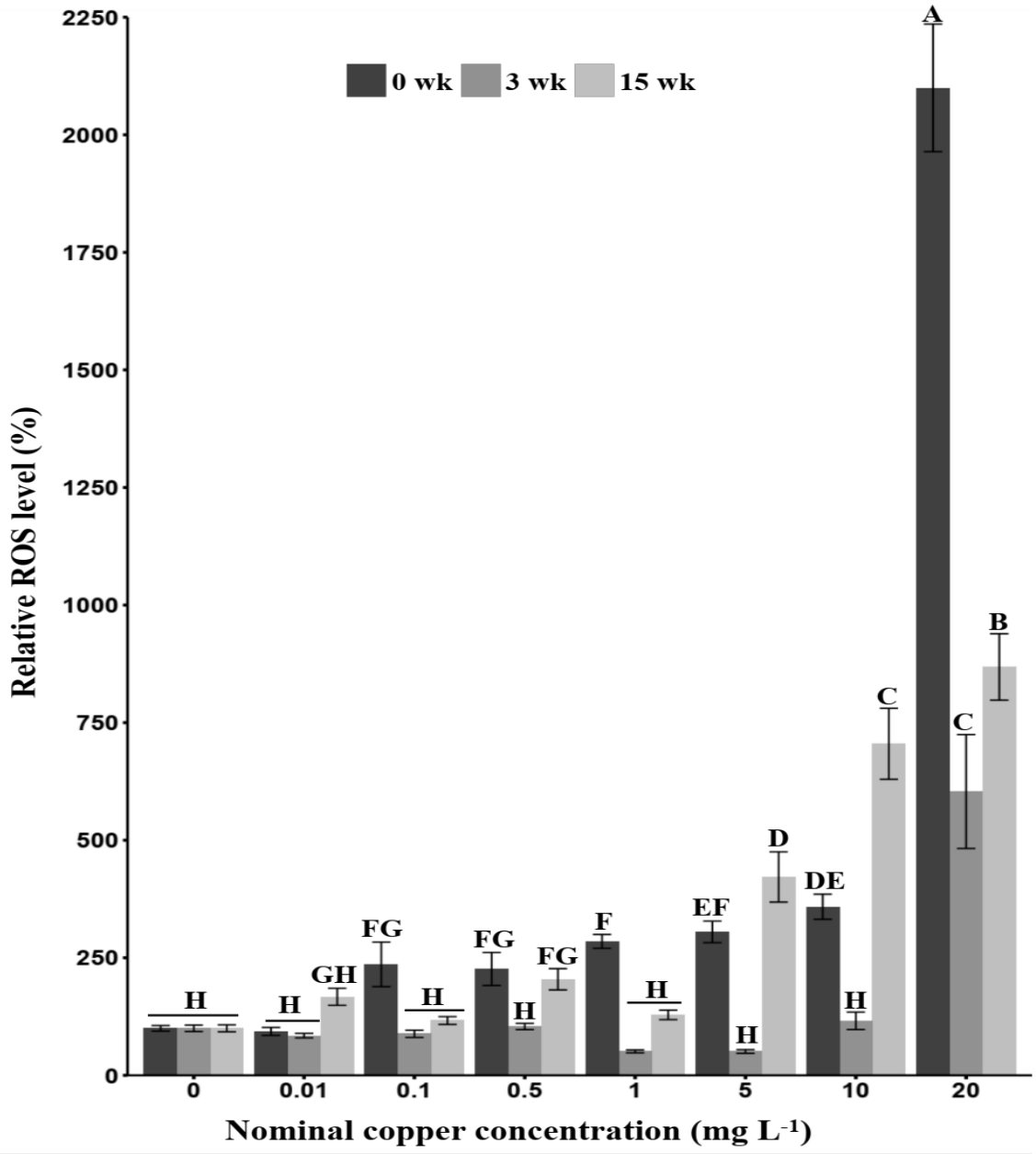
0 wk
3 wk
15 wk
Relative ROS level (%)
2250
2000
1750
1500
1250
1000
750
500
250
0
H
H
GH
FG
H
FG
H
FG
F
H
EF
H
D
DE
H
C
A
C
B
0
0.01
0.1
0.5
1
5
10
20
Nominal copper concentration (mg L-1)

Figure 5.

3.7. Appendix. Supporting Information

Table S1. Composition of simulated freshwater (pH 7.3) used for aging of Cu NPs, produced in accordance with EPA method 1003.0[3], without EDTA.

Nutrient	Concentration (mg L^{-1})
$NaNO_3$	25.5
$MgCl_2.6H_2O$	12.2
$CaCl_2.2H_2O$	4.4
$MgSO_4.7H_2O$	14.7
K_2HPO_4	1.0
$NaHCO_3$	15.0
H_3BO_3	0.2
$MnCl_2.4H_2O$	0.4
$ZnCl_2$	3.3×10^{-3}
$CoCl_2.6H_2O$	1.4×10^{-3}
$CuCl_2.2H_2O$	1.2×10^{-5}
$Na_2MoO_4.2H_2O$	7.3×10^{-3}
$FeCl_3.6H_2O$	0.2
Na_2SeO_4	2.4×10^{-3}

Table S2. Composition of artificial seawater (pH 8.1) used for culture of marine phytoplankton *D. tertiolecta*, produced in accordance with Kester and collaborators.

Nutrient	Concentration (mg L^{-1})
NaCl	23.0×10^3
Na_2SO_4	4.0×10^3
KCl	40.7×10^3
KBr	0.1×10^3
H_3BO_3	30.0
$MgCl_2.6H_2O$	10.8×10^3
$CaCl2.2H_2O$	1.5×10^3
$SrCl_2$	20.0
$NaHCO_3$	1.7×10^2

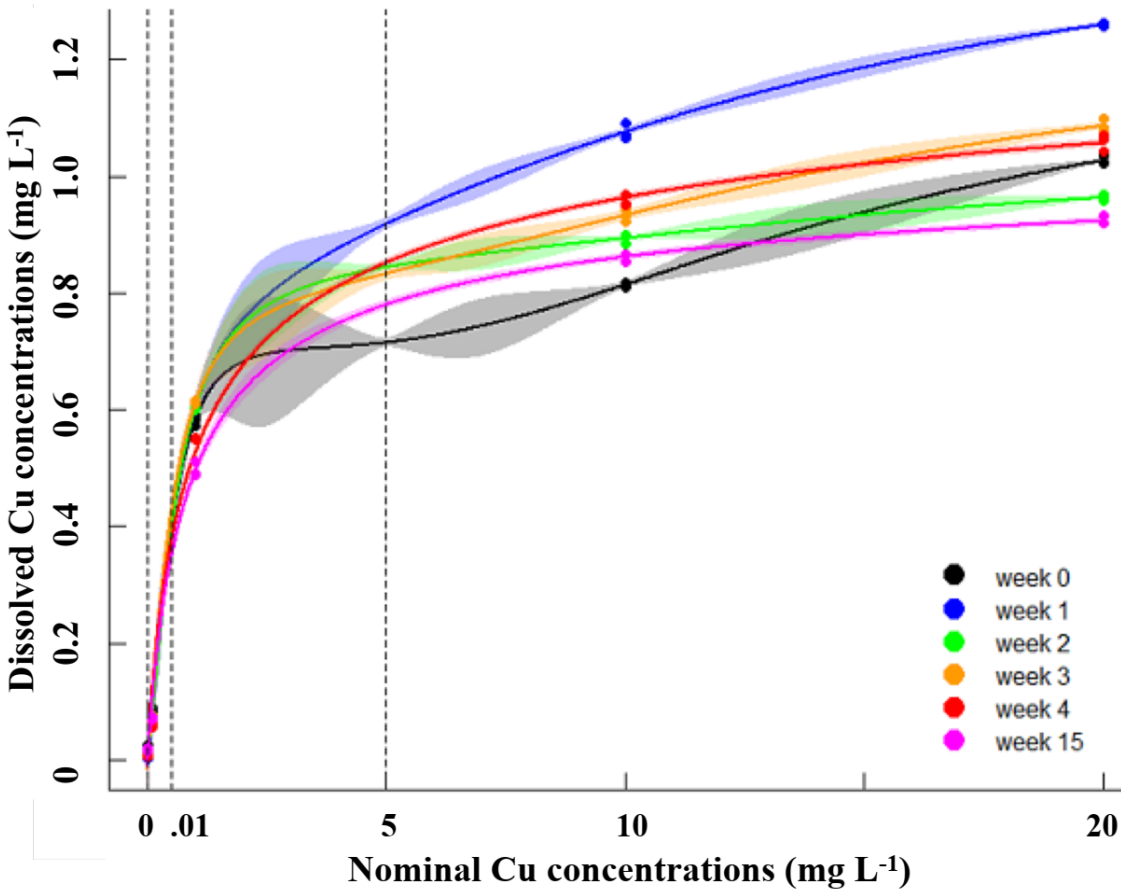

Figure S1. Variation in dissolved Cu concentrations (mg L^{-1}) measured in phytoplankton cultures as a function of nominal Cu concentrations (mg L^{-1}) over the experimental aging periods (weeks). Dots represent dissolved Cu concentrations (n=3). Lines and shading represent mean (95% C.I.) estimated dissolved Cu concentrations from semi-parametric regressions (detailed in the experimental section of this paper). Dashed lines represent nominal Cu concentrations (0.01, 0.5, and 5) where the corresponding estimated dissolved Cu concentration values were not measured from the solutions, but taken from the curves.

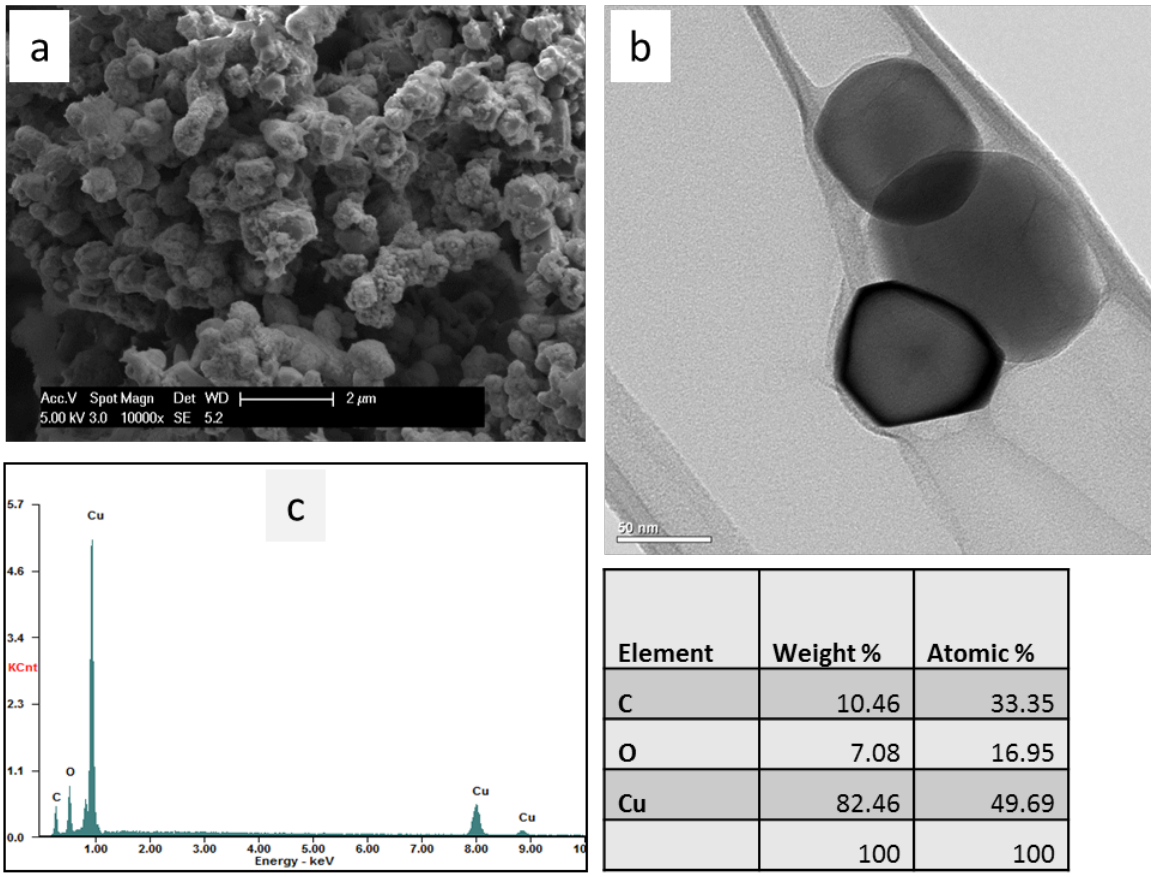

Element	Weight %	Atomic %
C	10.46	33.35
O	7.08	16.95
Cu	82.46	49.69
	100	100

Figure S2. Characterization of nanoparticles used in this study: (a) Scanning and (b) transmission electron micrographs of nanosized copper (Cu NPs), (c) EDS spectrum of Cu NPs, with elemental composition shown in table.

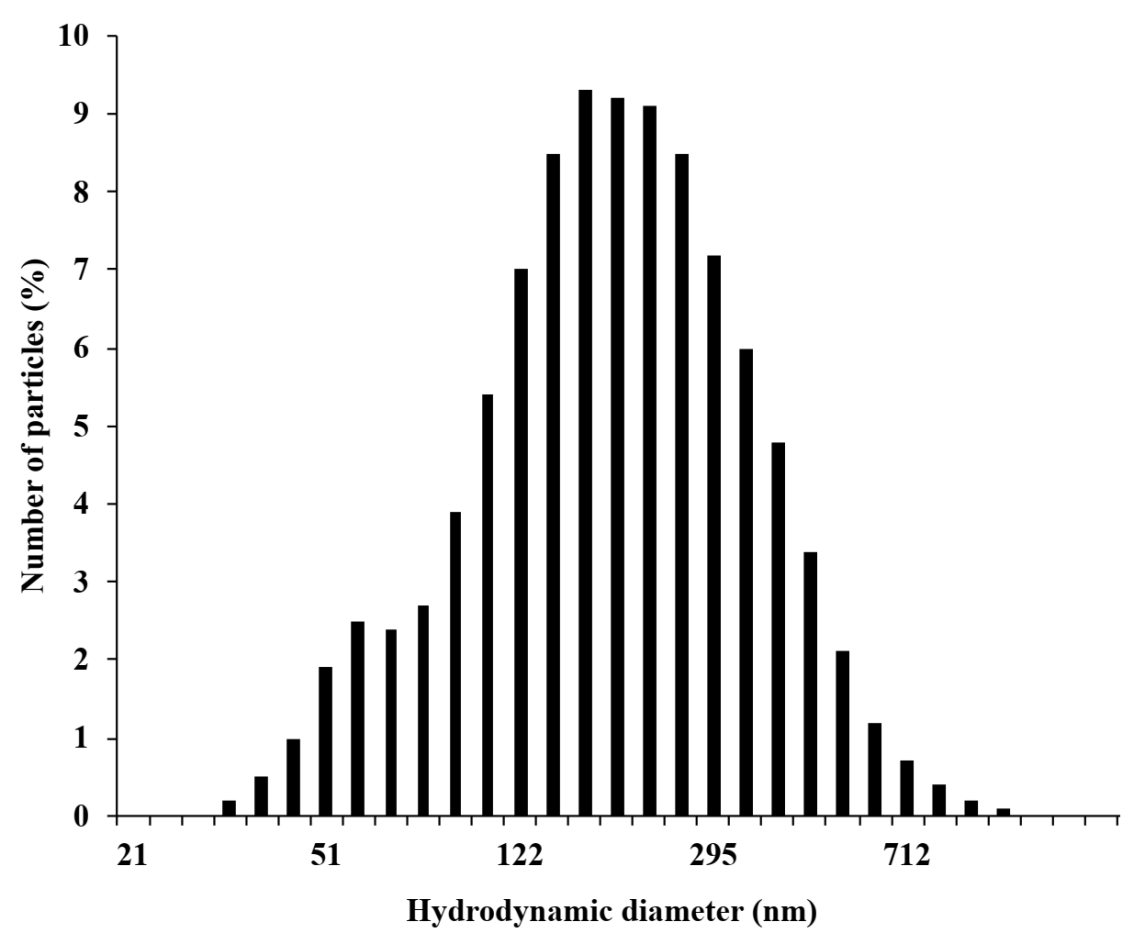

Figure S3. Size distribution of Cu NPs in freshwater aging media (20 mg L^{-1}) showing particle aggregation. Data was collected for 1 h.

Table S3. Concentrations of different copper fractions detected in Cu NPs (20 mg L^{-1}) aged in simulated freshwater.

Aging time (weeks)	Copper concentration (mg L^{-1})	
0	**Dissolved**	0.19
	Nano	0.00
	Bulk	18.93
1	**Dissolved**	0.18
	Nano	0.09
	Bulk	10.45
2	**Dissolved**	0.23
	Nano	0.17
	Bulk	17.77
3	**Dissolved**	0.24
	Nano	0.02
	Bulk	24.02
4	**Dissolved**	0.33
	Nano	0.28
	Bulk	36.01
15	**Dissolved**	0.39
	Nano	0.00
	Bulk	19.10

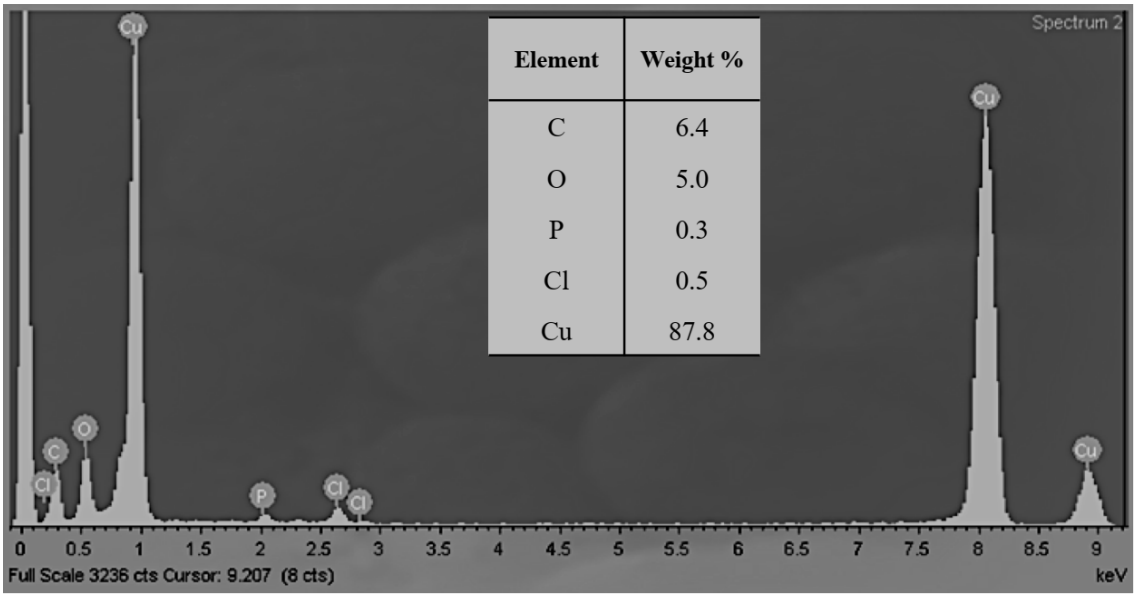

Element	Weight %
C	6.4
O	5.0
P	0.3
Cl	0.5
Cu	87.8

Figure S4. Energy-dispersive X-ray Spectroscopy (EDS) of Cu NPs aged in simulated freshwater, showing elemental composition by weight (%).

Table S4. Abundance of Cu species at equilibrium in simulated freshwater predicted by Visual MINTEQ.

Cu species	Abundance (%)
Cu^{+}	85.7
CuCl (aq)	13.9
$CuCl_2^{-}$	0.4
$CuCl_3^{2-}$	0.0
Cu^{2+}	0.0
CuBr (aq)	-

Table S5. Concentrations of dissolved and nanosized Cu (in mg L^{-1}) detected in cultures of *Dunaliella tertiolecta* exposed Cu NPs previously aged in simulated freshwater. ND = not detected.

Aging time (wk)	[Cu] (mg/L)	Day 1		Day 3		Day 5	
		Dissolved	Nano	Dissolved	Nano	Dissolved	Nano
0	0	0.031	0.000	0.030	0.002	0.022	0.008
	0.1	0.096	ND	0.100	0.001	0.086	0.006
	1	0.503	0.010	0.597	0.022	0.582	0.026
	10	0.888	0.031	0.852	0.016	0.814	0.035
	20	1.149	0.120	1.066	0.008	1.027	ND
1	0	0.010	0.051	0.011	ND	0.003	ND
	0.1	0.080	0.002	0.081	0.004	0.065	0.001
	1	0.560	0.008	0.594	0.022	0.604	0.014
	10	1.206	0.070	1.085	0.045	1.076	0.008
	20	1.404	0.032	1.269	ND	1.260	0.009
2	0	0.011	0.004	0.016	ND	0.015	0.003
	0.1	0.075	0.009	0.077	0.000	0.073	0.004
	1	0.559	ND	0.608	0.004	0.603	0.011
	10	0.924	ND	0.904	0.043	0.894	0.008
	20	1.024	0.007	0.962	0.006	0.963	0.000
3	0	0.017	ND	0.016	0.002	0.008	0.010
	0.1	0.086	ND	0.088	0.003	0.076	0.006
	1	0.518	0.020	0.607	ND	0.613	ND
	10	1.031	0.014	0.990	ND	0.932	0.003
	20	1.256	0.016	1.118	ND	1.087	0.009
4	0	0.011	ND	0.009	ND	0.005	0.000
	0.1	0.074	ND	0.076	0.001	0.058	0.007
	1	0.484	0.016	0.571	0.001	0.551	0.005
	10	1.111	0.019	0.993	ND	0.958	ND
	20	1.275	0.052	1.095	0.091	1.059	0.183
15	0	0.002	0.006	0.016	ND	0.018	ND
	0.1	0.051	ND	0.074	0.001	0.071	ND
	1	0.354	ND	0.481	0.009	0.497	0.013
	10	0.868	ND	0.859	ND	0.862	0.008
	20	0.937	0.008	0.929	ND	0.923	0.003

Table S6. Results of two-way ANOVA for dissolved Cu concentration data (mg L^{-1}) detected in phytoplankton cultures. Three different aging periods were used: 0 wk, 3 wk, and 15 wk. Three different media were used: aged stock solution (freshwater), and culture media at Day 1 (D1) and culture media at Day 5 (D5) (seawater). More detailed physicochemical water parameters are found in the Methods section.

Source	*df*	SS	*MS*	*F-value*	P-value
Aging (A)	2	0.06	0.03	550.9	$p < 0.0001$
Media (M)	2	3.81	1.91	37866	$p < 0.0001$
A x M	4	0.21	0.05	1050.6	$p < 0.0001$
Residuals	18	0.00	0.00		
Total	26	4.08	1.99		
Model R-squared: 0.99					

Note — *df* = Degree of freedom, SS = Sum squares, MS = Mean squares.

Table S7. Results of two-way ANOVA for Cu uptake data presented as Cu µg cells^{-1} x $(10)^6$, detected in phytoplankton cultures at the end of the experiment (D5). Three different aging periods were employed: 0 wk, 3 wk, and 15 wk. The nominal Cu concentrations were: 0, 0.01, 0.1, 0.5, and 1 mg Cu L^{-1}. All cells were rinsed with EDTA 0.1M solution to account for internal Cu only. *D. tertiolecta* cultures were exponential in all the experiments. All intracellular Cu uptake data were normalized by number of cells. More detailed uptake procedures are found in the Methods section.

Source	*df*	SS	*MS*	*F-value*	P-value
Aging (A)	2	122.7	61.4	192.4	$p < 0.0001$
Concentration (C)	4	259.0	64.7	203.0	$p < 0.0001$
A x C	8	194.9	24.4	76.4	$p < 0.0001$
Residuals	15	4.8	0.3		
Total	29	581.3	150.8		
Model R-squared: 0.98					

Note — *df* = Degree of freedom, SS = Sum squares, MS = Mean squares.

Table S8. Results of two-way ANOVA for phytoplankton population growth rate (μ, d^{-1}). Three different aging periods were employed: 0 wk, 3 wk, and 15 wk. The nominal Cu concentrations were: 0, 1, 5, 10, and 20 mg Cu L^{-1}. *D. tertiolecta* population growth rates were exponential in all the experiments. All growth rate data were normalized by cell number. More detailed growth rate procedures are found in the Methods section.

Source	*df*	SS	*MS*	*F-value*	P-value
Aging (A)	2	0.2	0.1	255.1	$p < 0.0001$
Concentration (C)	4	5.6	1.4	3574.0	$p < 0.0001$
A x C	8	0.4	0.0	117.7	$p < 0.0001$
Residuals	30	0.0	0.0		
Total	44	6.1	1.5		
Model R-squared: 0.97					

Note — *df* = Degree of freedom, SS = Sum squares, MS = Mean squares.

Table S9. Results of two-way ANOVA for intracellular reactive oxygen species (ROS) production data. Three different aging periods were employed: 0 wk, 3 wk, and 15 wk. The nominal Cu concentrations were: 0, 0.01, 0.1, 0.5, 1, 5, 10, and 20 mg Cu L^{-1}. All ROS data were normalized by number of cells and presented as relative ROS level (%). More detailed intracellular ROS assay procedures are found in the Methods section.

Source	*df*	SS	*MS*	*F-value*	P-value
Aging (A)	2	1.4×10^{7}	7.2×10^{6}	344.7	$p < 0.0001$
Concentration (C)	7	1.0×10^{8}	1.4×10^{7}	693.6	$p < 0.0001$
A x C	14	4.2×10^{7}	3.0×10^{6}	145.6	$p < 0.0001$
Residuals	840	1.7×10^{7}	2.1×10^{4}		
Total	863	1.7×10^{8}	2.5×10^{7}		
Model R-squared: 0.71					

Note — *df* = Degree of freedom, SS = Sum squares, MS = Mean squares.

II. Conclusions

This doctoral research project has increased our understanding of how natural processes directly and indirectly impact the behavior, transformations, and toxicity of copper-based nanoparticles (CBNPs) in complex environmental matrices. The role of the physicochemical properties of the CBNPs and environmental factors including ionic strength, pH, and natural organic matter (NOM) were considered, as well as how these interact with aquatic organisms to determine both Cu uptake and toxicity. The overall results showed that CBNPs negatively impacted marine/estuarine aquatic organisms, having a lethal or sublethal effect, and accumulating in both marine phytoplankton and estuarine amphipods.

In Chapter 1, the lethal and sublethal effects of CBNP pesticides on non-target estuarine amphipods were investigated. It was found that Cu-based nanopesticides reduced biomass and survival and increased respiration and Cu body burden in amphipods, in a similar manner to that of conventional Cu pesticides. While Cu ions are known to be toxic to amphipods, and considering that conventional Cu pesticides dissolve rapidly in aquatic systems, it is surprising that most of the toxicity seen in the acute exposure experiments was likely to be caused by the combination of Cu particles and ions. Additionally, the concentrations that elicited the sublethal impact in laboratory assays did not resemble the concentrations at which reduced biomass and increased respiration rates were observed in a dynamic energy budget model. Therefore, while the toxicity of copper nanoparticles (Cu NPs) was similar to that of the Cu ions in the experimental assays of the present study, the ability of amphipods to dictate the fate and behavior of Cu-based pesticides at very low environmental concentrations in the estuarine environment may not be detected by traditional toxicity

methods. This is important for our understanding of the impacts of Cu-based nanopesticides in the estuarine environment.

Chapter 2 of this study examined whether the aging process of Cu NPs in a mesocosm designed to simulate the surface water of a marine ecosystem impacted marine phytoplankton. It was found that the aging process of the Cu NPs in a marine ecosystem reduced the toxicity of aged Cu NPs to phytoplankton due to the lower concentration of dissolved Cu with an aging period of up to 30 days. The aging process also influenced the behavior of Cu NPs in seawater, as shown by a drastic transformation in the morphology of Cu over time. A threefold increase in aging time, however, resulted in a similar increase in the negative impacts of the aged Cu NPs. Greater Cu dissolution was observed at the 15 wk aging period, which was attributed to the formation of small aggregates of soluble Cu complexes, and primary particle sizes with a high surface area. Also, physical interactions between the particles and phytoplankton cells were responsible for an increased concentration of dissolved Cu in phytoplankton cultures. Increased dissolution in algal cultures resulted from heteroaggregation or Cu uptake by the cells. This study therefore showed that the effect of Cu NPs aged in the simulated marine environment can be influenced by the extent of aging in estuarine surface waters, as well as the concentrations of NOM present, including those released from algae.

In Chapter 3, the impacts of the aging process Cu NPs undergo as they flow downriver to the ocean on marine phytoplankton were examined. Unlike with the Cu NPs aged in seawater, where reductions in the bioavailability of Cu ions and toxicity over a month of aging were observed, the Cu NPs aged in freshwater media resulted in substantially increased dissolution rates, intracellular uptake, and toxicity as aging increased. The freshwater system slowed the morphological transformations of the Cu NPs over time, and also increased the

concentration of the released Cu ions. The effects of the greater bioavailability of toxic Cu ions released from the aged Cu NPs than the pristine Cu NPs was a determinant factor in Cu toxicity to phytoplankton. In fact, the growth of cells was greater in phytoplankton exposed to Cu NPs without aging than in phytoplankton exposed to aged Cu NPs.

Cu NPs aged in freshwater systems seemed to be more toxic than Cu NPs aged in seawater systems, as evidenced by reduced phytoplankton population growth rates and increased intracellular Cu uptake with greater aging periods. While Cu NPs aged in seawater reduced toxicity over a 4 wk period, when aged for up to 15 weeks, population growth rates declined and Cu uptake increased, suggesting that longer-term exposure may result in greater negative impacts. Additionally, the higher concentrations of toxic Cu ions found in algal cultures in comparison with aged stock solutions in both freshwater and seawater system phytoplankton exposed to Cu NPs raised concerns of impacts on pelagic organisms and suggested that such communities can play an important role in influencing the fate and transport of aged Cu NPs in estuarine systems.

Finally, the behavior and toxicity of CBNPs seemed to be more pronounced after aging in aquatic ecosystems, as evidenced by the generally greater toxicity in Cu NP exposed marine phytoplankton, while similar lethal and sublethal impacts on estuarine amphipods exposed to Cu-based nanopesticides and conventional Cu-based pesticides were detected in the present study. Traditional ecotoxicity tests and studies with pristine NPs allow the identification of potential hazards, but due to the vast array of Cu NPs incorporated in various products and processes, current methods for assessing their potential ecological impacts on aquatic ecosystems under environmentally realistic conditions are still lacking.